

1985

# A study of the chemistry and mutagenicity of welding fume

Ramkishore Tandon

*University of Wollongong*

---

## Recommended Citation

Tandon, Ramkishore, A study of the chemistry and mutagenicity of welding fume, Doctor of Philosophy thesis, Department of Chemistry, University of Wollongong, 1985. <http://ro.uow.edu.au/theses/1106>

Research Online is the open access institutional repository for the University of Wollongong. For further information contact Manager Repository Services: [morgan@uow.edu.au](mailto:morgan@uow.edu.au).

## **NOTE**

This online version of the thesis may have different page formatting and pagination from the paper copy held in the University of Wollongong Library.

## **UNIVERSITY OF WOLLONGONG**

### **COPYRIGHT WARNING**

You may print or download ONE copy of this document for the purpose of your own research or study. The University does not authorise you to copy, communicate or otherwise make available electronically to any other person any copyright material contained on this site. You are reminded of the following:

Copyright owners are entitled to take legal action against persons who infringe their copyright. A reproduction of material that is protected by copyright may be a copyright infringement. A court may impose penalties and award damages in relation to offences and infringements relating to copyright material. Higher penalties may apply, and higher damages may be awarded, for offences and infringements involving the conversion of material into digital or electronic form.

A STUDY OF THE CHEMISTRY AND MUTAGENICITY OF WELDING FUME

A thesis submitted in fulfilment of the  
requirements for the award of the degree of

DOCTOR OF PHILOSOPHY

from

THE UNIVERSITY OF WOLLONGONG

by

RAMKISHORE TANDON, M.Sc. Andhra, Ph.D. Melb.

DEPARTMENT OF CHEMISTRY

1985

Dedicated to Mary with love -  
for those special gifts she so readily shares.

## ACKNOWLEDGEMENTS

I wish to express my sincere gratitude to my supervisors, Dr John Ellis and Dr Phillip T. Crisp, for their interest and support throughout the course of this work. I thank Dr John Ellis for making it possible for me to come to Wollongong University to take up the project.

I am most grateful to Dr Robert S. Baker, Mr Andrew Arlauskas and Mr Antonio M. Bonin (Commonwealth Institute of Health, University of Sydney) for carrying out the mutagenicity assays and introducing me to the field. Significant contributions to the work by Dr Robert S. Baker are gratefully acknowledged. Thanks are due to Dr Richard Payling (John Lysaght (Australia) Ltd., Port Kembla) and to Dr Bryan E. Chenhall (Department of Geology, University of Wollongong) for their collaboration in the XPS and XRF/XRD studies. I gratefully acknowledge the assistance of Mr Ian S. Barrow (Australian Iron and Steel Co. Pty. Ltd., Port Kembla) in carrying out some of the XRF analyses, and thank Dr Roger St. C. Smart and Mr Colin F. Jones (School of Science, Griffith University, Brisbane), for performing the BET measurements.

The assistance of Mr Mervyn Fletcher and Mr John Forest during the building and testing of the welding and fume collection apparatus is gratefully acknowledged. Thanks are also due to Miss Ellen Wilke, to Mr Trevor Lewis, to Mr Peter Pavlik, to Mrs Roslyn Atkins, to Mrs Ethel Lee, and to Mr Ross Smith, for their ready assistance.

I gratefully acknowledge the receipt of a scholarship from the Australian Welding Research Association. Finally, I wish to express my sincere appreciation to Mrs Christine Peacock for her painstaking care in typing the manuscript.

This thesis describes physical, chemical and biological studies of fumes from six types of flux-coated welding rods, and a companion study of the bacterial mutagenicity of 24 metal salts. The choice of the welding rods was based on market availability and use, and chemical considerations. Fume was generated using an automatic arc welder (MMAW process). The mutagenicity study focussed on nickel (II) and chromium (VI), putative carcinogens present in certain welding fumes. Summaries of individual fume and mutagenicity studies are given below:

- (1) The generation rate and chemical composition of fume from AC welding of E316L-16 stainless steel electrodes were studied under a wide range of current (80-120A) and voltage (20-40V) conditions. The marked variations observed in the fume generation rates and fume composition are discussed in terms of arc temperature, gas shielding effects and the volatility and thermodynamic stability of fume components.
- (2) Fume from E316L-16 stainless steel electrodes was examined by x-ray photoelectron spectroscopy. Fourteen elements were determined. Necessary chemical information on the fume was obtained using various analytical techniques. It is demonstrated that NaF and KF are preferentially enriched on the particle surfaces and that Na, K, F and Cr(VI) are appreciably leachable by water. The toxicological significance of the results is discussed.

- (3) Fume generation rates (FGRs) and electrode melting rates (EMRs) of three types of hardfacing and two types of HSLA steel electrodes were determined at optimum values of current. Significant variations were observed in the FGRs and EMRs when arc voltage (and hence arc current and power) was varied at a fixed current setting on the power supply. The processes responsible for the observed variations are discussed. Both AC and DC processes are examined.
- (4) Fume from AC welding of a high-manganese hardfacing electrode showed no significant variation in chemical composition with particle-size range in the size fractions  $\leq 1.1$ , 1.1–2.0, 2.0–3.3, 3.3–7.0 and  $\geq 7.0$   $\mu\text{m}$  equivalent aerodynamic diameter. The physical properties of the fumes from the hardfacing and HSLA steel electrodes lie in the range: density = 3.0–4.4  $\text{g cm}^{-3}$ ; mass mean aerodynamic diameter = 0.5–0.9  $\mu\text{m}$  (92–96% of fume < 7  $\mu\text{m}$ ); and BET surface area = 13–28  $\text{m}^2 \text{g}^{-1}$ .
- (5) Elemental composition of the flux, fume and water-soluble fume fractions from the hardfacing and HSLA steel electrodes were determined using a wide range of analytical techniques. The results obtained (including chromium speciation data) are discussed alongside existing toxicological information.
- (6) Chromium(VI) and selenium(VI) were found to be mutagenic in standard Ames plate-incorporation assays. Cadmium(II), beryllium(II), chromium(VI) and ~~vanadium~~vanadium(V) were detected in

standard fluctuation assays. It was not possible to detect nickel (II) and cadmium (II) in modified Ames and fluctuation assays (trimetaphosphate in the nutrient media in place of orthophosphate to prevent precipitation of these metals as orthophosphates).

Metavanadate (V) was however detected in the modified Ames assays.

The results indicate that metal mutagens such as nickel (II) and chromium (VI) act by different mechanisms.

- (7) After treatment with potassium chromate at concentrations causing ultramicroscopic cellular lesions ( $3.7 \times 10^{-5}M$ ), only 25% of revertant colonies of Salmonella TA100 replicate on fresh minimal plates containing biotin. Detailed investigations show that temporary growth inhibition may be responsible for most of the non-replicating colonies detected in Ames plate-incorporation assays of chromium (VI).
- (8) Mitotic inhibitory activity and sister chromatid exchange (SCE) induction in cultured Chinese hamster lung (Don) cells correlate with the chromium (VI) contents of the water-soluble extracts of welding fumes. The growth inhibitory and genotoxic action of insoluble fume particles is more complex and cannot be explained on the basis of chromium (VI) alone.
- (9) Published values of equilibrium constants were used to calculate the percentage of  $CrO_4^{2-}$ ,  $Cr_2O_7^{2-}$ ,  $HCrO_4^-$  and  $H_2CrO_4$  present in aqueous solution at total chromium (VI) concentrations of

$10^{-2} - 10^{-6}$ M, in the pH range 1-8. This is the first compilation of such data.

## TABLE OF CONTENTS

	<u>Page No.</u>
<u>CHAPTER 1</u> INTRODUCTION	1
<u>CHAPTER 2</u> LITERATURE REVIEW	5
2.1      The welding process	5
2.2      Health effects of welding fume	7
2.3      Mutagenicity studies of welding fumes	11
2.4      Physical and chemical studies of welding fume	13
2.4.1    Effect of welding parameters on fume generation rates and fume composition	13
2.4.2    X-ray photoelectron spectroscopy and other studies	15
2.5      Direction of research	18
<u>CHAPTER 3</u> CHEMICAL COMPOSITION AND GENERATION RATES OF FUME FROM STAINLESS STEEL ELECTRODES	20
3.1      Introduction	20
3.2      Experimental	20
3.2.1    Equipment for fume generation and collection	20
3.2.2    Chemical analysis of fume and flux	24
3.3      Results	26
3.4      Discussion	32
3.5      Summary and conclusions	37

## Table of Contents (continued)

Page No.

<b><u>CHAPTER 4</u></b>	<b>XPS ANALYSIS OF STAINLESS STEEL WELDING FUMES</b>	<b>39</b>
4.1	Introduction	39
4.2	Experimental	39
4.3	Results	42
4.4	Discussion	46
4.5	Summary and conclusions	55
<b><u>CHAPTER 5</u></b>	<b>FUME GENERATION AND MELTING RATES OF HARDFACING AND HSLA STEEL ELECTRODES</b>	<b>56</b>
5.1	Introduction	56
5.2	Experimental	56
5.3	Results	58
5.4	Discussion	64
5.5	Summary and conclusions	67
<b><u>CHAPTER 6</u></b>	<b>GENERATION RATE, PARTICLE-SIZE AND SIZE-RELATED CHEMICAL MEASUREMENTS OF FUME FROM HARDFACING AND HSLA STEEL ELECTRODES</b>	<b>69</b>
6.1	Introduction	69
6.2	Experimental	69
6.3	Results	72
6.4	Discussion	78
6.5	Summary and conclusions	82

## Table of Contents (continued)

Page No.

<u>CHAPTER 7</u>	CHEMICAL INVESTIGATION OF FUMES FROM THE HARDFACING AND HSLA STEEL ELECTRODES	84
7.1	Introduction	84
7.2	Materials and methods	84
7.3	Results	89
7.4	Discussion	90
7.5	Summary and conclusions	102
<u>CHAPTER 8</u>	MUTAGENICITY OF METAL IONS IN BACTERIA	104
8.1	Introduction	104
8.2	Materials and methods	106
8.3	Results	113
8.4	Discussion	120
8.5	Summary and conclusions	123
<u>CHAPTER 9</u>	CHROMIUM (VI) AND APPARENT PHENOTYPIC REVERSION IN SALMONELLA TA100	125
9.1	Introduction	125
9.2	Materials and methods	126
9.3	Results	128
9.4	Discussion	136
9.5	Summary and conclusions	139
<u>CHAPTER 10</u>	ACTION OF WELDING FUMES FROM HARDFACING AND HSLA STEEL ELECTRODES ON CULTURED MAMMALIAN CELLS	141

## Table of Contents (continued)

Page No.

10.1	Introduction	141
10.2	Experimental	144
10.3	Results	147
10.4	Discussion	156
10.5	Summary and conclusions	157

<u>APPENDIX 1</u>	EFFECT OF pH ON CHROMIUM (VI) SPECIES IN SOLUTION	159
-------------------	---	-----

<u>REFERENCES</u>	166
-------------------	-----

<u>LIST OF PUBLICATIONS</u>	182
-----------------------------	-----

<u>PAPERS PRESENTED AT CONFERENCES</u>	183
--	-----

# CHAPTER 1

## INTRODUCTION

Welding is the principal industrial process used for metal bonding. The industrial use of welding is highly labour-intensive, labour accounting for 80–90% of production costs for all but the most automated processes (1). 0.2–2% of the total work force in typical industrialised countries is thus engaged in welding (1). The majority of welders are employed in the ship building, transportation, building construction, petrochemical, mining and metallurgical industries. These workers are exposed to fumes released in the welding process, which may create some health hazards.

There are about 20 major types of welding processes used on ten major classes of materials and hence an extremely wide range of possible working environments (1). The electric arc welding of metals using (i) a gas-shielded consumable wire electrode (Metal Inert Gas, MIG), and (ii) a flux-coated stick electrode (Manual Metal Arc, MMA), are the two most common types of welding. In general, the five combinations, MIG/mild steel, MIG/stainless steel, MIG/aluminium, MMA/mild steel and MMA/stainless steel account for 60–70% of all welding activity (1). The substances produced during the electric arc welding of metals include a mixture of complex oxides, fluorides, ozone and oxides of nitrogen. The acute and chronic health effects (mainly respiratory irritation and related effects) of the toxic substances present in welding aerosols are well documented in the literature (2, 3). Considerable concern has recently arisen over the presence of the potential cancer-causing agents, nickel and chromium (VI), in certain types of welding fumes (3).

The prime purpose of this study was to investigate the physical characteristics, chemical composition and biological activities of fumes from stainless steel, hardfacing and high-strength low-alloy (HSLA) steel MMA welding electrodes. A complementary study to evaluate possible mechanisms of action consisted of in vitro bioassays of 20 different metal ions including nickel and chromium (VI) using the Ames and other test systems. It should be pointed out that although most metal ions are reported to be mutagenic in at least one in vitro bioassay, the only metal salts which are suspected or demonstrated human carcinogens are those of nickel, chromium (VI), arsenic, cadmium and beryllium (4).

A review of literature on the physical, chemical and biological studies of welding fume is given in Chapter 2. Following this, the thesis is divided into three sections. The first section (Chapters 3 and 4) deals with the generation rate and the bulk and surface composition of fume from a common type of stainless steel electrode; the second section (Chapters 5, 6 and 7) deals with the physical characteristics and chemical composition of fumes from hardfacing and HSLA steel electrodes, some of which contain chromium and nickel; and the third section (Chapters 8, 9 and 10) deals with the toxic and genotoxic action of fumes from the hardfacing and HSLA electrodes, and the in vitro testing of metal ions for bacterial mutagenicity.

The diverse nature of the work lends itself to each individual study being presented as a separate and self-contained chapter in the

thesis. Chapter 3 discusses variations in generation rates and chemical composition of fume from a stainless steel (E316L-16) electrode. An automatic arc welder and fume collection system are described in this chapter. Chapter 4 describes the results of surface analysis of the fume and water-washed fume from the stainless steel (E316L-16) electrodes using x-ray photoelectron spectroscopy (XPS). Bulk analysis data obtained using a wide range of experimental techniques are also included in the chapter. Chapter 5 presents fume generation rate (FGR) and electrode melting rate (EMR) data for three types of hardfacing and two types of HSLA steel electrodes using both AC and DC welding. Chapter 6 deals with density, particle-size and BET surface area measurements of the fumes from the hardfacing and HSLA steel electrodes. The fume fractions produced using a 4-stage cascade impactor, were chemically analysed for one of the hardfacing electrodes to examine the relationship between fume composition and particle-size range. Results of these chemical measurements are also discussed in Chapter 6. Included in this chapter is also a detailed investigation of the variation of FGRs of this hardfacing electrode with arc voltage over a wide range of constant current conditions. Chapter 7 gives a detailed chemical analysis (including mass balances) of the flux, fume and water-soluble fume from the hardfacing and HSLA steel electrodes. Emphasis is given to the chromium speciation results. Chapter 8 contains results of standard and modified Ames and fluctuation assays of 24 metal salts. The different ions tested, some of

which may be present in welding fumes, were chosen on the basis of their coordination chemistry, redox properties, and/or known toxic action, and include  $\text{Be}^{2+}$ ,  $\text{Cd}^{2+}$ ,  $\text{Cr}^{3+}$ ,  $\text{Co}^{2+}$ ,  $\text{Cu}^{2+}$ ,  $\text{Pb}^{2+}$ ,  $\text{Mn}^{2+}$ ,  $\text{Hg}^{2+}$ ,  $\text{Ni}^{2+}$ ,  $\text{Os}^{3+}$ ,  $\text{Mo}_7\text{O}_{24}^{6-}$ ,  $\text{VO}_3^-$ ,  $[\text{Sb}(\text{OH})_6]^-$ ,  $\text{CrO}_4^{2-}$ ,  $\text{MnO}_4^-$ ,  $\text{HAsO}_4^{2-}$ ,  $\text{F}^-$ ,  $\text{AsO}_2^-$ ,  $\text{BiO}_3^-$ ,  $\text{SeO}_4^{2-}$  and  $\text{SeO}_3^{2-}$ . Modified culture media were prepared by using trimetaphosphate ions instead of the orthophosphate used in standard media. The media modifications were introduced to prevent precipitation of metals such as nickel and cadmium as their insoluble phosphates.

Chapter 9 looks specifically at 'false' reversion in *Salmonella* TA100 assays of chromium (VI). The investigation was undertaken to find out if 'false' reversion affects quantitative estimates of chromium (VI) mutagenesis in *Salmonella*. Chapter 10 describes an investigation of the water-soluble and the water-insoluble fume fractions from the hardfacing and HSLA steel electrodes for mitotic inhibition and sister chromatid exchange (SCE) in cultured Chinese hamster lung (Don) cells. This work complements the chemical results described in Chapter 7. The major objective here was to find a relationship between the chromium (VI) contents of the welding fumes and their SCE activities.

Appendix 1 describes the chromium (VI) system in solution (concentration range  $10^{-2}$  –  $10^{-6}\text{M}$ ) over the pH range 1–8. The study was carried out in the context of the Ames test.

## CHAPTER 2

### LITERATURE REVIEW

In this chapter, the literature on welding fume is reviewed under the following sections:

- (1) the welding process,
  - (2) health effects of welding fume,
  - (3) mutagenicity studies of welding fumes,
- and (4) physical and chemical studies including new areas of welding fume research.

This review is general; literature relevant to individual topics is discussed, where appropriate, in the relevant sections of Chapters 3–10.

## 2.1 THE WELDING PROCESS

Manual metal arc welding (MMAW), is a process which uses electrodes coated with a mixture of materials which by melting and decomposition provide readily ionised compounds for arc maintenance, slag formers, and a non-oxidising atmosphere. Fume is an extremely complex by-product of the arc welding process. In manual metal arc welding, fume arises by vaporisation of the core metal and flux components of the electrode. The various constituents of the core metal and flux react at the high temperatures of the welding arc to produce a mixture of oxides, which rapidly condense to form particles of less than 1 µm in diameter (5, 6), and then appear to grow in size with time due to agglomeration (7). Particles in the range 1–7 µm thus develop with time (7). These constitute the greatest health hazard because of their ability

to penetrate deep into the lungs and because they are not readily cleared by the cilia lining the respiratory tract (7).

A generalised representation of fume and other by-products of welding is given in Table 2.1.

Table 2.1 By-products of welding operations.

Fume (Particulate content)	Radiant Energy	Gases	Other
Aluminium	UV	Carbon dioxide	Heat
Chromium	Visible	Carbon monoxide	Noise
Copper	Infrared	Nitrogen oxides	
Fluorides		Ozone	
Iron			
Lead			
Magnesium			
Manganese			
Nickel			
Silica, silicates (amorphous)			
Titanium			
Vanadium			
Zinc			

From: Effects of Welding on Health, American Welding Society, Miami, 1979.

Fume concentrations (particulate content) of the order of 100–400 mg/m<sup>3</sup> may be produced in the rising column of hot air directly above the arc (1). Average breathing zone concentrations depend to a large extent on the type of welding process used, but levels of 5 mg/m<sup>3</sup> are currently typical throughout the welding industry (8, 9).

High temperatures produced by the arc can cause emission of infrared, visible and ultraviolet radiation and in turn, ozone and oxides of nitrogen (Table 2.1). These potential hazards are well understood and several excellent review papers are available in the literature (3, 10–13). The discussion below is limited to the particulate form of fume.

## 2.2 HEALTH EFFECTS OF WELDING FUME

Doig and McLaughlin (14) as early as 1936 reported x-ray findings in welders of fine nodulation and stripping described as "siderosis". Parkes (15) later defined this as a "benign pneumoconiosis due to inhalation of dust and fume of metallic iron or iron oxide". Many of the later papers, however, are concerned not so much with the health hazards from iron but from nickel, chromium, manganese, cadmium, zinc, lead and fluorides, etc., in the welding fume. It is since about 1970 that the scientific method has been brought to bear on welding fume health studies. Stern (16) carried out an extensive literature search of the toxic substances to which welders may be exposed and their effects on health. From this study, Stern identified 20 papers and reports prior to 1970, 61

prior to 1975 and 153 prior to 1980.

The acute effects of the inhalation of various welding fume components (e.g., nickel, chromium (VI), manganese, cadmium) have been reported and recently reviewed (17, 18). Such effects can generally be related to a particular exposure and process. Chronic effects have received less attention, because of the confounding effects due to population dynamics e.g., job mobility (1), and from the masking of welding-related health effects by cigarette-smoking (19, 20). Stern (1) has reviewed pneumoconiosis (silicosis, asbestosis and silico-asbestosis), siderosis and pulmonary function studies of welders. The literature discussed in Stern's review demonstrates the existence of statistically significant exposure-related incidence of chronic respiratory tract disease in welders. There are certain health hazards which are not general but entirely process-dependant: e.g., exposure during the welding of stainless steel in confined spaces to high concentrations of fume containing water-soluble chromium (VI) has been reported to lead to both acute and chronic chrome intoxication, dermatitis and asthma (21-27).

Baker (3) has reviewed the carcinogenic effects of stainless steel and other nickel and chromium-bearing welding fumes. Some welding fume components, for which there is already evidence of carcinogenicity or which are suspect, are summarised in Table 2.2.

Table 2.2 Potential or known carcinogens in welding fume.

Chromium (VI)	Cancer in chromate workers.
Nickel	Cancer in nickel-refinery workers.
Ozone	Suspect carcinogen in laboratory animals.
Silica	Possible co-carcinogenic effects of silica in haematite miners.
UV radiation	200-315 nm wavelengths are known to be carcinogenic in animals.
Particulate form of fume	Possible co-carcinogen or tumour promoter due to irritant effects.

From: Baker (3).

The effect of the individual fume components is generally considered to be additive (e.g., in the calculation of threshold limit value (TLV) indices).

However, detailed scientific studies on possible synergistic or antagonistic effects still remain to be done.

The prime target organ for welding fume particles is the lung (28).

There are several papers in the literature on the examination of lung tissue in welders and in animals exposed to welding fumes. A discussion of these studies is, however, not within the scope of the present thesis.

The literature on the biological monitoring of chromium (VI) in welders, and the absorption, transport and excretion of chromium in man and animals, has been reviewed by Langard (29). MMAW stainless steel welders are exposed to much larger concentrations of chromium (VI) than MIG stainless steel welders (3, 29).

### Epidemiological studies on welders:

The various epidemiological studies in the literature have been reviewed and summarised by Stern (1, 4), and Baker (3). The reviews in Refs 3, 4 are specific to epidemiology of lung cancer among welders whereas the review in Ref. 1 includes surveys of both respiratory tract disease and lung cancer. Baker has pointed out the limitations of epidemiological studies, for example; a number of studies have not been corrected for smoking habits or for the ethnic background of the welders. The crude lung cancer mortality rates among the welding populations range from 54/100,000 (30) to 183/100,000 (31); age distribution, tobacco use and other factors among the welders and choice of reference population will significantly affect the relative results in each case (4).

A search of the world literature up to 1982 has revealed 22 epidemiological studies of lung cancer among welders (4). Of these, 17 report more than 3 cases of lung cancer, and 16 of the 22 collectively report a total of 586 cases (4). After excluding effects for shipyard employment and smoking (shipyard welders have in the past been exposed to asbestos), there still appears to be a "small but irreducible excess risk" of lung cancer for general welding populations (4).

Epidemiological studies (and animal tests) have confirmed chromium (VI) and nickel as occupational carcinogens (3). These health risks have been determined from non-welding occupations (see Table 2.2). There appear to be no conclusive epidemiological studies of cancer among

welders involved in stainless steel and nickel-plated mild steel welding.

### 2.3 MUTAGENICITY STUDIES OF WELDING FUMES

For the vast majority of metal compounds, there is insignificant human exposure and insufficient numbers of exposed individuals to permit satisfactory epidemiological studies. Since full scale inhalation testing using animals, is slow and expensive, the use of mutagenicity tests as indicators of carcinogenicity, is now gaining acceptance as a means of rapidly screening substances for potential hazard (32-41). These short-term screening tests rely on the hypothesis that most chemical carcinogens are able to interact with DNA before they can induce cancer. The same reactive molecules can attack either microbial or mammalian genetic material in similar ways (3). Reaction with microbial DNA induces mutations which can easily be detected by the Ames test (42, 43). Thus, most short-term in vitro tests have as their measured endpoints phenomena that can be directly related to mutation or malignant transformation (36, 44). In the particular case of the sister chromatid exchange (SCE) test, however, no such relationships have been established and the biological significance and the molecular mechanisms involved have yet to be identified (45, 46). Despite this, the SCE test (see also chapter 10) is an important test for the evaluation of genetic risk for man and a good complementary test for the Ames test. The former conclusion is based on the reasoning that a number

of steps which determine genotoxicity in vitro (e.g., solubility, rate of formation of chemical species, activity of intermediate metalorganic metabolites, membrane diffusion, and particle cell interactions such as phagocytosis) can be expected to occur in vivo as well.

A number of studies have been reported in the literature on the mutagenicity of welding fumes. Hedenstedt et al. (47) and Maxild et al. (48) showed stainless steel welding fumes to be positive in the Ames Salmonella histidine revertant plate-incorporation assay. Chromium (VI) has been shown to be an active mutagen in stainless steel welding fumes (49, 50). An antagonistic effect has been proposed to explain the reduced activity of chromium (VI) in MMA/stainless steel welding fumes (50). MIG/stainless steel welding processes have been found to produce particles of lower mutagenicity than MMA/stainless steel welding, and particulates from mild steel welding are reported to be inactive in the Ames Salmonella assay (48).

A slight but statistically significant increase in mutagenicity was observed for stainless steel welding fumes in the N-thioguanine resistance of V79 Chinese hamster cells which survive exposure to the highly toxic material (47).

The recessive lethal test in drosophila gave a negative response for exposure in the larval stage to MIG/nickel-containing welding fumes and to MIG/stainless steel fume, and to fresh MIG/stainless steel fume in the adult stage (49).

Water-soluble chromium (VI) and fumes from a MMA/stainless steel welding process representing an equivalent chromium (VI) dose showed similar transplacental genotoxic potency in intraperitoneal administration in the mouse spot test (Fleckentest) (51, 52). Stainless steel welding fume particles have also been shown to be cytotoxic and genotoxic in cultured mammalian cells (53).

There is still a general uncertainty in the relationship between mutagenicity and carcinogenicity of metals (see also Chapter 1). To the author's knowledge, there are not many long-term animal carcinogenicity experiments of welding fumes currently in progress. Such studies may be useful to further understand the effect of fume particles on the health of welders.

## 2.4 PHYSICAL AND CHEMICAL STUDIES OF WELDING FUME

### 2.4.1 Effect of welding parameters on fume generation rates and fume composition

A large number of parameters can be varied during a manually carried out MMA welding process. In addition, there are a wide variety of applications for which the welding process may be used. The fume generation rate and the composition of the fume are affected by both the welding parameters and the type of application. Listed below are the most important factors which have been shown to affect the rate of fume formation and fume composition (54).

- Voltage drop across the welding arc which is related to the arc length being maintained (55, 56, 57).
- Welding mode, i.e., AC, DC electrode positive (DCEP) or DC electrode negative (DCEN) (56).
- Arc current (55, 56, 57).
- Angle between electrode and workpiece (56).
- Position and type of weld, i.e., fillet, bead-on-plate, etc.

Arc voltage has been shown to affect both fume generation rate (FGR) and fume composition (55, 57). Increasing the arc current has been shown to increase the FGR measured with respect to time (g/min), but if the FGR was measured with respect to the weight of electrode consumed (a dimensionless quantity), then the rate was found to remain constant with increasing current (55, 56, 57). The increase in FGR measured in g/min may be due to the increase in electrode melting rate (EMR) at increased currents. More detailed studies are essential to further understand variations in both electrode melting and fume formation rates with welding parameters.

Previous standard techniques for the measurement of fume have been based on hand welding techniques, e.g., the Swedish standard (58). Results obtained using the Swedish fume box technique (58) have not been found to be reproducible between different laboratories (59, 60). Recently, a specially constructed equipment to control the various welding parameters during the production of fume from MMA electrodes has been

described in the literature (61). Laboratory research on welding fume using controlled and reproducible conditions is certainly of great value in assessing health risks. Breathing zone considerations, for example, the stance adopted by the welder and the positioning and type of headshield used, are critical in determining the exposure of any individual welder to fume (62).

#### 2.4.2 X-ray photoelectron spectroscopy and other studies

X-ray photoelectron spectroscopy (XPS) provides surface identification and quantitation (at depths of 2–5 nm without ion beam etching) of a large number of elements, including those with low  $Z$ , with reasonably high sensitivities (63, 64). The applications of XPS in welding fume research have however so far been limited to chromium speciation studies (65, 66). XPS analysis of chromium in welding fume is important because there still does not exist a totally unambiguous chemical method for the bulk analysis of chromium (VI) (67, 68), and because instrumental methods such as neutron activation analysis (NAA) and proton-induced x-ray emission (PIXE) measure only total chromium and not the individual chromium species, i.e., Cr(VI), Cr(III) or Cr<sup>0</sup>.

Lautner et al. (65) used XPS along with NAA, spectrophotometry and atomic absorption to analyse the chromium in fumes from the MMA welding of E308-16 stainless steel electrodes welded onto stainless steel 304. These authors used a deconvolution technique to resolve the Cr(VI) and Cr(III) peaks, and peak areas to determine the atomic ratios of the

surface chromium species. Lautner et al. conclude that surface ratios of chromium (VI) to chromium (III) may be used to calculate bulk chromium (VI) and bulk chromium (III) once total bulk chromium has been determined. Although the authors substantiate this claim with their experimental findings, extrapolations of surface concentrations to bulk concentrations using XPS data, may not be reliable except in the case of very small ( $< 0.01 \mu\text{m}$ ) particles and particles comprising aggregates of small identical particles.

Bohgard et al. (66) used XPS in conjunction with PIXE, spectrophotometry and transmission electron microscopy (TEM) to measure the water-soluble and water-insoluble chromium (VI) and chromium (III) in stainless steel welding fumes. The authors used TEM as a guide for interpreting their XPS data and making surface vs. bulk composition comparisons.

Senkevich and Prokopenko (cited in Ref. 69) studied the XPS spectra of welding fume from rutile-coated electrodes and found that when a 5 nm layer was removed by ion beam etching, the concentration of potassium became halved. Also, after etching, the authors claim the XPS spectra showed the presence of  $\text{Fe}_3\text{O}_4$  and  $\text{MnO}$  while the immediate surface of the fume particles contained the more oxidised  $\text{Fe}_2\text{O}_3$  and  $\text{Mn}_2\text{O}_3$ . The compounds were distinguished on the basis of small peak position shifts and minor differences in peak shapes.

The heterogeneity of welding fume particles has been demonstrated using scanning electron microscopy/energy-dispersive x-ray analysis (SEM / EDAX), particle-size fractionator/proton-induced x-ray emission (PIXE), and other techniques (2, 70-72). By far the most detailed investigations in this area are those of Stern (70, 71). A discussion of this work is beyond the scope of the present thesis.

Voitkevich (69) has reviewed some new areas of welding fume research which include spectroscopic, diffraction and resonance methods for investigating welding fumes. He concludes that XPS, infra-red spectroscopy, x-ray diffraction (XRD), electron diffraction and electron paramagnetic resonance (EPR) methods should be used in conjunction with each other in order to obtain maximum chemical information. Auger electron analysis may be applied to determine the local concentration of adsorbed gases on welding fume particles (71). EPR may be used to study compounds of iron and manganese, and free radicals, etc., in welding fumes (73).

The American Welding Society (74) has recently published a comprehensive study of six welding fumes, representing a variety of welding rods and wires. Fumes were analysed by XRD, SEM/EDAX and automated electron beam analysis, and by scanning transmission electron microscopy (STEM)/electron diffraction. The suspended particulate evaluation and classification system used in this study combines three basic analytical instruments to produce its particle-by-particle analysis;

an electron beam analyser is joined to a scanning electron microscope and an energy-dispersive x-ray analyser. No correlation was found between average diameter and particle chemistry or between average diameter and fume type. Even though no crystalline features were observed on the STEM, all particles examined produced electron diffraction patterns, indicating that individual fume particles contained crystalline material. Since the bulk composition of the fumes from several different ferrous electrodes was found to be similar, the investigators (74) were able to tailor a single list of chemical categories for the suspended particulate evaluation and classification system to identify particle types in a wide variety of fumes.

## 2.5 DIRECTION OF RESEARCH

An evaluation of previous welding fume studies showed the following gaps in the literature:

- (i) lack of detailed and mechanism-oriented fume generation rate measurements;
- (ii) lack of x-ray photoelectron spectroscopy (XPS) experiments to study possible surface enrichment of species;
- (iii) only one previous study on 'false' reversion of chromium (VI) (75); and
- (iv) only one previous published study (not detailed) of the effect of MMA welding fume particles on sister chromatid exchange (SCE) in cultured mammalian cells (53).

The focus of the present work was to provide, where possible, new data and to verify and extend pertinent studies reported in the literature.

## CHAPTER 3

### CHEMICAL COMPOSITION AND GENERATION RATES OF FUME FROM STAINLESS STEEL ELECTRODES

### 3.1 INTRODUCTION

Welders commonly experience increased fume production when the arc length is increased beyond its normal value or when the current setting on the power supply is raised. Variations in the rate of fume generation have been reported for a variety of electrodes under different current and voltage conditions (76-78). Kimura et al. (78) found that the rate of fume generation increases with the apparent power (V.A) of the arc. The elemental composition of welding fume has also been shown to vary with the arc conditions (77). Studies to date have concentrated on examining a broad range of electrodes and provide only a small amount of data for each electrode under different arc conditions. The present investigation involves an exhaustive study of the welding fume from a single type of stainless steel MMA electrode under a wide range of precisely controlled AC arc conditions. The data may be used to test proposed theories of fume formation and is essential for evaluating the toxicology of stainless steel welding fume.

### 3.2 EXPERIMENTAL

#### 3.2.1 Equipment for fume generation and collection

The automatic welder and fume collection system (Figs 3.1 and 3.2) comprised the following:

- (i) An AC Weldarc 230 power supply with rated input current 13.5A at 415V, set on low current range (open circuit voltage 78V).

- (ii) An automatic deposition machine (Steel Mains Pty. Ltd.) with a horizontal work table driven by a variable speed motor set at 150 mm/min and an electrode feeder mechanism set at 45° to the table.
- (iii) An electronic controller (Steel Mains Pty. Ltd.) for the electrode feeder mechanism which maintains a constant preset voltage between the electrode and the work by raising or lowering the electrode.
- (iv) A galvanised steel hood (base dimensions 30 cm x 30 cm) with a Fibrafax skirt connected by galvanised steel tubing (5 cm I.D.; wrinkles at bends filled with plastic) to a galvanised steel cowl (base dimensions 25 cm x 20 cm).
- (v) A high-volume air sampler (General Metal Works Model 2000) with motor speed regulated by a variable transformer and fitted with a 20 cm x 25 cm glass-fibre filter paper (air flow rate  $\approx$  14 L/s).

The horizontal table moves on rollers with a total movement of 500 mm at speeds adjustable from 100 to 700 mm/min. The electrode feeder mechanism comprises an insulated electrode holder mounted on a worm thread which is driven by a DC Servo-motor. The electronic controller operates both the horizontal drive table and the welding power supply while continuously displaying the welding current and voltage, which may be continuously recorded.

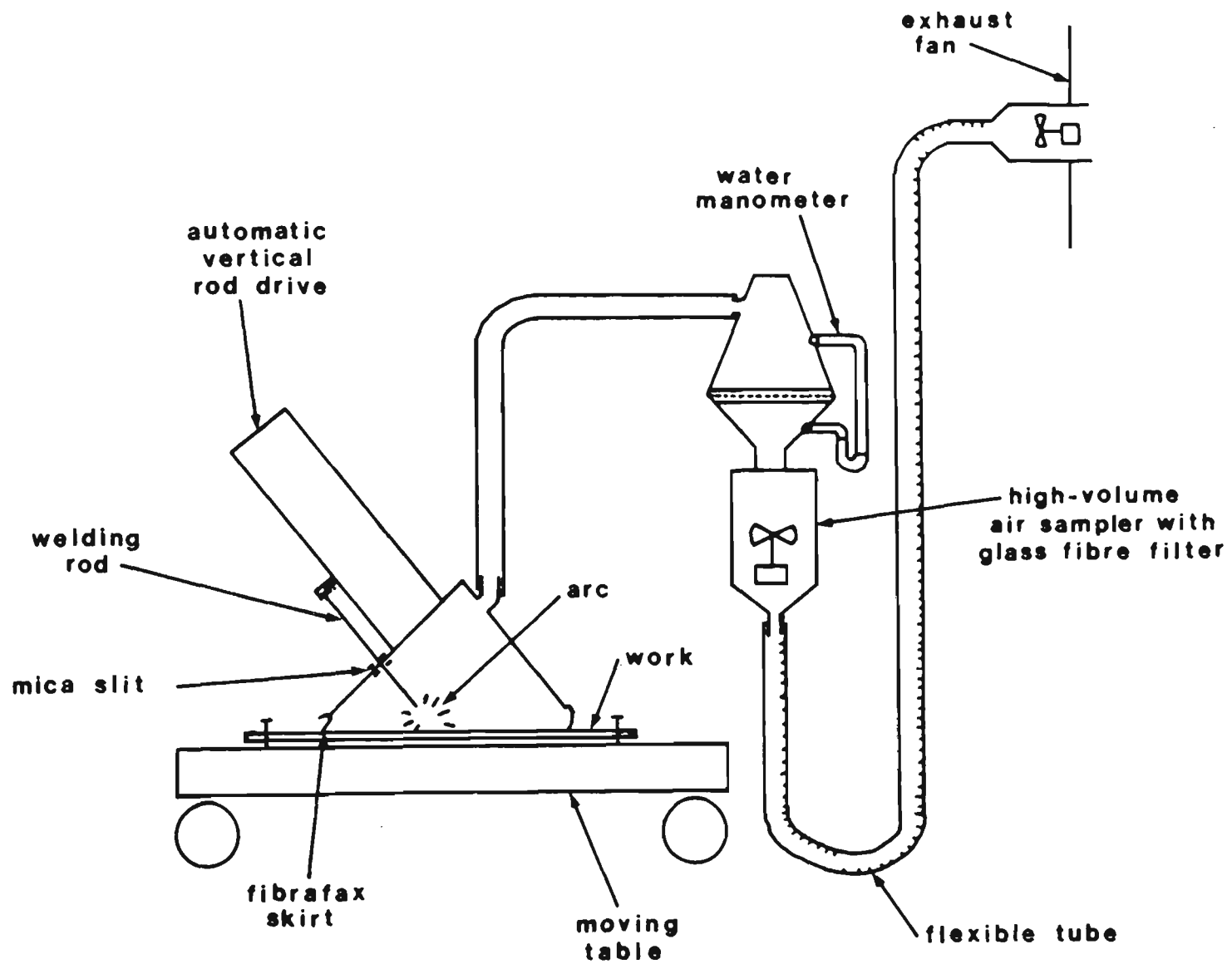


**Fig. 3.1** Schematic diagram of automatic welder and fume collection system.

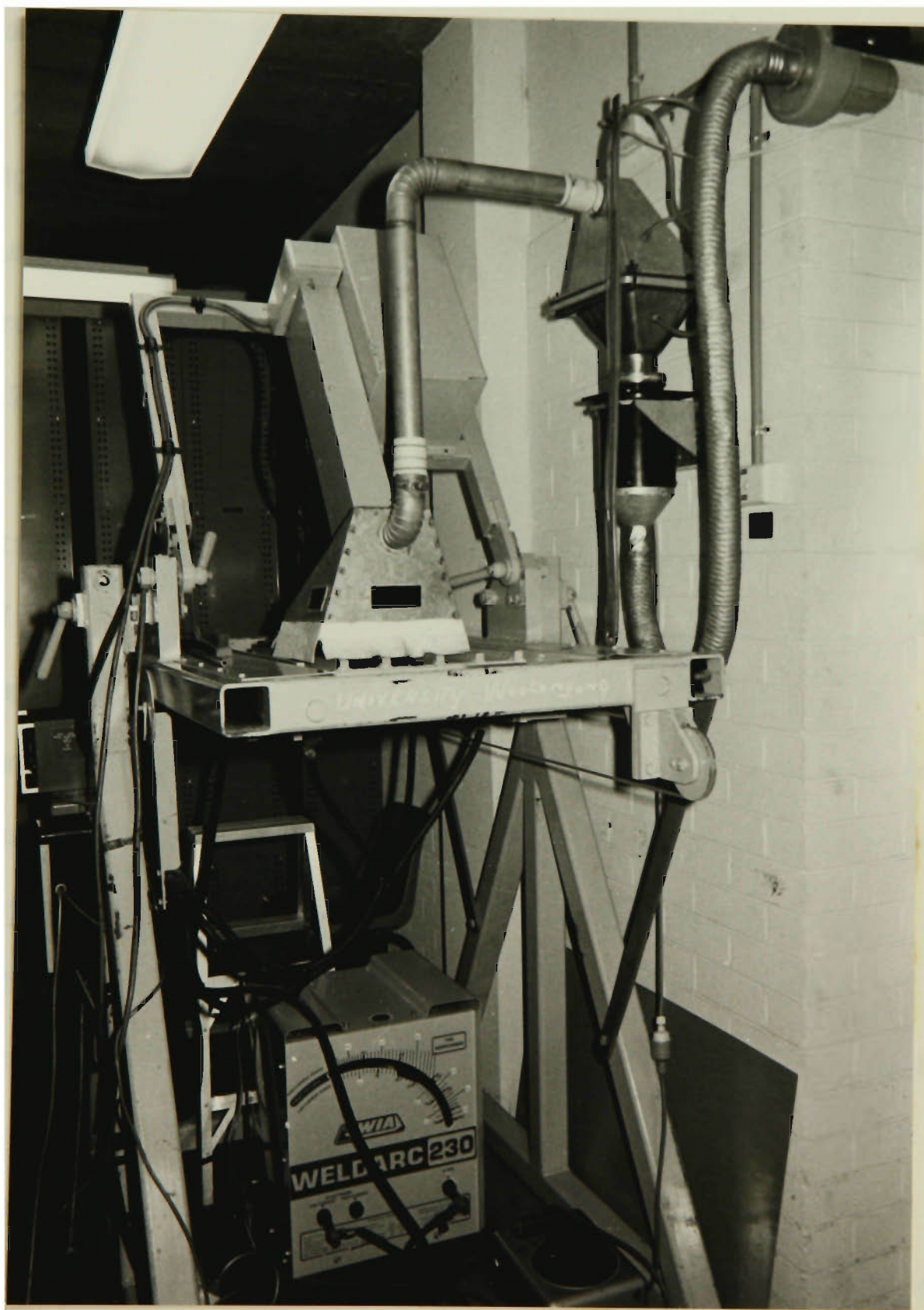


Fig. 3.2 The welding and fume collection system.

Welding was initiated by placing a 1 cm ball of steel wool between the electrode and the work. The voltage setting on the electrode feed controller kept the arc length within close limits with a hunting action of  $\pm 2$  mm superimposed on the downward feed. The flow rate of the high-volume air sampler was the minimum required to prevent escape of fume from beneath the hood skirt. Filter loading was monitored by making pressure drop measurements (data not shown).

### 3.2.2 Chemical analysis of fume and flux

Fume was generated using 3.15 mm E316L-16 electrodes on stainless steel 304 plates 6.25 mm thick. Fume from 2-4 electrodes (50% of total filter capacity on filter-loading curve) was collected on the filter paper, dried at 100°C and weighed prior to the chemical analysis. The fume deposit was carefully brushed from the filter paper. The deposit was examined for glass fibres or brush hairs and contaminated samples were rejected. Duplicate 0.1g samples of fume were extracted with nitric/hydrochloric and nitric/perchloric acids following the method described by Miller and Jones (79). Acid insoluble material was removed by filtration, ignited and weighed. The filtrate was analysed for the metals iron, chromium, manganese, nickel, copper, potassium, sodium, calcium, magnesium, using atomic absorption spectrophotometry. Fluoride was analysed following nitric/hydrochloric acid digestion, using an ion-selective electrode. Atomic absorption measurements were made on an Instrumentation Laboratory Model 551 instrument using flame

atomisation with automatic background correction in the double beam mode. An air-acetylene flame was used for all elements except chromium and calcium, where nitrous oxide-acetylene was used. The matrices of standard and unknown solutions were matched and standard instrument and analytical conditions (80) were used. Appropriate ionisation suppressants and releasing agents were added to standards and unknowns for the following elements: potassium (1000 ppm caesium), sodium (2000 ppm potassium), calcium (2000 ppm potassium) and magnesium (10,000 ppm lanthanum). Fluoride analyses were made using an Orion Model 901 Ionanalyser and a Model 94-09 fluoride selective electrode. Standards were prepared containing the same concentration of iron (III) as the unknowns and all fluoride concentrations were measured using solutions at pH = 5-6 containing sodium acetate (0.9M), hydrochloric acid (<sup>0.5M</sup>5M), sodium tartrate (0.5M) and trishydroxymethylaminomethane (0.9M).

Qualitative analyses of the electrode flux coating were carried out by x-ray fluorescence (XRF) spectrometry. Samples of flux coating were pelletized by fusing with lithium metaborate and analysed using a United Scientific instrument fitted with an energy dispersive Si (Li) detector and a Tracor Northern TN2000 multichannel analyser.

A second-order polynomial least-squares fit was applied to the fume generation data using standard programs on a Univac 1100 computer. Both fume generation rate and chemical results correspond to experiments in which welding was carried out at different arc voltages at fixed power

supply (current) settings. Varying the arc voltage at a fixed current setting on the power supply also varies the arc current and power.

### 3.3 RESULTS

The compositions of the stainless steel 304 base metal and the weld deposit from E316L-16 electrodes are given in Table 3.1. Qualitative XRF analysis of the electrode flux indicated the following components: titanium, zirconium, (major); potassium, calcium, chromium, manganese, nickel, silicon, niobium (minor); iron, rubidium, strontium, aluminium (trace). Phosphorus, molybdenum, sulphur and chlorine were not detected; magnesium and sodium were not determined.

The reproducibility of fume generation rates using the automatic deposition machine (relative standard deviation of six determinations) was 2% at 21.5V, 91A and 1% at 37.5V, 101A. Replicate values for the rates of fume generation during sample collection were determined periodically and lay within 5% of each other. The hunting action of the electrode feeder mechanism (designed to mimic the manipulation by an experienced welder) caused a variation of  $\pm 0.5V$  and  $\pm 8A$ . Average voltage and current values at a particular power supply setting varied by  $\pm 3\%$ .

Variations in the rate of fume generation under different welding conditions are shown in Fig. 3.3. Points with similar fume generation rates were contoured using a least-squares curve fit to yield "isofume"

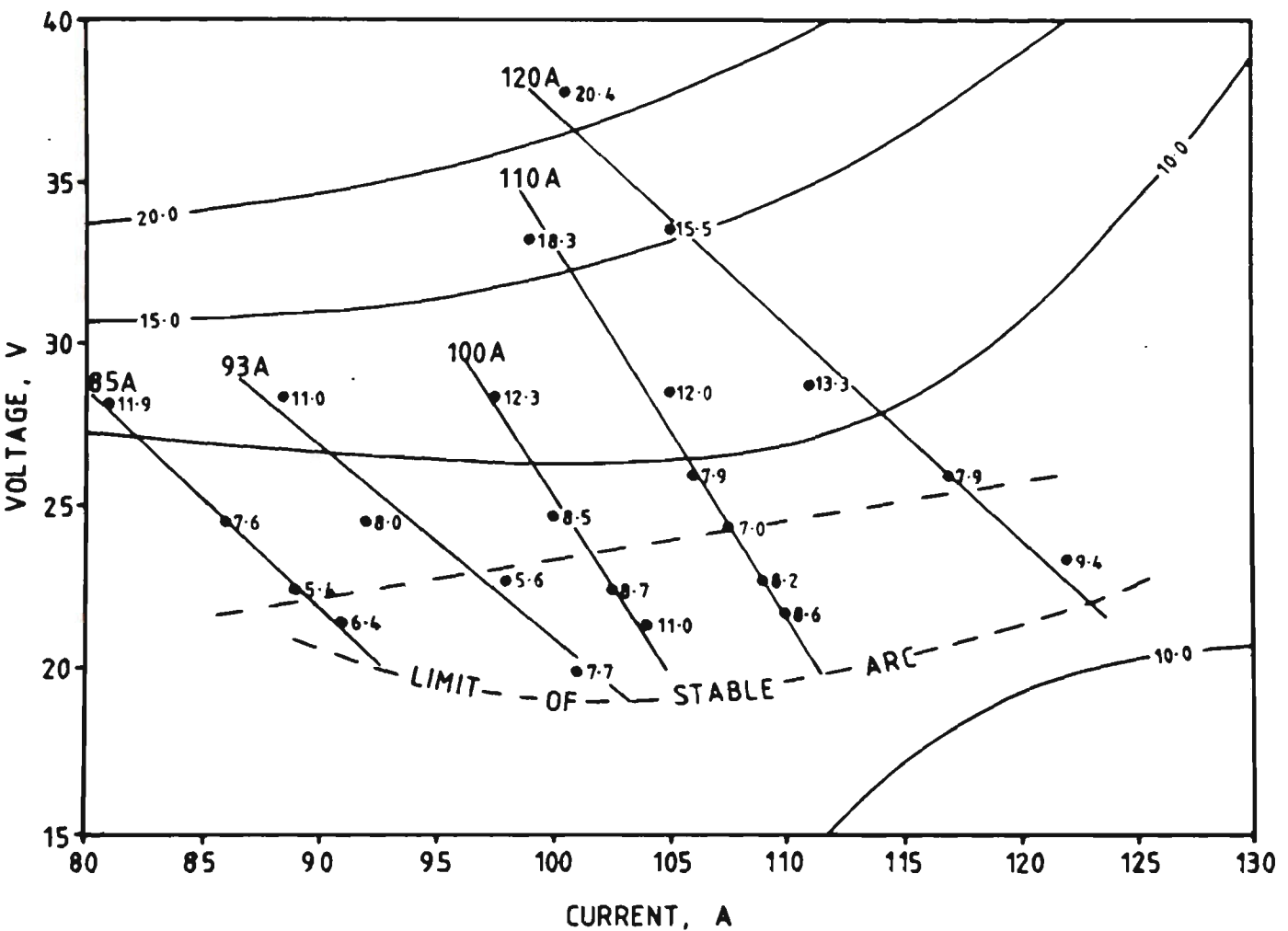
lines (goodness of fit 88%). The effect of V.A upon the rate of fume generation is given in Fig. 3.4. The effects of arc voltage on the fume composition and rates of element release in fume are given in Figs 3.5 and 3.6 for 100A and 120A power supply settings. Duplicate chemical analyses differed by an average of 2% (maximum 5%). Approximately 20% of the fume was acid insoluble.

Table 3.1. Composition of the base metal (S.S.304) and the weld deposit (E316L-16 electrodes).

Element	Percentage by weight <sup>(a)</sup>	
	Base metal (S.S.304)	Weld deposit <sup>(b)</sup> (E316L-16)
Fe	70.64	64.98
Cr	18.35	19.02
Mn	1.29	1.76
Ni	8.85	11.34
Cu	0.05	0.04
Mo	0.17	2.27
Nb	≤ 0.005	0.02
Ta	-	0.01
Ti	-	0.02
Si	0.54	0.49
C	0.05	0.023
P	0.03	0.017
S	0.02	0.004

(a) Percentage values for iron were obtained by difference.

(b) Certificate of analysis provided by the manufacturer for a batch of electrodes.



**Fig. 3.3** Isofume curves for 3.15 mm E316L-16 electrodes. Machine-electrode characteristic curves at 85, 93, 100, 110 and 120A settings are shown as lines of best fit to the experimental data points (●). Fume generation rates (g fume/kg electrode melted) are indicated at each point on the machine-electrode curves. Isofume curves (10.0, 15.0, 20.0 g fume/kg electrode) are drawn using a bivariate least-squares polynomial fit. The dashed line (----) indicates the minimum fume generation rate in each of the machine-electrode curves.

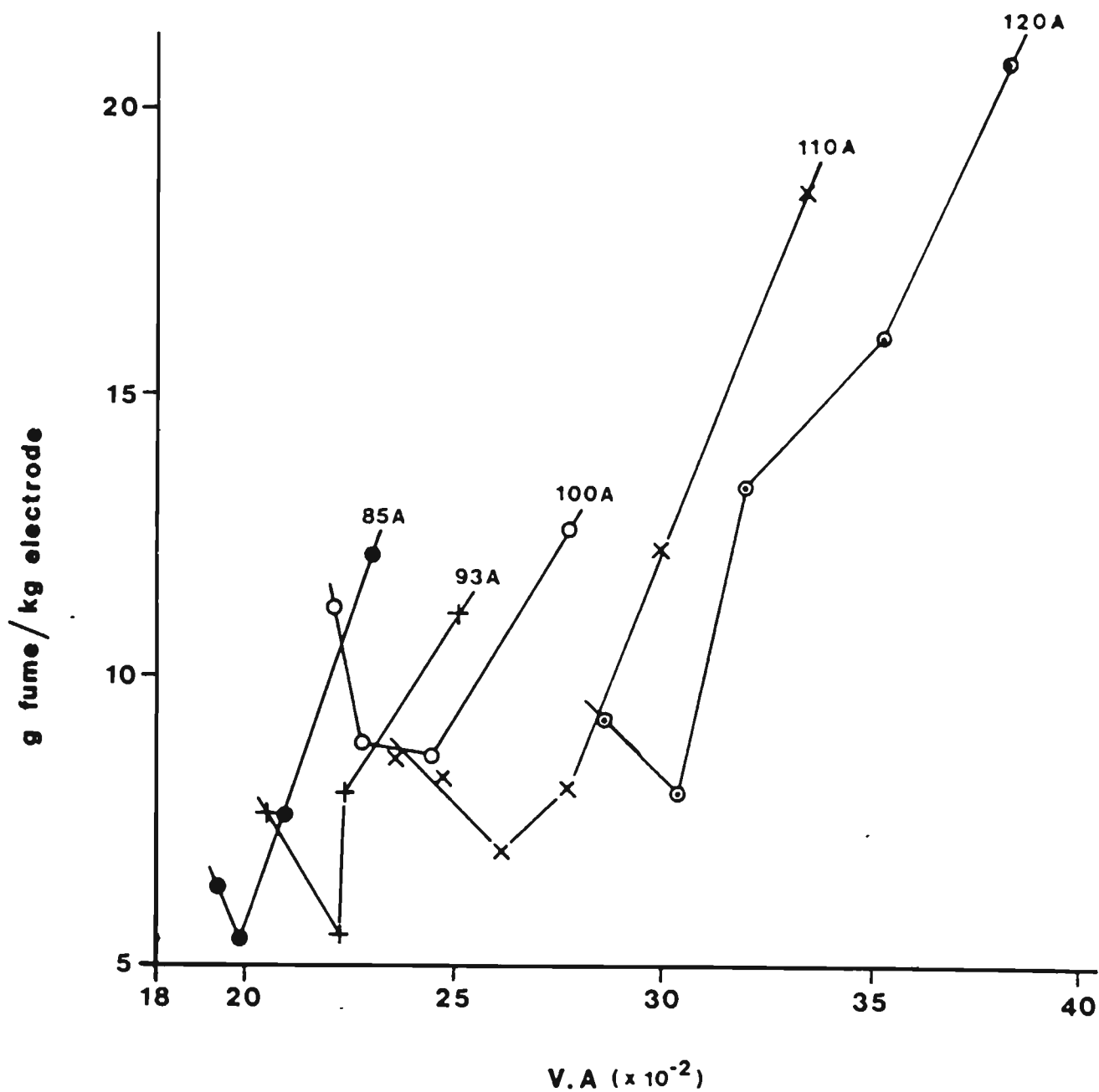


**Fig. 3.4** Effect of apparent power (V.A) on the rate of fume generation using 3.15 mm E316L-16 electrodes at power supply settings of 85, 93, 100, 110 and 120 amps.

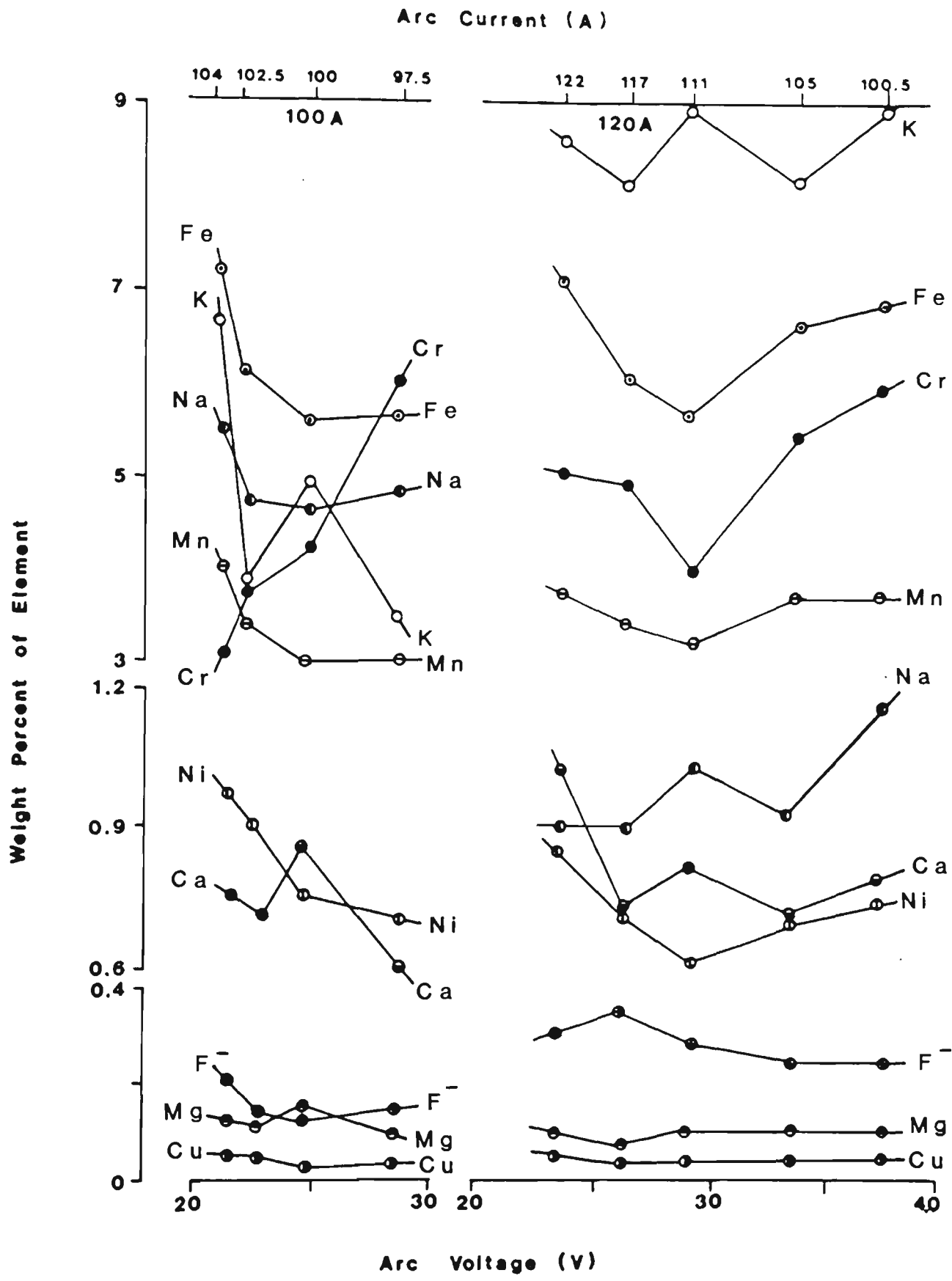


**Fig. 3.5** Effect of arc voltage on the composition of welding fume from 3.15 mm E316L-16 electrodes at 100A (left) and 120A (right) power supply settings.



### 3.4 DISCUSSION

Within the limits of stable arc, fume generation rates varied by a factor of four (Fig. 3.3). For each machine-electrode curve, there was an arc length (corresponding to particular current and voltage values) which resulted in a minimum fume generation rate. The rate of fume generation varied so critically with arc length that even an experienced welder might choose to operate under conditions which would result in substantially more than the minimum rate of fume generation. An inexperienced welder using the same machine setting might easily produce fume at twice the minimum rate. The highest and lowest voltages do not represent practical welding conditions, but were chosen in order to probe the physical and chemical processes occurring in the arc. The increase in fume production with increasing arc length (increasing voltage) is probably due to more vapour being expelled from the arc (78) as it becomes larger and hotter (greater rate of energy dissipation). The relationship between fume generation rate and apparent power in the arc (Fig. 3.4) supports this view: for each setting of the power supply, the relationship is approximately linear in the region away from the short arc (low voltage) condition. Kimura et al. (78) have reported a similar linear relationship between fume generation rate and apparent power for a variety of electrodes. The increase in fume generation under short arc conditions does not appear to have been reported previously. It may result from the erratic operation of the arc causing spattering and loss of gas shielding.

The fumes generated at power supply settings of 100A and 120A have generally similar elemental compositions (Fig. 3.5). The most notable exceptions are sodium and potassium: at 100A sodium and potassium have similar abundances, while at 120A potassium is nine times as abundant as sodium. Sodium and potassium salts with the same anion boil at similar temperatures (81) and are likely therefore to have similar volatilities in the arc. Ejection of liquid droplets from the arc is unlikely to favour one alkali metal over another. The different ratios of sodium to potassium may be explained by each metal being associated with a different anion (either in the original flux or in the arc) to produce compounds with different volatilities. Although the ratio of sodium to potassium varied, the sum of mean sodium and potassium concentrations in fume evolved at 100A and 120A settings respectively was constant.

There is a marked increase in the abundance of most elements in fume produced under low voltage conditions, especially with a power supply setting of 100A. These increased abundances must be associated with decreased abundances of constituents which were not determined (e.g., titanium and zirconium). Under the cooler conditions of a short arc, metals such as titanium and zirconium, which form refractory compounds, may be relatively less volatile than at higher temperatures. Chromium is exceptional in having a lower abundance in fume produced under low voltage conditions than under normal welding conditions at 100A. This may be due to an increased concentration of oxygen in the erratic arc

leading to the formation of poorly-volatile chromium (III) oxide.

Chromium (III) oxide is more stable than iron, manganese, nickel and copper oxides at 2000°C (Table 3.2) and should be formed preferentially from the vapour of the electrode alloy. While reliable data for the boiling points of metal oxides could not be obtained, the order of the melting points (Table 3.2) indicates that chromium (III) oxide should be less volatile than the other metal oxides.

Table 3.2 Physical and thermodynamic properties of relevant metals and metal oxides.

Metal	Boiling point <sup>(a)</sup> (°C)	Composition of stable oxide at 2000°C	Melting point of oxide <sup>(b)</sup> (°C)	$\Delta G_f^\circ$ of metal oxide per mole of metal <sup>(c)</sup> (kJ mol <sup>-1</sup> at 2000°C)
iron	2750	FeO	1424	-120
chromium	2480	Cr <sub>2</sub> O <sub>3</sub>	2400	-255
manganese	2100	MnO	1875	-200
nickel	2730	NiO	1960	- 30
copper	2600	Cu <sub>2</sub> O	1230	- 15

- (a) Handbook of Chemistry and Physics, 55th edition, 1974-75.
- (b) Kubaschewski, O. and Hopkins, B.E., Oxidation of Metals and Alloys, Butterworths, London, 1962.
- (c) Richardson, F.D. and Jeffes, J.H.E., J. Iron St. Inst., 160 (1948) 261.

The approximately linear relationship between the chromium content of the fume and arc voltage at a power supply setting of 100A is notable: the abundance of chromium in the fume doubles as the arc voltage increases from 20 to 30V. Since chromium compounds are suspected of having adverse health effects (82), this result may be significant.

The composition of the welding fume is very different from the composition of the electrode metal. Comparative figures for the electrode core wire and fume generated with a 120A power supply setting are given in Table 3.3 (average fume compositions at 100A are similar). It appears from the work of Gray et al. (83) that the volatilisation of elements from the molten electrode core wire is an important mechanism for the formation of fume particles in the arc. The simplest model assumes that the metals behave ideally and that their partial pressures above the liquid alloy surface may be calculated from Raoult's law (84). Due to the dilution of electrode core wire elements in the fume by volatilised flux constituents, comparisons must be made relative to a particular element. Table 3.3 gives this comparison in terms of "enrichment factors" relative to iron. For the major elements, chromium, manganese and nickel, direct application of Raoult's law provides values which are in fair agreement with the experimental values. However, the concentration of copper in the fume differed by an order of magnitude from the Raoult's law prediction, and this may reflect non-ideal behaviour of this trace constituent in the liquid metal solution. A more rigorous model is one which takes into

Table 3.3 Comparison of electrode and fume composition using the 120A power supply setting.

Metal	% in electrode core wire <sup>(a)</sup>	% in fume <sup>(b)</sup>	Relative enrichment factors <sup>(c)</sup>		
			Experimental	Raoult's law <sup>(d)</sup>	Gray et al. <sup>(e)</sup>
Fe	65.0	6.5	1	1	1
Cr	19.0	5.1	3	4	2
Mn	1.8	3.3	19	11	27
Ni	11.3	0.7	0.6	0.9	0.5
Cu	0.04	0.04	10	185	-

- (a) Values for the weld metal deposit have been used. Contribution to the weld deposit from metals present in the flux are not significant.
- (b) Average of values obtained at 23.4, 26.0, 28.8, 33.6 and 37.8V.
- (c) The relative enrichment factor (E) for each metal (relative to iron) is given by 
$$E = \frac{C_{\text{metal in fume}} \times C_{\text{iron in electrode}}}{C_{\text{metal in electrode}} \times C_{\text{iron in fume}}}$$
 where C values are concentrations expressed as percentage by weight.
- (d) Calculated from the composition of the equilibrium vapour obtained by direct application of Raoult's law to liquid electrode alloy at 2600°C (total vapour pressure = 1 atm).
- (e) Based on Raoult's law calculations by Gray et al. (83) for a similar electrode alloy (64.7% Fe, 18.7% Cr, 1.9% Mn, 12.9% Ni, 2.3% Mo) using estimated activity coefficients.

account the activity coefficients of the metals in the liquid alloy. Such a model has been used by Gray et al. (83) for metal inert gas welding using an electrode core wire of similar composition to that used here. Their results have been used to calculate enrichment factors which are presented in Table 3.3 for comparison. The concentration of nickel in the fume is better represented by this model.

The amount of each element released in fume per kilogram of electrode consumed (Fig. 3.6) may vary by a factor of between two and four under different welding conditions. The variation with arc voltage is larger at the higher power supply setting (120A). The minimum rate of all elements released in the fume (g element/kg electrode consumed) occurs under arc conditions corresponding to the minimum rate of total fume generation. The results demonstrate the importance of welding under optimum arc conditions in order to minimise the release of metal aerosols to the work environment.

### 3.5 SUMMARY AND CONCLUSIONS

The generation rate and chemical composition of fume from manual metal arc welding type AWS A5.4 E316L-16 electrodes (3.15 mm) were studied under a wide range of current (80-120A) and voltage (20-40V) conditions using an AC electrode deposition machine. Welding conditions, generation rates and chemical analyses were reproducible to within 5%. A summary of the results of the different experiments is given

below:

- (i) For each setting on the power supply, there was an optimum arc length which minimised fume generation. The rates of fume generation were up to 4 times greater than the minimum under high voltage conditions, and up to 1.5 times greater under low voltage conditions.
- (ii) Marked variations were found in the elemental composition of fume produced under different welding conditions using power supply settings of 100A and 120A. The metal content of the fume increased under low voltage conditions, except in the case of chromium at 100A where a linear increase with arc voltage was observed. At 100A, sodium and potassium had similar abundances in the fume, while at 120A potassium was nine times as abundant as sodium.
- (iii) For each power supply setting, the rates of release of individual metals in fume (g metal/kg electrode) have minimum values at the same arc conditions as the minimum in total fume generation rate; rates of metal release under unfavourable conditions may be up to three times the minimum value.

Data on rates of fume generation and element release should permit the occupational health aspects of welding to be evaluated and may lead to improvements in the formulation and operation of welding rods to minimise the emission of potentially toxic constituents.

## CHAPTER 4

### XPS ANALYSIS OF STAINLESS STEEL WELDING FUMES

## 4.1 INTRODUCTION

As pointed out in Chapter 2, the manual metal arc welding of stainless steel with flux-coated electrodes produces fume which is suspected of causing a number of lung diseases including cancers (3). The fume is known to contain both water-soluble and to a lesser extent water-insoluble chromium (VI) compounds (70) and has been found to damage microbial DNA as expressed in the Ames test (47). When fume particles are deposited in the human lung, the particle surfaces come into immediate contact with lung tissues and lung fluids. An examination of particle surfaces by x-ray photoelectron spectroscopy (XPS) is therefore fundamental to the chemical toxicology of welding fumes.

Previous applications of XPS to welding fumes (65, 66) have concentrated on the measurement of chromium (VI) / total chromium ratios. Reported here is the determination of fourteen elements in the surface of welding fume particles both before and after washing with water and argon ion-etching to a range of subsurface depths.

## 4.2 EXPERIMENTAL

The equipment and method for producing and collecting welding fume have been described in Chapter 3. 3.15 mm E316L-16 stainless steel electrodes were AC welded bead-on-plate to 6.25 mm stainless steel 304 at 100A, 24V. The electrodes used were from a different production batch to those used in the study described in Chapter 3, the major

differences being in the silicon, fluoride and aluminium flux contents.

Fume particles were collected on glass-fibre filter papers as a thick ( $\approx 0.05$  mm) layer and removed by gentle sweeping. The absence of filter fibres was confirmed by optical microscopy. Particle samples were washed by stirring with water at  $60^{\circ}\text{C}$  for 2h, recovered by filtration through a  $0.45\text{ }\mu\text{m}$  nylon membrane filter and dried at  $45^{\circ}\text{C}$ .

Bulk analyses of the fume particles were performed by:

- (i) infra-red spectrophotometry (Perkin-Elmer Model 283B; Nujol mull),
- (ii) thermogravimetry and differential thermal analysis (Rigaku TGA/DTA;  $\text{Al}_2\text{O}_3$  reference),
- (iii) x-ray fluorescence (as described in Chapter 3),
- (iv) x-ray diffraction (Phillips PW 1316/90 specimen/camera housing with PW 1050/70 goniometer;  $\text{Cu K}_{\alpha}$  radiation; graphite crystal monochromator; calibrated with Si crystal) and
- (v) electron microprobe analysis (Hitachi S-450 scanning electron microscope fitted with Tracor Northern TN2000 Si (Li) detector).

The flux (outer coating) of the E316L-16 electrodes was analysed by x-ray fluorescence ( $\text{Li}_2\text{B}_4\text{O}_7/\text{LiBO}_2$  fusion; Philips PW1600), x-ray diffraction (as for fume); for Ni, V and Mo by atomic absorption spectrophotometry (acid digestion/ $\text{Na}_2\text{O}_2$  fusion followed by  $\text{KHSO}_4$  fusion; Varian AA475) and for total carbon by combustion (Leco EC12). The water-soluble

fraction of the fume particles was analysed:

- (i) spectrophotometrically for chromium (VI) using s-diphenylcarbazide (85),
- (ii) for metals by atomic absorption spectrophotometry (see Chapter 3) and
- (iii) for fluoride using an ion-selective electrode (see Chapter 3).

For XPS analysis, particle samples (0.1 g) were pressed between two 2.5 cm aluminium foil discs in a Buehler Speed Press to 20 MPa. On peeling the two foils apart, the compressed powder adhered largely to one of the foils which was used as a support for the particles. A Perkin-Elmer 551 x-ray photoelectron spectrometer (Al  $K_{\alpha 1,2}$  excitation at 1486.6 eV; residual pressure  $< 5 \times 10^{-7}$  Pa) with a scanning Auger microprobe was used for XPS measurements. The energy scale was calibrated with gold, copper and palladium standards using the energy values of Asami (86). An analyser pass energy of 100 eV in conjunction with large aperture settings was used to obtain high sensitivity and a resolution of 2 eV. Noise problems prevented work at higher resolutions. During ion-etching, the pressure was increased to  $7 \times 10^{-3}$  Pa ( $5 \times 10^{-5}$  Torr) with argon. The ion beam (2 mm diameter) was rastered over an area 7 mm x 7 mm, greater than the effective analyser image size ( $\approx 3$  mm diameter). The etching rate was calibrated at 1 nm/min in the standard manner using Ta<sub>2</sub>O<sub>5</sub> (100 nm) on Ta. Since welding fume components may sputter at different

rates from tantalum oxide, the calibrated etching rate provides only a semi-quantitative estimate of sputtered depth. Concentrations were determined from peak areas using elemental sensitivity factors from Ref. (87) or from peak heights using sensitivity factors from Ref. (88) relative to peak areas from Ref. (87).

### 4.3 RESULTS

The elemental composition of the flux on the E316L-16 electrodes is given in Table 4.1 and the crystalline materials identified by x-ray powder diffraction of the flux were  $\alpha$ -SiO<sub>2</sub>, TiO<sub>2</sub>, CaCO<sub>3</sub> and ZrO<sub>2</sub> (Fig. 4.1a). The elemental composition of the weld deposit from the electrode (similar to that of the electrode core metal) and the composition of the stainless steel 304 base metal are given in Chapter 3.

The elemental composition of the fume from the electrodes is given in Table 4.1. Nearly 30% of the fume was soluble in water and the composition of the water-soluble material is given in Table 4.2. Analysis of fume samples by IR spectrophotometry indicated the presence of chromate ions ( $\nu(\text{Cr-O}) = 880 \text{ cm}^{-1}$ ) which were not detectable in the water-washed fume. The following transitions were observed during DTA of fume samples: 260-360°C, exothermic oxidation of Fe<sub>3</sub>O<sub>4</sub> to  $\alpha$ -Fe<sub>2</sub>O<sub>3</sub> (89); 650°C, endothermic polymorphic transition of K<sub>2</sub>CrO<sub>4</sub> (90); and 730°C, endothermic melting of Na<sub>2</sub>CrO<sub>4</sub> (90).

Table 4.1 Bulk analyses of electrode flux and fume particles from E316L-16 stainless steel electrodes.

Element	Concentration (% w/w) <sup>(a)</sup>	
	Flux	Fume particles
C	1.5	N.D.
F	1.6	3.0
Na	1.0	4.3
Mg	0.25	< 0.04
Al	3.8	5.9
Si	11.3	20.2
P	0.02	< 0.1
S	< 0.01	n.d.
K	4.2	19.4
Ca	5.3	0.6
Ti	17.6	1.4
V	0.04	n.d.
Cr	9.5	4.2 <sup>(b)</sup>
Mn	1.3	3.2
Fe	2.9	5.3
Ni	0.9	1.0
Zn	< 0.01	N.D.
Zr	1.0	n.d.
Mo	< 0.01	n.d.

(a) Based on dry weight.

Elements determined by XRF except for C (combustion); F(ion-selective electrode); Ni, V, Mo in flux (AAS); and Na, Cr, Mn, Ni in fume particles (AAS); n.d. = not detected; N.D. = not determined. Elements not determined (esp. 0) account for remainder of mass.

(b) Low chromium figure due to volatilisation losses during digestion of fume samples by  $\text{HNO}_3$  /  $\text{HCl}$  /  $\text{HClO}_4$ .

RELATIVE INTENSITY

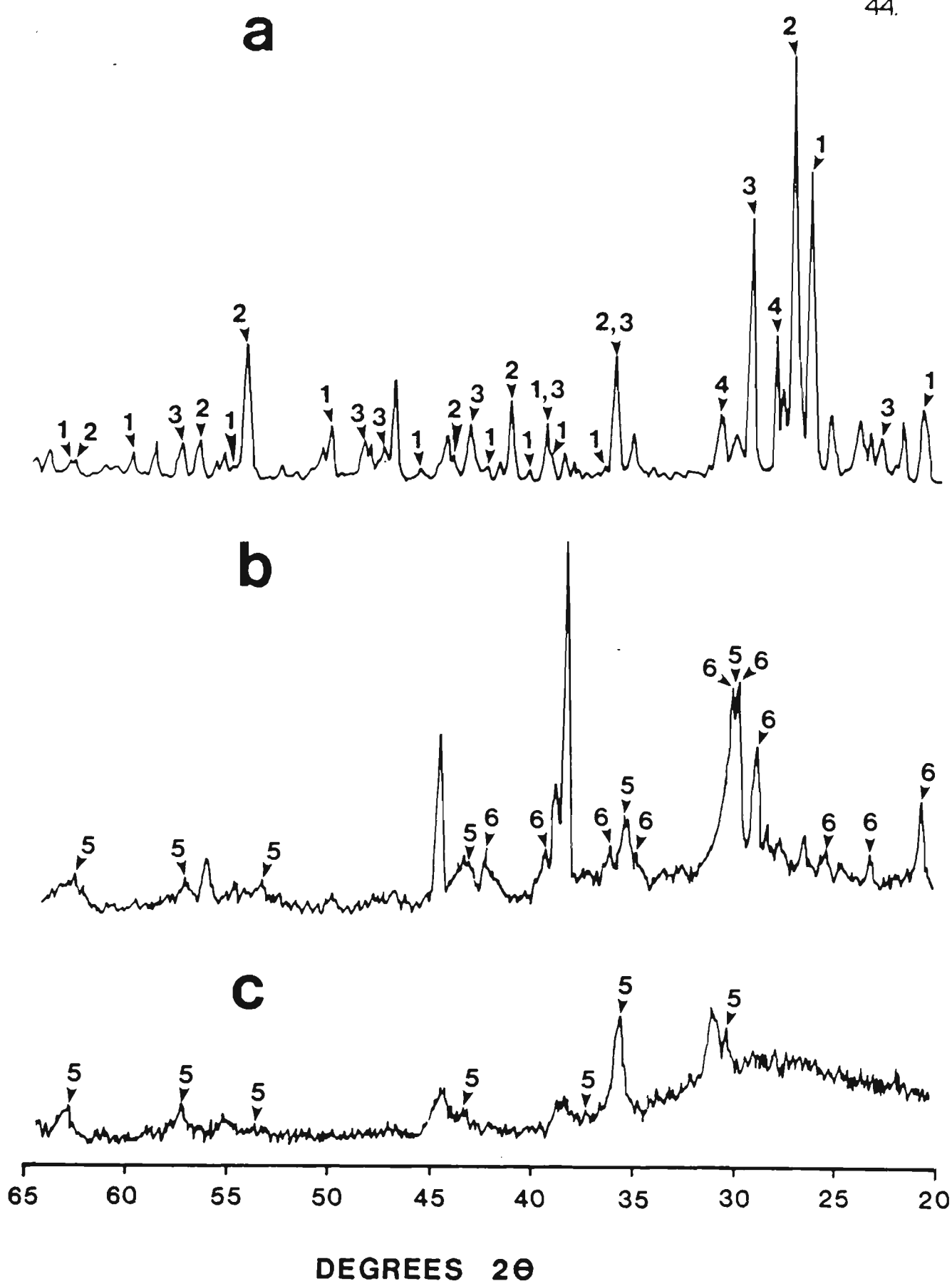


**Fig. 4.1** X-ray powder diffractograms of electrode flux (a), fume particles (b) and washed-fume particles (c) from E316L-16 stainless steel electrodes. 1 =  $\alpha$ - $\text{SiO}_2$ , 2 =  $\text{TiO}_2$ , 3 =  $\text{CaCO}_3$ , 4 =  $\text{ZrO}_2$ , 5 =  $\text{Fe}_3\text{O}_4$  or  $\text{FeCr}_2\text{O}_4$ , 6 =  $\text{K}_2\text{CrO}_4$ .

Table 4.2 Analysis of the water-soluble fraction of the fume particles from E316L-16 stainless steel electrodes.

Element	Concentration (% w/w in fume)
F	2.5
Na	4.0
Mg	0.06
K	6.7
Ca	0.15
Cr	5.1 <sup>(a)</sup>
Mn	0.7
Fe	0.15
Ni	0.08
Total	<u>19.4<sup>(b)</sup></u>

(a) All the water-soluble chromium is present as chromium (VI).

(b) 30% w/w of the fume was water-soluble; elements not determined (esp. O) account for remainder of the 30% w/w.

The endothermic phase transition of  $\text{Na}_2\text{CrO}_4$  at 395°C (90) was absent.

No transitions involving chromate species were observed with samples of water-washed fume. Examination of the fume by x-ray powder diffraction (Fig. 4.1b) indicated  $\text{K}_2\text{CrO}_4$  and either  $\text{Fe}_3\text{O}_4$  or  $\text{FeCr}_2\text{O}_4$  (or both).

Diffraction peaks due to  $\text{K}_2\text{CrO}_4$  were not detected with the water-washed fume (Fig. 4.1c). The presence of silicon in the washed-fume particles

was confirmed by XRF and by large-area electron microprobe analysis ( $\approx 60$  wt.% Si as  $\text{SiO}_2$ ).

X-ray photoelectron spectra of fume particles and washed-fume particles are given in Fig. 4.2. Quantitative results for the analysis of fume and washed-fume particles at various sub-surface depths are given in Table 4.3. Accurate peak positions were determined by high-resolution scans of individual peaks. Shifts in the kinetic energy of electrons due to charging of the sample were estimated for Na and for F using the modified Auger parameter (91) and indicated a charge shift of 7.1 eV for the NaF phase in the fume. Experimental values of photo-electron energies are compared with literature values (87, 92) for pure compounds in Table 4.4 (for fume) and in Table 4.5 (for water-washed fume). The Cr  $2p_{3/2}$  peak was resolved into Cr(VI) and Cr(III) components in some samples and quantitation was performed on the basis of peak areas (Table 4.3).

#### 4.4 DISCUSSION

Welding fume is considered (93) to contain two components: particles derived from molten droplets of flux or alloy ("unfractionated fume") and material derived from the condensation of volatile compounds ("fractionated fume"). The latter material may either condense onto the surface of "unfractionated fume" particles or condense to form separate particles.

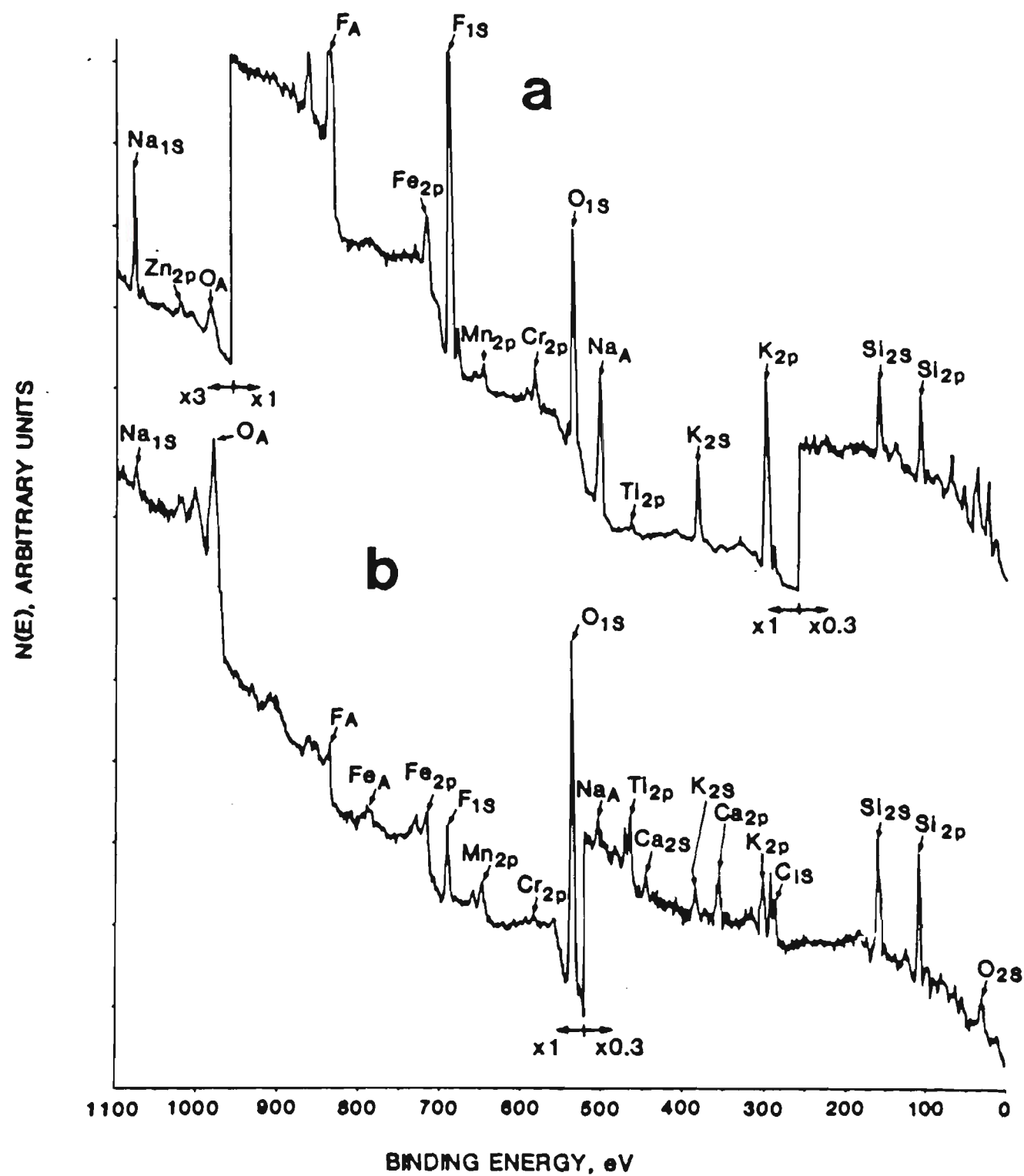


**Fig. 4.2** X-ray photoelectron spectra of fume particles (a) and washed-fume particles (b) from E316L-16 stainless steel electrodes.

Table 4.3 XPS analyses of fume and washed-fume particles at different subsurface depths.

Element	Concentration (at.%) <sup>(a)</sup>					
	<u>Fume particles</u>			<u>Washed-fume particles</u>		
	0 nm	≈10 nm	≈50 nm	0 nm	≈3 nm	≈10 nm
C	7	2	n.d	7	1	n.d.
O	21*	36	45	55	56	60
F	30*	18	11	6	6	4
Na	9*	9	6	0.9	1.7	0.4
Si	9*	14	17	21	23	24
K	19*	15	11	2.4	1.8	2.3
Ca	0.5	0.5	0.5	1.8	1.3	1.1
Ti	0.6	1.0	1.2	1.5	1.8	1.8
Cr <sup>(b)</sup>	1.3*	1.6	2.0	0.1	n.d.	n.d.
Mn	0.8	1.1	2.3	1.8	4.0	2.7
Fe	0.8	1.6	2.6	2.2	2.8	3.7
Ni	n.d.	n.d.	0.3	n.d.	n.d.	n.d.
Zn <sup>(c)</sup>	0.5	0.4	0.9	n.d.	n.d.	n.d.

(a) The concentrations indicated with an asterisk were calculated from peak areas; all others were calculated from peak heights.

n.d. = not detected.

(b) Approximate ratios of Cr(VI) / total Cr in fume particles:

0 nm, 0.7; 10 nm, 0.4.

(c) May be derived from the brass electrode holder of the welder.

Table 4.4 Energies and assignments of photoelectrons from fume particles.

Element	Peak <sup>(a)</sup>	Observed Electron energy (eV)	Assignment			
			Formula	Electron energy (eV)	Charge shift (eV)	Phase <sup>(b)</sup>
O	1s	538.3	silicates	531.4	6.9	A
			$\alpha$ -SiO <sub>2</sub>	532.2	6.1	
			SiO <sub>2</sub> gel	533.3	5.0	
O	1s	536.7	Fe <sub>3</sub> O <sub>4</sub> /Fe <sub>2</sub> O <sub>3</sub>			B
			MnO/Mn <sub>2</sub> O <sub>3</sub>	529.7	7.0	
			TiO <sub>2</sub>			
F	1s	691.4	NaF	684.2	7.2	B
			CaF <sub>2</sub>	684.6	6.8	
F	F <sub>A</sub>	648.1	NaF	655.2	7.1	B
Na	1s	1078.4	NaF	1071.1	7.3	B
Na	Na <sub>A</sub>	981.7	NaF	988.8	7.1	B
Si	2p	108.7	Silicates	≈102.6	6.1	A
			$\alpha$ -SiO <sub>2</sub>			
			SiO <sub>2</sub> gel	103.4	5.3	
K	2p <sub>3/2</sub>	299.4	KF	292.2	7.2	B
Cr	2p <sub>3/2</sub>	585.4	K <sub>2</sub> CrO <sub>4</sub>	579.4	6.0	C
			Cr <sub>2</sub> O <sub>3</sub>	576.6	8.8	
			CrF <sub>3</sub>	580.1	5.3	

(a) Photoelectron peaks in binding energy (eV) and Auger peaks in kinetic energy (eV).

(b) Proposed phases: A = SiO<sub>2</sub> gel; B = metal oxides and hydroxides, NaF, KF; C = Na<sub>2</sub>CrO<sub>4</sub>, K<sub>2</sub>CrO<sub>4</sub>, possibly in phase B.

Table 4.5 Energies and assignments of photoelectrons from washed-fume particles.

Element	Peak	Observed Electron energy (eV)	Assignment			
			Formula	Electron energy (eV)	Charge shift (eV)	Phase <sup>(a)</sup>
O	1s	535.7 ( $\approx 3$ peaks)	$\alpha$ -SiO <sub>2</sub>	532.2	3.5	
			SiO <sub>2</sub> gel	533.3	2.4	A
			silicates	531.4	4.3	C
			Fe <sub>3</sub> O <sub>4</sub> /Fe <sub>2</sub> O <sub>3</sub>			
			MnO/Mn <sub>2</sub> O <sub>3</sub>	529.7	6.0	B
F	1s	690.0	TiO <sub>2</sub>			
			NaF	684.2	5.8	B
			CaF <sub>2</sub>	684.6	5.4	
Na	Na <sub>A</sub>	982.5	NaF	988.8	6.3	B
Si	2p	105.8	$\alpha$ -SiO <sub>2</sub>			
			SiO <sub>2</sub> gel	103.4	2.4	A
			silicates	102.6	3.2	
K	2p <sub>3/2</sub>	297.5	KF	292.2	5.3	B
Ca	2p <sub>3/2</sub>	349.0	CaF <sub>2</sub>	347.8	1.2	
			CaCO <sub>3</sub>	346.8	2.2	D
Ti	2p <sub>3/2</sub>	462.5	TiO <sub>2</sub>	458.5	4.0	C
Mn	2p <sub>3/2</sub>	645.8	MnO/Mn <sub>2</sub> O <sub>3</sub>	641.2	4.6	C
Fe	2p <sub>3/2</sub>	715.7	Fe <sub>2</sub> O <sub>3</sub> /Fe <sub>3</sub> O <sub>4</sub>	711.1	4.6	C

(a) Proposed phases: A = SiO<sub>2</sub> gel; B = metal oxides and hydroxides, Na, K, F compounds; C = metal silicates/titanates; D = calcium compounds, possibly in phase A.

Compared to the electrode flux, the fume particles are rich in elements (e.g., F, Na, K) which form volatile compounds and poor in elements (e.g., Ti) which form refractory compounds (Table 4.1). The concentration of Ti in the fume is only 8% of that in the flux. Since neither the electrode core nor the base metal contain Ti, this figure should represent the maximum possible contribution of molten flux droplets to the fume. If volatilisation of  $\text{TiF}_4$ ,  $\text{TiO}_2$  or metal titanates occurred, the contribution may be substantially less.

The composition of the water-soluble fraction of the fume (Table 4.2) indicates that  $\text{Na}^+$  and  $\text{K}^+$  (mole ratio 1 : 1) are the principal cations, while  $\text{F}^-$  and  $\text{CrO}_4^{2-}$  (mole ratio 3 : 2) are the principal anions.  $\text{CaF}_2$  is insoluble in water ( $K_{\text{sp}} = 3 \times 10^{-11}$ ) (94) and the presence of significant quantities of dissolved  $\text{Ca}^{2+}$  is probably due to the co-ordination of  $\text{F}^-$  to transition-metal ions to form fluoro-complexes. This also explains the failure of transition-metal chromates to precipitate.

Mass balances may be obtained for the flux, fume and water-soluble fume (Tables 4.1, 4.2) by including the mass of O which would be associated with elements such as Si ( $\text{SiO}_2$ ,  $\text{SiO}_3^{2-}$ ), Ti ( $\text{TiO}_2$ ,  $\text{TiO}_3^{2-}$ ), Cr ( $\text{Cr}_2\text{O}_3$ ,  $\text{CrO}_4^{2-}$ ), Al ( $\text{Al}_2\text{O}_3$ ,  $\text{Al}_2\text{O}_4^{2-}$ ) and Fe ( $\text{Fe}_2\text{O}_3$ ,  $\text{Fe}_3\text{O}_4$ ). Contributions from elements which were not

determined are expected to be minor.

Thermal methods of analysis detected  $\text{Fe}_3\text{O}_4$ ,  $\text{K}_2\text{CrO}_4$  and possibly  $\text{Na}_2\text{CrO}_4$  in the fume. The uncertainty concerning  $\text{Na}_2\text{CrO}_4$  arises from the absence of an endothermic phase transition which occurs in the pure substance. The absence of this transition may be due to crystallinity defects or to the formation of mixed Na/K chromates. Alternatively,  $\text{CrO}_4^{2-}$  ions may condense from the gas phase preferentially with  $\text{K}^+$  ions due to their larger size (leading to a more stable ion-packing arrangement) and  $\text{Na}_2\text{CrO}_4$  may be absent.  $\text{Na}_2\text{CrO}_4$  could not be detected in the fume by XRD (Fig. 4.1b) although the unidentified peaks in the diffractogram ( $2\theta = 38.3^\circ, 38.8^\circ, 44.5^\circ$ ) may be due to a Na / K chromate (water-soluble) for which no diffraction data are available. The disappearance of chromates from the fume following washing (IR, DTA and XRD data) is consistent with the appearance of chromates in the water-soluble fraction.

The elemental analysis of the surface layers of the fume particles which were determined by XPS (Table 4.3) must be regarded as approximate due to the different depths sampled for each element and the use of sensitivity factors for pure homogeneous substances as the basis for quantitation. Also, since the analysed area for XPS was approximately  $10 \text{ mm}^2$ , the analyses represent an average composition of the surfaces of fume particles. The atomic ratios O/Si vary from 2.3 to 2.7 and indicate

that  $\text{SiO}_2$  rather than silicates must be the principal Si species near the surface. The exposure of deeper Si due to the crushing of particles in the press is possible. In the surface of the fume particles, the atomic percentages of Na (9%) and K (19%) approximately equal those of F (30%) and Cr (1.3%) and suggest a mixture of NaF, KF,  $\text{Na}_2\text{CrO}_4$  and  $\text{K}_2\text{CrO}_4$ . Some of the F may be co-ordinated to transition-metal ions such as Fe, since 6 at.% F remains on the surface of the washed-fume particles. Chromium must be present on the surface of the fume largely as alkali metal chromates since it is removed by washing with water. Other metals may occur as their oxides or as silicates. The carbon on the surface is probably an artefact (95), known to be adventitiously present on most material surfaces exposed to air.

Assignment of photoelectrons to particular compounds is complicated by the apparent presence of a number of different charge-phases in both the fume and water-washed fume. With such complex chemical systems, confidence in XPS peak assignments rests to a large extent on evidence from chemical analyses and from understanding of possible chemical processes. The surface of the fume sample (Table 4.4) contains at least two different charge-phases. The first contains Na and F, as indicated by the modified Auger parameter, with a charge shift of  $\approx 7.0$  eV. In this phase are found K, metal oxides and hydroxides and possibly Cr(VI) (if its charge shift is 1 eV less than in pure

$K_2CrO_4$ ). A second charge-phase (charge shift  $\approx 5.1$  eV) is comprised of Si and O, apparently as  $SiO_2$  gel. It should be noted that the O of metal silicates has the correct charge shift for inclusion in the first phase, but this assignment is unlikely to be correct due to the atomic ratio O/Si and the different charge shift of Si. Small amounts of metal silicates would not have been detected, however.

Assignment of the photoelectrons from the washed-fume is especially complicated (Table 4.5). A silica gel phase (charge shift 2.4 eV) is apparent and the water insoluble Na, K and F compounds have the same charge shift ( $\approx 5.7$  eV) as the O of metal oxides. Ti, Mn, Fe and Si occur as a separate charge-phase with charge shift  $\approx 4.3$  eV, possibly as a mixture of Fe and Mn silicates and titanates; while Ca may be present also in phase A (Table 4.5). Assignment of peaks is limited by the lack of data on suitable reference compounds (e.g., metal silicates and titanates).

Marked changes in elemental abundance occurred during ion-etching of the fume particles (Table 4.3). The at.% F for instance, decreased by a factor of 3 after etching to a nominal depth of 50 nm. This may be related to the high volatility of NaF (compared to other fume components) which causes it to condense last from the welding vapour. Substantial reductions in at.% K and Na also occurred (cf. Ref. 69). The at.% Cr increased during etching and the proportion of Cr(VI) decreased, although the latter may be an artefact of the etching process (96).

#### 4.5 SUMMARY AND CONCLUSIONS

The surface of fume particles from the manual metal arc welding of stainless steel with E316L-16 electrodes comprises  $\approx 50$  at.% sodium and potassium fluorides,  $\approx 8$  at.% soluble (probably potassium) chromate,  $\approx 30$  at.% silica and several at.% of transition-metal oxides, hydroxides or silicates. The fluorides and chromates are removed by washing with water to reveal a surface which is predominantly silica ( $\approx 60$  at.%) with the remainder comprising of transition-metal oxides, silicates and fluorides.

The presence of large quantities of fluoride (50 at.%) on the surface of the fume particles is especially significant since the combined effects of soluble fluorides and chromates on lung tissue have not been investigated. The quantity of fluoride (6 at.%; presumably transition-metal fluoro-complexes) which is not readily removed by washing from the fume particles may slowly leach into the lung tissues and pose additional health problems.

The general toxicological significance of surface enrichment of potentially toxic species is twofold. First, surface enrichment results in enhanced concentrations of potentially toxic species being in immediate contact with body fluids. Second, if the surface-enriched species are soluble, they can be readily mobilised to produce possibly adverse toxicological effects.

## CHAPTER 5

### FUME GENERATION AND MELTING RATES OF HARDFACING AND HSLA STEEL ELECTRODES

## 5.1 INTRODUCTION

A large proportion of the electrodes currently produced are of the hardfacing and high-strength low-alloy (HSLA) steel types. Hardfacing manual metal arc welding (MMAW) electrodes are extensively used in agriculture, mining and engineering where resistance to abrasion, impact and erosion are essential weld requirements (97, 98). HSLA steel MMAW electrodes have numerous industrial applications, such as the welding of tubes and vessels in chemical plants and steam generating equipment (98). Both types of electrodes contain varying amounts of chromium, and it is important therefore to study the formation rate and chemical composition of the fume emitted from such electrodes. In this chapter, data are presented on three hardfacing MMAW and two HSLA steel MMAW electrodes in order to show the effect of electrical parameters on fume generation rates and electrode melting rates. Both welding and fume collection were carried out under precisely controlled and reproducible conditions. This study is the first phase of an investigation on the physical characteristics, chemical composition and biological activities of fume particles from the hardfacing and HSLA steel electrodes.

## 5.2 EXPERIMENTAL

The equipment and method used for generating and collecting welding fume have already been described. For AC welding (see Chapter 3), the low current range (open circuit = 78V) was used for all electrodes

except E11 (Table 5.1) for which the high current range (open circuit = 55V) was used. DC welding (not described in Chapter 3) was performed with a Lincwelder DC 250 MK generator (open circuit = 60V). For both AC and DC welding, the current setting on the power supply was set to the mid-point of the recommended operating range and welding was performed at arc voltages between 20 and 35V. The automatic welding apparatus was thus used to simulate both practical welding conditions and unstable long-arc conditions. The electrodes used could not be welded under short-arc (unusually low voltage) conditions.

All measurements were made at a welding speed of 150 mm/min with the electrode feeder mechanism set at an angle of 45° to the table. All welding was done on 8 mm mild steel plates. Voltage measurements were made between the top of the electrode and the work table and between points 50 mm apart near the top of each electrode; current was determined by measuring the voltage drop across a shunt of known resistance. Dynamic properties of the arc (99) and phase angle were measured using a cathode-ray oscilloscope.

Fume collection was carried out following the procedures described by the American Welding Society (100) and the Australian Welding Research Association (101). An air flow rate of approximately 16 L/s was used; this is within the range of fume-plume conditions in practical welding.

### 5.3 RESULTS

The electrodes used in the study and their recommended operating conditions are given in Table 5.1. Electrode efficiencies, deposition efficiencies and fume generation rates under optimum or near-optimum current and voltage conditions are given in Table 5.2. The relationships between the electrical parameters: current, voltage and power, are shown in Fig. 5.1 and the variations in fume generation rate and electrode melting rate with current and power are shown in Figs 5.2 and 5.3. It must be borne in mind that both fume generation rates and electrode melting rates relate to a situation where power (V.A) is increasing as voltage (V) is increasing and current (A) is decreasing (see Fig. 5.1). We are thus working along points on the voltage-current curve at constant current setting on the power supply. The experiments were not designed to make comparisons of fume generation rates at equivalent power levels ( $\text{power (kW)} = \text{current (A)} \times \text{voltage (V)} \div 1000$ ). However, in all instances where equivalent power levels were obtained, higher fume generation rates were found with higher arc voltages. (See also Chapter 3, Fig. 3.4, p.29, for a similar observation with stainless steel electrodes).

Values for average current, fume generation rate and electrode melting rate were reproducible within  $\pm 5\%$  using the same voltage setting on the electronic controller and electrodes of the same production batch. During welding, voltage and current fluctuated within  $\pm 1\text{V}$ ,  $\pm 1\text{A}$  with electrode E11 and within  $\pm 2.5\text{V}$ ,  $\pm 5\text{A}$  for the other electrodes.

Table 5.1 Description of the hardfacing and high-strength low-alloy steel electrodes used.

Code*	Type	Diameter (mm)	Recommended operation and current (A)	Nominal weld deposit analysis (wt.%)	
E01	Hardfacing, medium-chromium	3.25	AC : 90-135 DCEP : 90-135	Cr : 7 Mo : 0.5 V : 0.5	C : 0.4 Mn : 0.3
E04	High-strength-low-alloy-steel	3.25	AC : 105-150 DCEP : 105-150	Ni : 1.6 Mn : 1.0 Mo : 0.3	C : 0.07 Si : 0.04
E05	High-strength-low-alloy-steel	3.25	DCEP : 75-130	Cr : 2.12 Mo : 0.95 Mn : 0.72 Si : 0.38	C : 0.045 P : 0.022 S : 0.019
E11	Hardfacing, high-manganese	4.0	AC : 125-230 DCEP : 125-210 DCEN : 125-210	Mn : 14.5 Ni : 3.2 Mo : 0.75 C : 0.65	Si : 0.14 P : ≤0.05 S : 0.01
E12	Hardfacing, high-chromium	6.0	AC : 120 DCEP : 120	Cr : 30-35 C : 4-5	Mn : 3-3.5

DCEP = DC electrode positive.

DCEN = DC electrode negative.

\* Electrode classification - E01: 1855A4<sup>a</sup>; E04: E9018G;  
E05: E9015B3; E11: 1215A4<sup>a</sup>; E12: 2355A1<sup>a</sup>.

<sup>a</sup> Australian Welding Research Association (AWRA) system of classification.

Table 5.2 Electrode efficiencies and fume generation rates of the hardfacing and HSLA steel electrodes.

Electrode code	Operation <sup>(a)</sup>	Electrode efficiency <sup>(b)</sup>	Deposition efficiency <sup>(c)</sup>	Fume generation rate <sup>(d)</sup>		
				g/kg electrode melted	g/kg weld deposit	g/min
EO1	AC:24V, 125A	65	96	30	46	0.63
	DCEP:24V, 120A	63	93	42	67	0.90
EO4	AC:25V, 125A	69	99	17	25	0.42
	DCEP:25V, 128A	68	97	16	24	0.43
E05	DCEP:23V, 125A	65	90	12	18	0.35
E11	AC:25V,200A	53	85	49	92	2.10
	DCEP:26V, 200A	53	85	38	72	1.80
	DCEN:24V, 200A	54	87	30	56	1.80
E12	AC:24V, 128A	78	95	40	51	0.78
	DCEP:25V, 124A	76	93	42	55	0.87

(a) Welding speed = 15 cm/min; FGRs at speeds < 15 cm/min may be greater due to the increased heat input.

(b) defined as 
$$\frac{\text{Weight of weld deposit}}{\text{Weight of electrode (including flux) melted}} \times 100$$

(c) defined as 
$$\frac{\text{Weight of weld deposit}}{\text{Weight of core metal melted}} \times 100$$

(d) Fume generation rates measured with respect to the weight of weld deposit, and as g/min, are included for purposes of comparison.

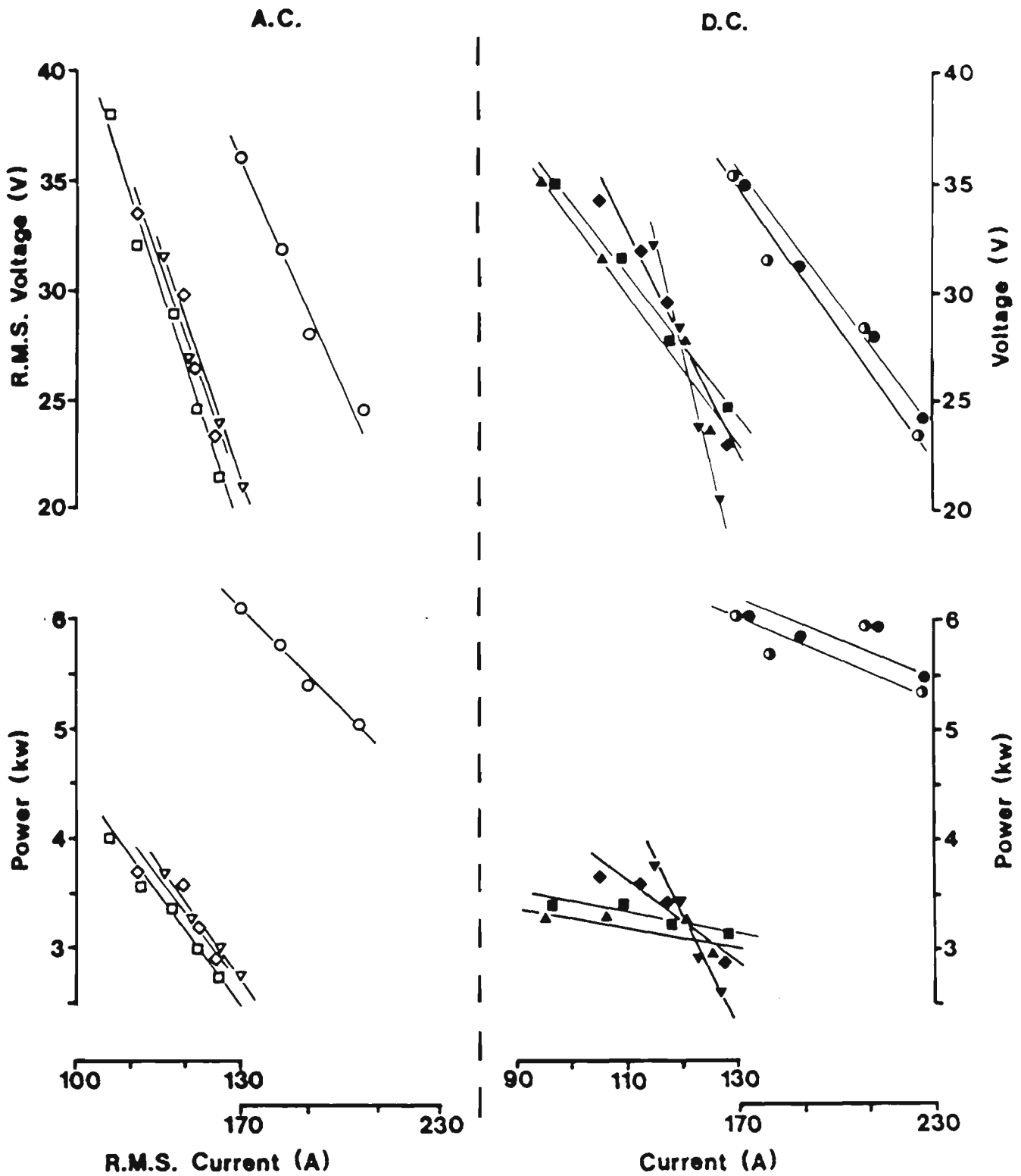


**Fig. 5.1** Effect of current on arc voltage and power.  
 Electrodes: E01, AC  $\nabla$ , DCEP  $\blacktriangledown$ ; E04, AC  $\square$ ,  
 DCEP  $\blacksquare$ ; E05, DCEP  $\blacktriangle$ ; E11, AC  $\circ$ , DCEP  $\bullet$ ,  
 DCEN  $\odot$ ; E12, AC  $\diamond$ , DCEP  $\blacklozenge$  (see Table 5.1 for electrode  
 code designations).

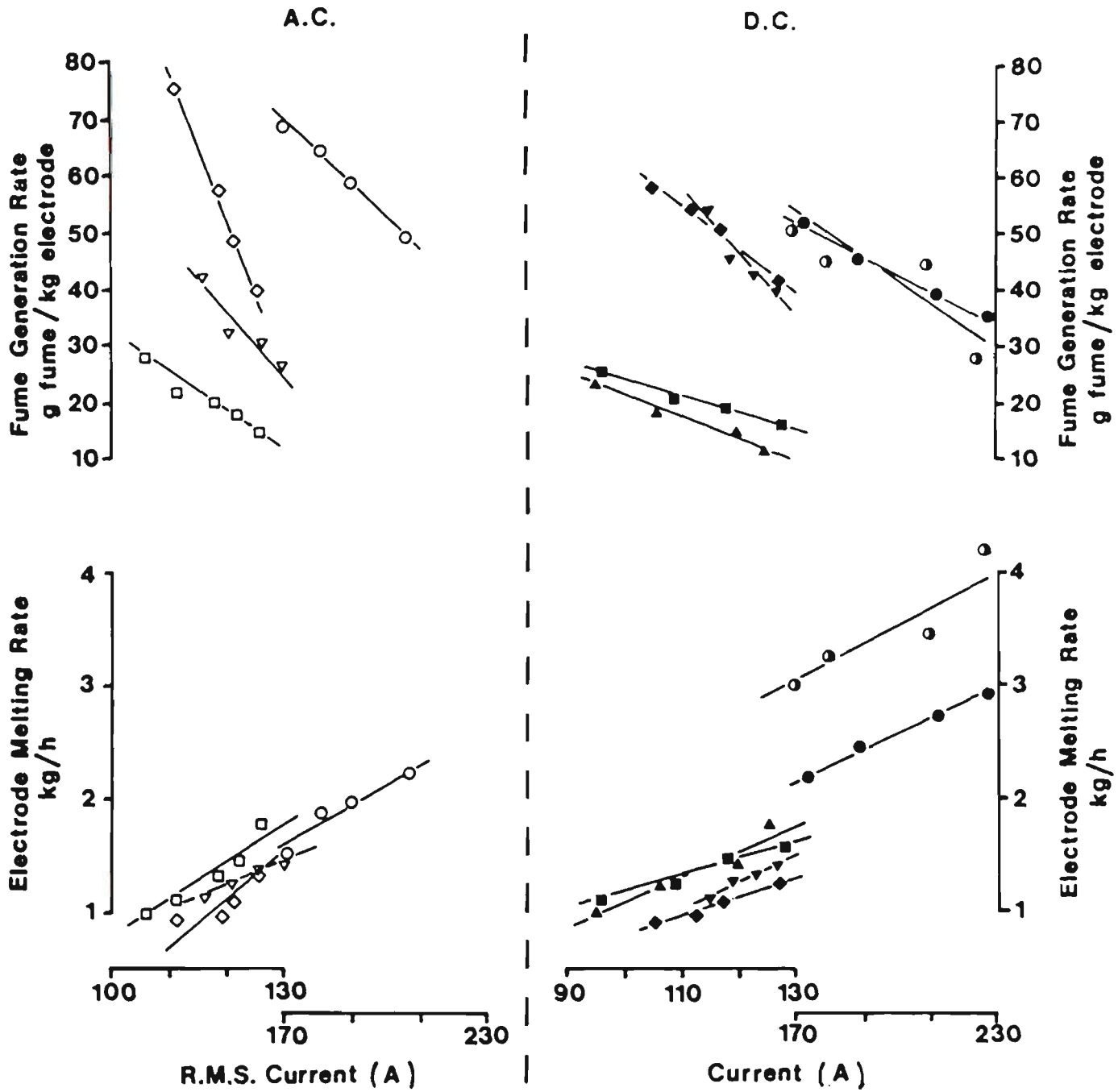


**Fig. 5.2** Effect of current on the fume generation rate and electrode melting rate.  
 Electrodes: E01, AC  $\nabla$ , DCEP  $\blacktriangledown$ ; E04, AC  $\square$ , DCEP  $\blacksquare$ ; E05, DCEP  $\blacktriangle$ ; E11, AC  $\circ$ , DCEP  $\bullet$ , DCEN  $\odot$ ; E12, AC  $\diamond$ , DCEP  $\blacklozenge$  (see Table 5.1 for electrode code designations).

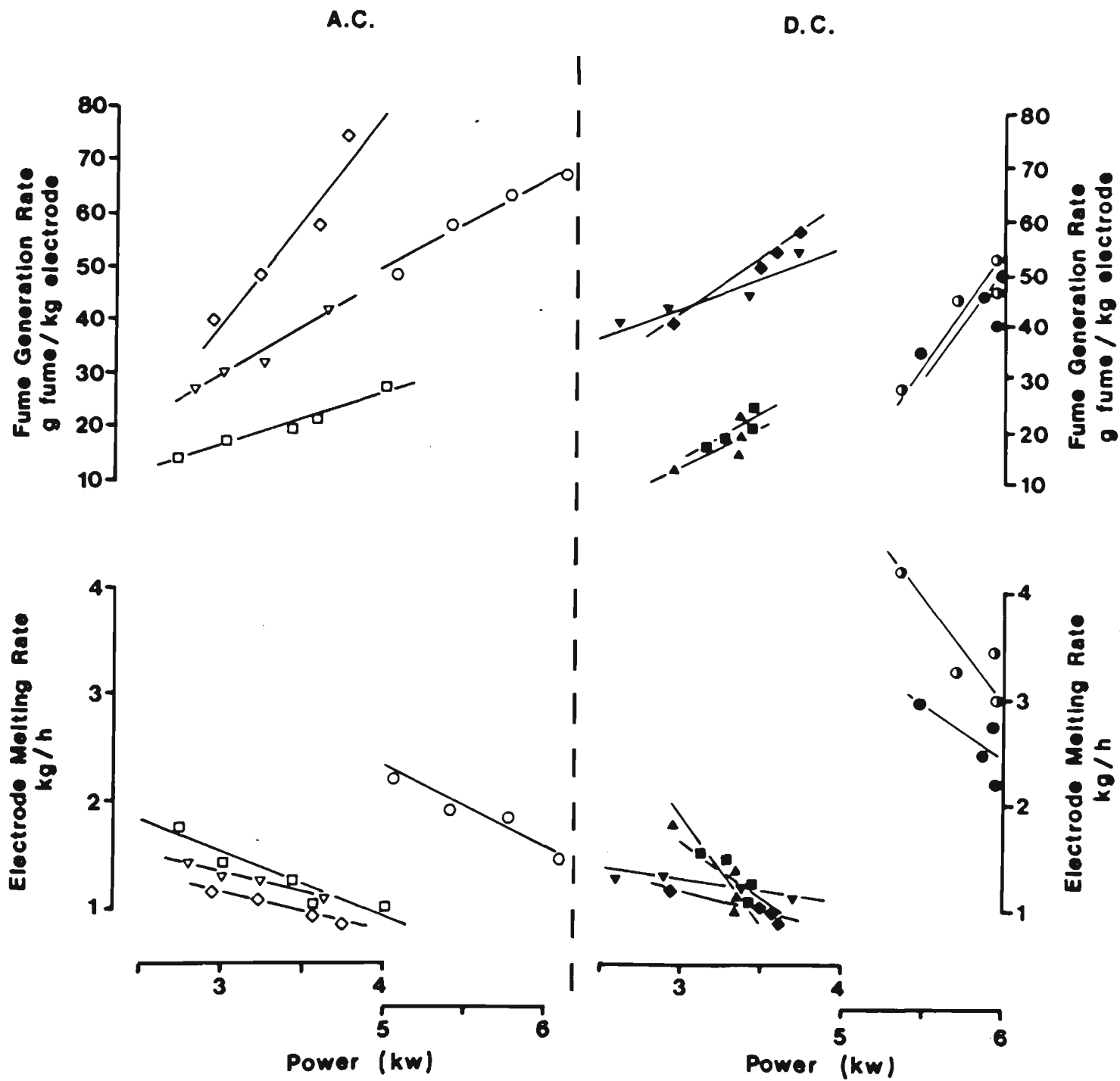


**Fig. 5.3** Effect of power on the fume generation rate and electrode melting rate.  
 Electrodes: E01, AC  $\nabla$ , DCEP  $\blacktriangledown$ ; E04, AC  $\square$ , DCEP  $\blacksquare$ ; E05, DCEP  $\blacktriangle$ ; E11, AC  $\circ$ , DCEP  $\bullet$ , DCEN  $\odot$ ; E12, AC  $\diamond$ , DCEP  $\blacklozenge$  (see Table 5.1 for electrode code designations).

Resistive heating of the unused portion of electrode was small since the voltage drop along the electrode was 20–50 mV/cm corresponding to  $\approx 1$  V along a full rod. Current and arc voltage were in phase (phase angle  $< 3^\circ$ ) confirming the absence of significant capacitance or inductance in the arc. All electrodes formed a gun barrel tip during use and the welded seams were generally flat and uniform. Electrode E12 formed considerably less slag than the other electrodes. No leakage of fume around the collecting hood was visible during welding and loss of fume due to deposition in the steel tubing and hood was  $< 5\%$ . The glass-fibre filter collects particles below  $0.3\ \mu\text{m}$  with decreasing efficiency but such particles constitute only a small percentage of the total mass collected on the filter (102).

#### 5.4 DISCUSSION

The fume generation rates (FGRs) for each electrode varied by a factor of approximately two, while acceptable arc length was maintained using the recommended nominal current settings on the power supplies. FGRs increased almost linearly with voltage and with power; and decreased almost linearly with current (Figs 5.2, 5.3) while constant setting was maintained on the power supply. As with stainless steel electrodes (Chapter 3), the power of the arc is probably the principal factor determining the FGRs (78) since an increase in the rate of heat input to the arc should lead to greater evaporation and sputtering of molten metal and molten flux. The arc voltage may also be important

since it determines the arc length (97) and thus the surface area of the plasma column through which material can escape as well as the time the material spends in the plasma (See also Chapter 3). No systematic difference was observed in FGRs with AC compared with DC welding. The results obtained here do not agree with the findings of Eichhorn et al. (103) who claim that AC welding generally produces less fume than DC welding. The mechanism of metal transfer during MMAW welding is difficult to establish but under optimum conditions consists of a showery spray of metal and slag droplets (97). Gray et al. (93) proposed that during spray transfer the bulk of the fume formation occurs in the arc plasma by evaporation of droplets in the plasma jet, rather than by processes at the cathode or anode. This proposal explains the similar FGRs obtained with DCEN and DCEP welding for electrode E11, and the generally similar fume generation rates obtained with AC and DC welding at the same power (Fig. 5.3).

The electrode melting rates (EMRs) displayed opposite behaviour to the FGRs in their variation with the electrical parameters. EMRs increased almost linearly with current and decreased almost linearly with voltage and power while constant setting was maintained on the power supply. EMRs obtained using AC and DCEP were generally similar, but the EMR for electrode E11 using DCEN was approximately 40% greater than that using DCEP. The high melting rates obtainable with DCEN arcs are well known (97, 104). The transfer of metal is globular and spattery unless trace

constituents such as metal oxides and calcium salts are included in the flux to make the cathode more thermionic; if this is done, spray transfer of metal predominates and the melting rate decreases (97). It appears therefore that the differences in EMRs with different DC polarities arise from differences in the proportions of globular transfer (fast) and spray transfer (slow). It is suggested that globular transfer occurs when there are relatively few arc roots releasing heat ("plasma emission", Ref. 104) and that spray transfer occurs when the arc roots are relatively numerous ("field emission", Ref. 104). The increase in EMRs with increasing current (decreasing voltage and power) may be due to the increasing frequency of charge-transfer processes per unit area of the electrode surface, resulting in a greater rate of heat dissipation. It is notable that EMRs increase with decreasing power. This is probably due to the relatively small amount of radiative heating of the electrode by the plasma or workpiece surface (97); resistive heating of these components of the arc therefore has little bearing on events at the electrode surface.

Interpretation of fume-generation and electrode-melting data for covered electrodes is hindered by the limited information available on the physics of metal arcs. In particular, processes occurring at the anode and cathode surfaces are poorly understood and, to date, studies of the arc plasma have concentrated on the simplest cases, viz., inert-gas shielding, non-consumable electrode and cooled workpiece (e.g., Refs 93, 105). The flux coatings of covered electrodes provide additional charge carriers to

the plasma (readily ionisable elements such as sodium, potassium and calcium), modify the emissivity of the cathode and anode surfaces (metal oxide and ionisable atomic films) and probably affect most other arc parameters. Further interpretations of fume-generation and electrode-melting data must wait until the chemical physics of flux coatings and electrode processes are better understood.

## 5.5 SUMMARY AND CONCLUSIONS

Reproducible fume generation rate and electrode melting rate data were obtained for three hardfacing and two high-strength low-alloy steel MMAW electrodes at optimum current settings for each electrode. The results from the different experiments are summarised below:

- (i) At each current setting on the power supply, fume generation rates (FGRs, g fume/kg electrode melted) varied by a factor of 1.5 to 2.0 while acceptable arc length was maintained. At each current setting, FGRs increased while simultaneously voltage and power increased (almost linearly) and current decreased (almost linearly).
- (ii) AC welding gave FGRs which ranged from 50% greater (hardfacing high-manganese electrode) to 30% lesser (hardfacing medium-chromium electrode) than DC welding at the same current. No difference was found in the FGRs between DCEN or DCEP welding with a hardfacing high-manganese electrode.

- (iii) Electrode melting rates (EMRs, kg electrode melted/h) increased almost linearly with current and decreased almost linearly with voltage and power while constant setting was maintained on the power supply. For the same current with a hardfacing high-manganese electrode, EMRs varied:  $AC < DCEP < DCEN$ .

Variations in fume generation rates are important for determining the precautions which should be taken during welding operations and must be known for chemical and biological studies of fume toxicity. In addition, rate data for welding processes under different conditions are important in testing hypotheses concerning electrode and plasma behaviour.

## CHAPTER 6

GENERATION RATE, PARTICLE-SIZE AND SIZE-RELATED CHEMICAL  
MEASUREMENTS OF FUMES FROM HARDFACING AND HSLA STEEL ELECTRODES

## 6.1 INTRODUCTION

In this chapter, the following data on fume from the hardfacing and HSLA steel electrodes are presented:

- (i) more extensive generation rate measurements for one of the hardfacing electrodes (high-manganese hardfacing electrode E11);
- (ii) particle-size distribution and mass mean aerodynamic diameter (MMAD) values obtained using an Andersen 4-stage fractionator;
- (iii) surface areas determined by the BET method (106, 107); and
- (iv) analytical results showing the relationship between particle-size range and chemical composition for electrode E11.

The additional fume generation rate (FGR) measurements on electrode E11 were carried out at the manufacturer's request. FGR data in this study are expressed as g/kg weld deposit and g/min.

## 6.2 EXPERIMENTAL

Fume generation rate measurements were made using the equipment described in Chapters 3 and 5. FGRs for the high-manganese hardfacing electrode (E11; Table 5.1) were determined at selected constant current values at three or four different voltages for each current. The power supply setting (AC or DC) was adjusted to obtain constant welding current when the voltage was varied.

Bulk densities of the fume powders were determined in duplicate at 20°C by the Archimedes method using kerosene as the immersion liquid

(0.5 - 1 g fume; 50 cm<sup>3</sup> pyknometer). The fume powders were outgassed for two hours under vacuum with half the volume of the pyknometer filled with kerosene before adjustment to final volume.

Particle-size distributions and mass mean aerodynamic diameters were determined by means of an Andersen 4-stage 20CFM (9.4 L/s) cascade impactor (108) connected to the General Metal Works Model 2000 high-volume air sampler described in Fig. 3.1. The 50% effective cutoff diameters (ECDs) for the four impactor stages were 7.0, 3.3, 2.0 and 1.1  $\mu\text{m}$ , with the backup filter collecting particles 0.01 - 1.1  $\mu\text{m}$ . Depending upon the FGRs, welding times of 3-15s were required for satisfactory loading. The glass-fibre fractionation and backup filters were encased in aluminium foils and weighed on a balance housed in a specially designed perspex chamber. The procedures described for Andersen sampler particle-sizing in Refs 108 and 109 were closely followed. The performance of the cascade impactor was checked by using the following sizes of monodisperse polystyrene latex (PSL) spheres: 11.9, 7.6, 5.7, 2.0, 1.1, 0.8, 0.46 and 0.23  $\mu\text{m}$  mean diameter. The PSL spheres (density = 1.05 gcm<sup>-3</sup>) were obtained from Duke Scientific Corporation, U.S.A. A heterodisperse aerosol was prepared by dispersing 0.1 cm<sup>3</sup> of a 10% w/w aqueous solution of each size in 50 cm<sup>3</sup> methanol. 1 cm<sup>3</sup> of this solution was made up to 500 cm<sup>3</sup> in methanol and the entire aerosol sprayed in a small clean room. The solvent evaporated from the aerosol droplets leaving dry PSL spheres. The PSL spheres were collected on 5 x 5 mm

glass coverslips painted matt black. Four coverslips were placed on each impactor stage. A total of 50 – 100 particles were measured for each stage using scanning electron micrographs.

Surface areas of the fume powders were measured by the BET method (106, 107) with nitrogen gas at liquid nitrogen temperature (area assumed per  $\text{cm}^3$  monolayer nitrogen at S.T.P. =  $4.39 \text{ m}^2$ ). A Perkin-Elmer 212 D sorptometer was used. Pretreatment of the samples (0.1 – 0.3 g) consisted of outgassing at  $20^\circ\text{C}$  for 48 hours. All the BET determinations were made using a one-point method (110). The accuracy of the one-point measurements was checked by carrying out a three-point determination on one of the samples.

Scanning electron microscopy (SEM) specimens were prepared by re-depositing the fume powders by air-brushing them on to double-sided sticky tape on an aluminium stub. A  $200 \text{ \AA}$  film of gold-palladium alloy was evaporated on to the fume particles in a Dynavac CE 12/14 coating unit at a pressure of  $7 \times 10^{-4} \text{ Pa}$  ( $5 \times 10^{-6} \text{ Torr}$ ). Specimens thus prepared were examined in a Hitachi S-450 SEM operated at 20 kV.

Chemical analyses were performed on duplicate fractionated fume samples from the AC welding of electrode E11. The five fractions (4 fractionation filters and the backup filter) were dissolved in 6M hydrochloric acid at  $60^\circ\text{C}$  (111). Metals were determined by atomic absorption spectrophotometry and fluoride by an ion-selective electrode using the methods described in Chapter 3. All solutions for the atomic

absorption analyses were prepared in 0.1M hydrochloric acid. Separate blanks were run for the two configurations of fractionation filters and for the backup filter. Further details relevant to the chemical analysis are provided in Chapter 7.

### 6.3 RESULTS

The electrodes used in this study are listed in the previous chapter (Table 5.1). Fig. 6.1 shows the effect of arc voltage on fume generation rates of electrode E11 for AC, DCEP and DCEN welding. The data were reproducible to within  $\pm 5\%$ .

Bulk densities, mass mean aerodynamic diameters (MMAD) and surface areas of the welding fume from the electrodes are presented in Table 6.1. (See Chapter 5, Table 5.2, for electrode operating conditions). Bulk densities varied by  $\leq 0.03 \text{ gcm}^{-3}$  for the duplicate measurements. The reproducibility of MMAD determinations was 20% for fume from the DCEP welding of electrode E12 (relative standard deviation of 6 determinations) and 10% for fume from the AC welding of electrode E11 (average deviation of 3 measurements from the mean). The diameters of the PSL spheres collected on the four impactor stages showed no gross variations in their size distribution from the 50% effective cutoff diameters stated by the manufacturer. Some of the deviations observed may be due to the discontinuous size distribution of the particles, imperfect aerosol generation, particle agglomeration and particle

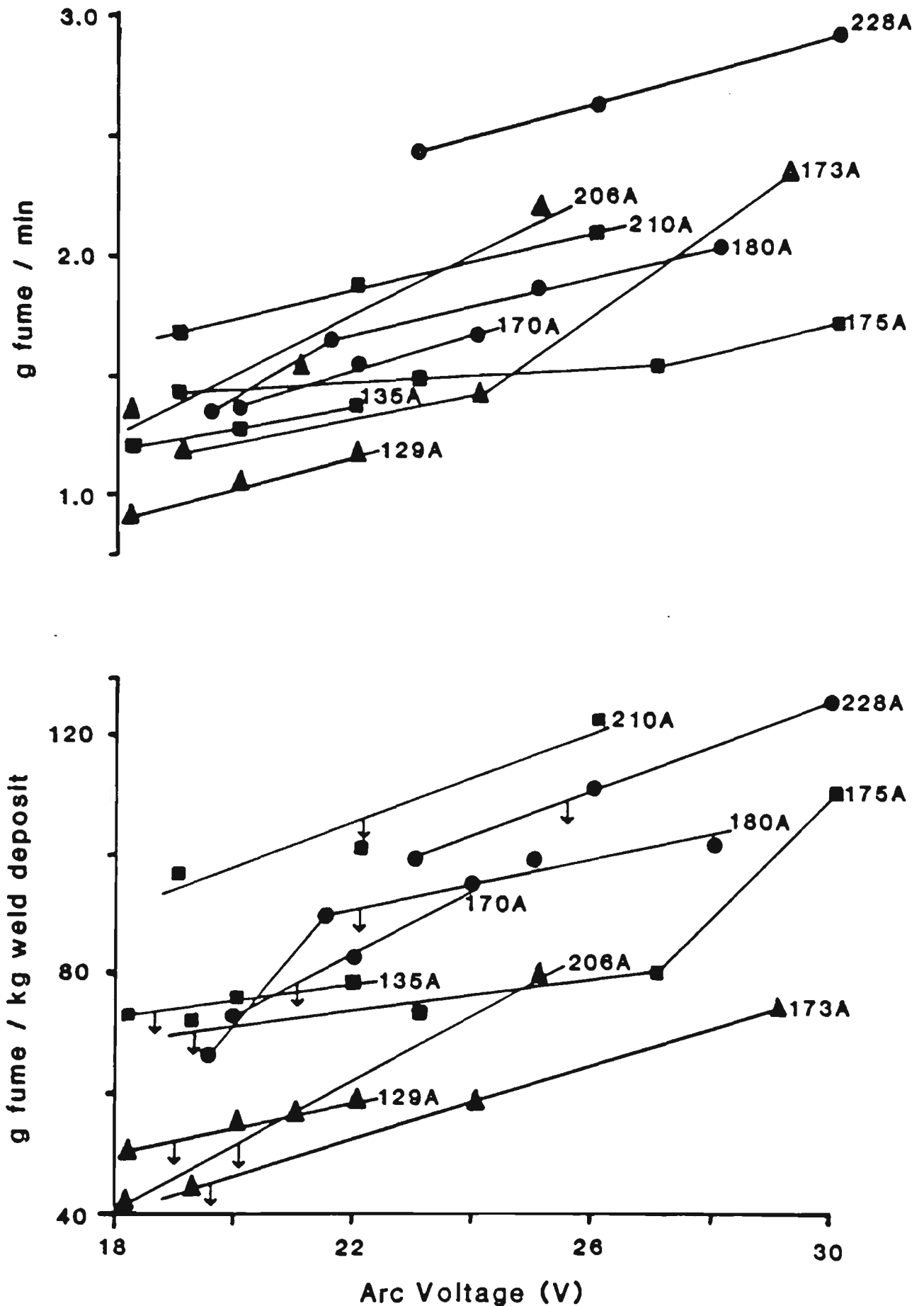


**Fig. 6.1** Effect of arc voltage on fume generation rates for high-manganese hardfacing E11 electrodes under conditions of AC (●), DCEP (■) and DCEN (▲). The current values (AC: 170A, 180A, 228A; DCEP: 135A, 175A, 210A; and DCEN: 129A, 173A, 206A) are within the ranges recommended by the manufacturer. The recommended voltage for each current is indicated on the bottom figure by an arrow (↓).

fragmentation. The method allowed only a general check on instrument performance and was not suitable for precise calibration.

The accuracy of the surface area measurements was estimated to be about 10% with the one-point method. The method is a variation of the classical BET technique and relies on working in an area of the adsorption isotherm where the BET equation exhibits a linear form. The three-point determination (full BET adsorption isotherm) for fume from AC welding of electrode E12 gave a surface area of  $13 \text{ m}^2\text{g}^{-1}$  (Table 6.1). The three points on the isotherm individually gave figures of  $13.5 \text{ m}^2\text{g}^{-1}$ ,  $13.6 \text{ m}^2\text{g}^{-1}$  and  $13.8 \text{ m}^2\text{g}^{-1}$  (the intercept in the BET plot (106,107) is assumed to be zero in the one-point method).

Fig. 6.2 shows the particle-size distribution of fume from AC welding of electrode E11. The mass mean aerodynamic diameter (MMAD) is read from this figure by noting the aerodynamic diameter corresponding to 50% cumulative mass. The plot is typical of the fumes tested. Assuming log-normal behaviour, the particle-size geometric standard deviation  $\sigma_g = (84.13\% \text{ diameter}) / (50\% \text{ diameter})$ , is  $3.8 \mu\text{m}$ . For the other fume samples,  $\sigma_g$  lay between 3.2 and  $5.0 \mu\text{m}$ . In Fig. 6.3 are shown typical electron micrographs illustrating the size, shape, surface texture and agglomeration of fume particles from the AC welding of electrode E11. Particles from other fume samples showed similar structures.

Table 6.1 Bulk densities, mass mean aerodynamic diameters and BET surface areas of welding fume particles.

Electrode code	Operation <sup>(a)</sup>	Bulk density (gcm <sup>-3</sup> )	Mass mean aerodynamic diameter <sup>(b)</sup> (μm)	Surface area (m <sup>2</sup> g <sup>-1</sup> )
E01	AC	3.8	0.8	27
	DCEP	3.6	0.9	28
E04	AC	3.3	0.7	22
	DCEP	3.0	0.7	25
E05	DCEP	3.4	0.8	25
E11	AC	3.6	0.8	19
	DCEP	4.4	0.6	17
	DCEN	4.3	0.8	17
E12	AC	3.5	0.7	13
	DCEP	3.6	0.5	13

(a) See Table 5.2 for voltage and current conditions used.

(b) For equivalent spheres of density 1gcm<sup>-3</sup>.

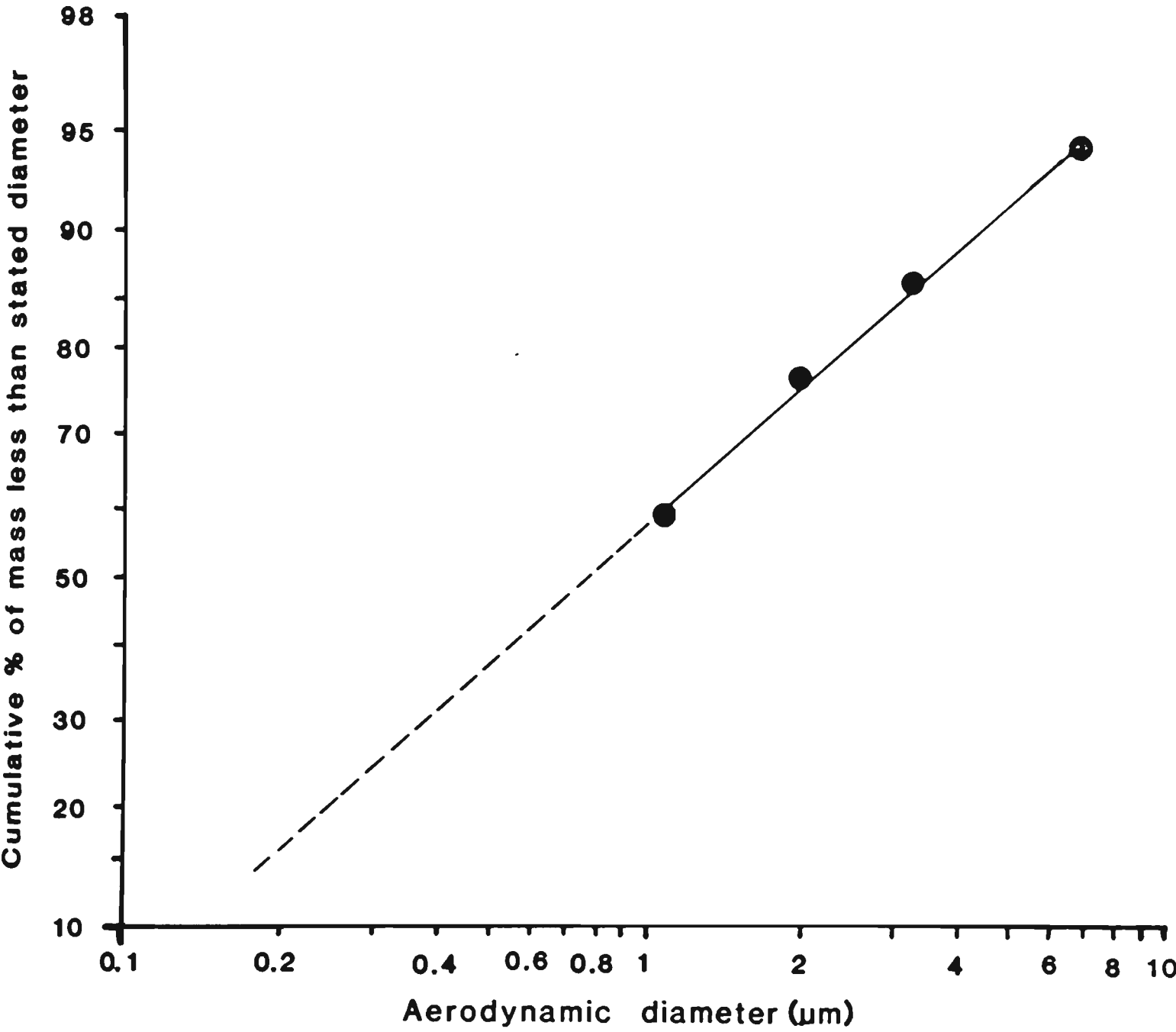
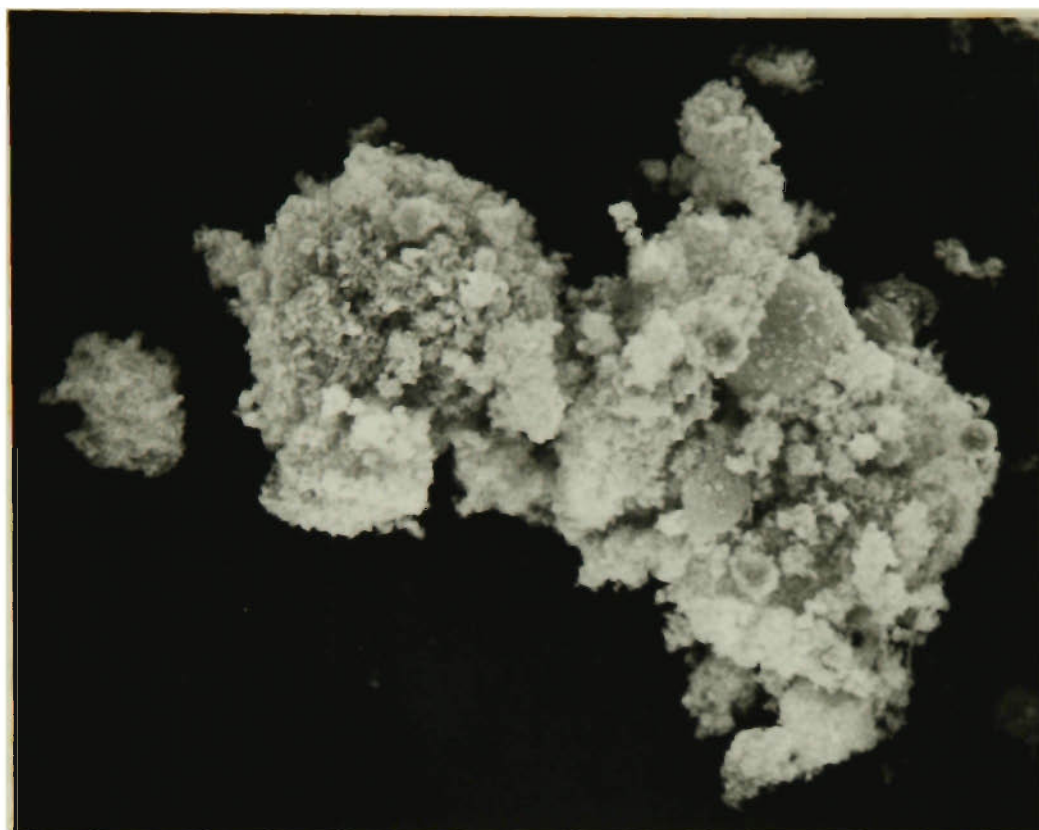


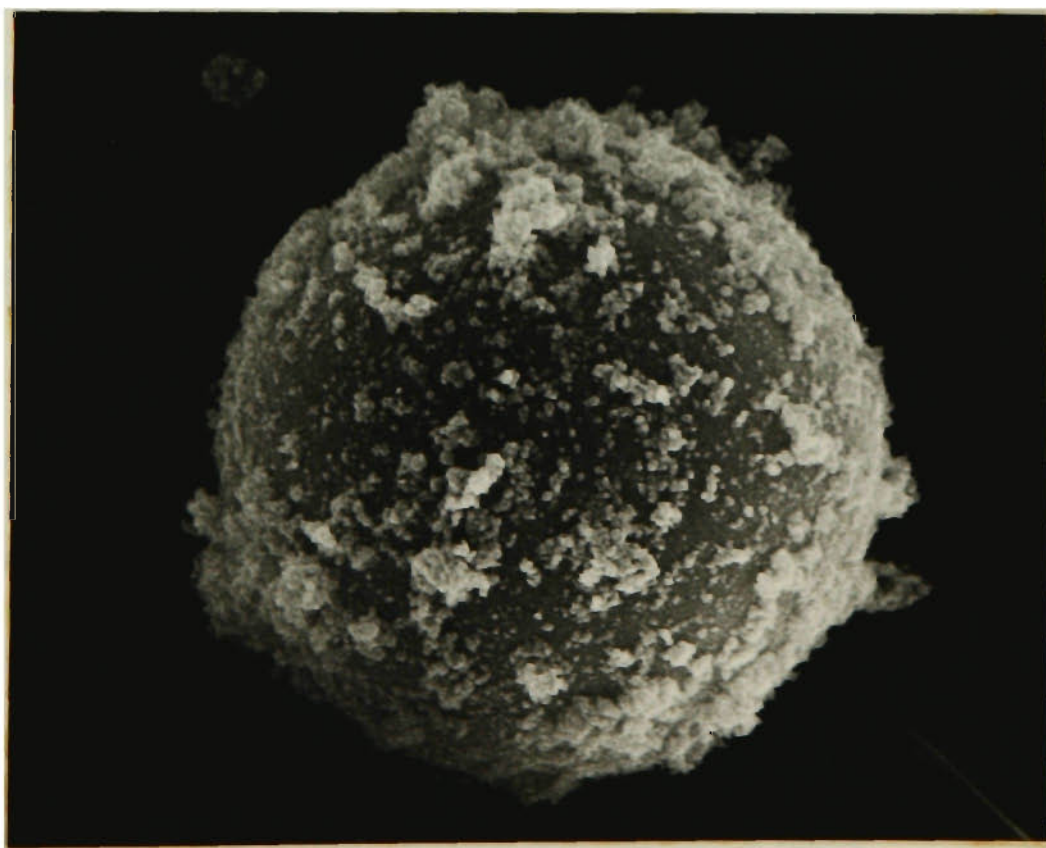
Fig. 6.2 Particle-size distribution of fume from AC welding of E11 electrodes determined by means of an Andersen 4-stage cascade impactor. Results are plotted using log-probability scales.

a)



10 μm

b)



1 μm

Fig. 6.3 Scanning electron micrographs of fume particles from AC welding of E11 electrodes : an aggregate (a) and a large spherical particle (b).

Table 6.2 gives the chemical composition of the different particle-size fume fractions obtained from the cascade impactor for AC welding of electrode E11 (25V, 200A). Duplicate chemical analyses of the fractionated fume varied by an average of 5% (maximum of 10%). An analysis of the total fume (unfractionated; duplicate determinations) is included in Table 6.2 for comparison.

#### 6.4 DISCUSSION

The constant-current measurements on the high-manganese hardfacing E11 electrodes were made to cover the wide range of conditions recommended by the manufacturer, and to thus obtain FGR data (i) at the minimum, the middle and the maximum of the recommended current range, and (ii) at low, optimum and high arc voltages, for each current value, where the optimum arc voltage is the voltage an operator would be expected to use. Fig. 6.1 shows that within the range of stable operation, FGRs for E11 electrodes may vary by a factor of three. There is an approximately linear relationship between FGR and arc voltage (V) at each current. The ratios of fume generation rates at the lowest and highest arc voltages range between 1.1 and 1.8 (average of 1.5). Since the data were obtained under conditions of constant current, a linear relationship between FGR and arc voltage also implies a linear relationship between FGR and arc power and between FGR and arc length.

**Table 6.2** Chemical analysis of fume fractions from the AC welding of  
high-manganese hardfacing MMAW electrodes<sup>(a)</sup> (E11; Table 5.1).

Element	% w/w of element in fume of stated size range <sup>(b)</sup> ( $\mu\text{m}$ )					% w/w in total fume	
	$\leq 1.1$	1.1–2.0	2.0–3.3	3.3–7.0	$\geq 7.0$	based on impactor fractions	based on total fume analysis
F	1.8	2.4	1.5	1.9	2.6	1.9	2.2
Na	2.8	3.6	3.8	2.4	3.4	3.0	3.5
Mg	0.2	0.3	0.3	0.2	0.3	0.2	0.2
K	0.2	0.1	0.2	0.1	0.2	0.2	0.1
Ca	0.5	0.8	0.7	0.6	0.8	0.6	0.5
Cr	0.06	0.05	0.08	0.04	0.1	0.06	0.05
Mn	34.6	32.6	29.2	32.4	28.4	33.0	31.0
Fe	24.8	25.8	27.5	28.1	25.6	25.5	27.3
Ni	1.4	1.2	1.6	1.1	2.0	1.4	2.0
Total <sup>(c)</sup>	66.4	66.9	64.9	66.8	63.4	65.9	66.9

- (a) The electrode contains 14.5% Mn in the weld deposit and 36.3% Mn in the flux.
- (b) Fraction of total mass collected in each impactor stage:  $\leq 1.1 \mu\text{m}$ , 60%; 1.1 – 2.0  $\mu\text{m}$ , 17%; 2.0 – 3.3  $\mu\text{m}$ , 10%; 3.3 – 7.0  $\mu\text{m}$ , 8%; and  $\geq 7.0 \mu\text{m}$ , 5%.
- (c) Concentrations of other flux elements (Si, 1.0% and Ti, 0.4%) were determined in the total fume by x-ray fluorescence; other elements (especially O) account for the remainder of the mass.

The densities of the welding fume particles (Table 6.1) are similar to a density value reported in the literature (2). In moist air (e.g., human respiratory tract), the hygroscopic fume particles would become larger and their density would decrease. Fume from the AC welding of electrode E11 has a density about 20% less than that from DC welding and this may be related to differences in the corresponding FGRs.

The cascade impactor measures the 50% effective cutoff aerodynamic diameter (ECD) for each fractionating stage. This is the particle diameter for which the collection efficiency is 50%, i.e., half of the particles with the ECD are captured and half escape to the next stage (112, 113). The ECDs quoted by the manufacturer (based on the theory of Ranz and Wong; Refs 109, 114) were found to be satisfactory in a field trial (115). Approximately 95% of the fume from the AC welding of electrode E11 is  $< 7.0 \mu\text{m}$  in equivalent aerodynamic diameter (Fig. 6.2) and is therefore respirable (109). The other fumes give respirable fractions ranging from 92 – 96%. The MMAD values range between 0.5 and 0.9  $\mu\text{m}$  (Table 6.1). The large  $\sigma$  g/MMAD values ( $3.8 / 0.8 = 4.8$  for E11 AC) indicate a high degree of polydispersity in the fumes tested (multimodal distribution not observed in the size range 1 – 7  $\mu\text{m}$ ). There ~~is~~<sup>are</sup> a great deal of data in the literature on the size of welding fume particles. Count median diameters (CMD) (116) of 0.1 – 0.15  $\mu\text{m}$  have been obtained for MMAW fumes using transmission electron microscopy (2, 78, 117–119). The CMD is not the same as the MMAD since the former does not take into

account the density of the particles.  $CMD \approx MMAD / \sqrt{\text{density}}$  (112,116). The MMAD values obtained (0.5 – 0.9  $\mu\text{m}$ ) are therefore equivalent to CMD values of approximately 0.25 – 0.5  $\mu\text{m}$ .

Surface areas of fume from the different electrodes range between  $13 \text{ m}^2\text{g}^{-1}$  and  $28 \text{ m}^2\text{g}^{-1}$  (Table 6.1). The results are consistent with the findings of Hewitt et al. (119), who measured the BET surface of fume from a MMAW electrode to be  $13 \text{ m}^2\text{g}^{-1}$ . The large amount of surface area per unit mass is a characteristic feature of fine welding fume particles and should be a consideration in work environments and pollution control systems. It must also be realised that BET surface areas are usually greater than calculated particle surface areas since the former includes the area of cracks, crevices and pores.

Under electron microscopic examination it was found that individual welding fume particles range in size from 0.1 to 10  $\mu\text{m}$  in diameter and that agglomeration is common. In Fig. 6.3a, it is not possible to say whether the agglomerated particles are held together by van der Waals forces, and magnetic forces (in the case of magnetite), or whether they have been fused together. Fig. 6.3b shows a large ( $\approx 10 \mu\text{m}$ ) spherical particle which presumably contracted to this shape when molten. Optical microscopy also showed that the larger fume particles were generally spherical. Particle morphology is an important consideration in assessing fume toxicity since irregular particles with sharp edges or fibres may be more irritating to the lung than regular and smooth spherical ones (74).

Fume fractions from the AC welding of electrode E11 obtained with the 4-stage cascade impactor do not show any significant variation in chemical composition with particle-size range (Table 6.2). The present result is different to that of Thomsen and Stern (67), who found that MMAW fume components from the core metal (principally metal oxides), concentrate in the smaller particle-size range and those from the slag/flux (principally silicates, titanates and chromates), concentrate in the larger particle-size range (core aerosol: MMAD =  $0.2\ \mu\text{m}$ ; slag aerosol: MMAD =  $2\ \mu\text{m}$ ). The difference may be explained by the composition of the electrodes (an electrode with a high-manganese flux was used here) and by the fact that silicon and titanium were not determined in the fume fractions in the present study.

## 6.5 SUMMARY AND CONCLUSIONS

- (i) Fume generation rates (FGRs) for a high-manganese hardfacing MMAW electrode vary by a factor of three over the wide range of current conditions for which a stable arc can be obtained and, at constant current, FGRs for the electrode vary with arc voltage by a factor of up to two.
- (ii) Fume from the AC welding of the high-manganese hardfacing electrode showed no significant variation in chemical composition with particle-size range in the size fractions  $\leq 1.1$ ,  $1.1 - 2.0$ ,  $2.0 - 3.3$ ,  $3.3 - 7.0$  and  $\geq 7.0\ \mu\text{m}$  equivalent aerodynamic diameter

( $\approx$  physical diameter  $\times \sqrt{\text{density}}$ ). The constant chemical composition of the different particle-size fractions of the fume was unexpected. A wider range of fumes need to be examined, however, before any generalisations are made.

- (iii) The physical properties of the fumes from the three MMAW hardfacing and two MMAW HSLA steel electrodes lie in the range: density =  $3.0 - 4.4 \text{ gcm}^{-3}$ ; mass mean aerodynamic diameter =  $0.5 - 0.9 \mu\text{m}$  (92-96% of fume  $< 7 \mu\text{m}$ ); and BET surface area =  $13 - 28 \text{ m}^2\text{g}^{-1}$ .
- (iv) The morphology of the fume particles indicates no obvious problems with regard to fume toxicity.

The respirable fractions (92-96% of total fume collected) do not represent the actual percentages of the total fume which would be deposited in a welder's lungs since fume particle-size will vary with physiological humidity and, in addition, efficiencies of respiratory deposition for different size ranges must be considered (5).

## CHAPTER 7

### CHEMICAL INVESTIGATION OF FUMES FROM THE HARDFACING AND HSLA STEEL ELECTRODES

## 7.1 INTRODUCTION

The toxic action of welding fumes, metal fumes and related metal salts on target organs is known to have a chemical basis (29, 120, 121). The toxicity or inertness of welding fume particulates may therefore be assessed by factors such as solubility, chemical composition (both surface and bulk), chromium oxidation state and crystallinity of constituents (67, 74). This chapter contains a rigorous and detailed chemical analysis of the flux, fume and water-soluble fume fractions from the hardfacing and high-strength low-alloy (HSLA) steel manual metal arc welding (MMAW) electrodes. As pointed out earlier, MMAW is one of the two most commonly practiced welding technologies, and hardfacing and HSLA steel electrodes are a major class of electrodes used in the welding industry.

## 7.2 MATERIALS AND METHODS

### Electrodes

The electrodes used in the study are listed in Table 5.1. The electrodes were stored in an oven at 100°C. Electrodes exposed to moisture were dried at 200°C for two hours prior to welding. The manufacturer specified DC electrode positive (DCEP) welding for E05; all the other electrodes were suitable for welding on either AC or DC.

### Chemicals

All chemicals (reagents, standards, etc.) used were of analytical grade or better. Triple glass-distilled water was used. The hydrochloric,

nitric and perchloric acids used were BDH, Aristar (ultrapure). Atomic absorption spectrophotometry (AAS) standards (1,000 mg/L stock solutions) were prepared from pure metals (99.9 – 99.999%) or from pure salts ( $\geq 99.9\%$ ) using standard methods (122). The working AAS standards were prepared freshly each day. The AAS standard for total chromium determination was made by dissolving 99.999% chromium metal in hydrochloric acid (1,000 mg/L  $\text{Cr}^{3+}$  stock solution). Both AAS and colorimetric standards for Cr(VI) determinations were made from a stock solution of 1,000 mg/L potassium dichromate. Sym-diphenylcarbazide ( $\underline{\text{s}}$  - DPC) reagent was prepared by dissolving 0.50g of the solid in a mixture of 100mL acetone and 100mL of distilled water. The solution was stored in an opaque bottle at 4°C (stable for up to a month).

### Fume sampling

Fume from the electrodes was generated using the automatic arc welder described in Chapter 3, and collected on glass fibre media. All the electrodes were AC welded bead-on-plate to 8mm mild steel at speeds around 15cm/min (E05 : DCEP). Operating conditions for the different electrodes are described in Table 5.2. The fume particles collected were carefully brushed from the glass-fibre substrates and dried at 100°C prior to analysis. Fume was generally analysed immediately after collection. Some fume samples (dried) were stored in sealed glass vials in a vacuum desiccator at 4°C for up to two weeks before analysis was commenced.

## Analysis

### Weld deposit

Each manufacturer provided data based on the analysis of a typical batch of electrodes. Weld metal deposit compositions are similar to the compositions of the electrode core metal except where there is a contribution from the metal present in the flux.

### Flux

Analysis of the flux (outer coating) of the electrodes was carried out by:

- (i) x-ray fluorescence ( $\text{Li}_2\text{B}_4\text{O}_7/\text{LiBO}_2$  fusion; Philips PW 1600; ZAF corrections program) and
- (ii) combustion (Leco EC 12) for total carbon.

### Fume

X-ray fluorescence (XRF) analysis was carried out as for flux.

X-ray diffraction (XRD) was carried out using Philips PW 1316/90 specimen/camera housing with PW 1050/70 goniometer ( $\text{Cu K}_\alpha$  radiation; graphite crystal monochromator;  $2\theta$  calibrated with silicon crystal).

The following analyses were also performed:

- (i) AAS: Duplicate 0.1g samples of fume from electrodes E01, E04, E05 and E11 were dissolved in 6M hydrochloric acid at 60°C (111). Fume samples from electrode E12 were dissolved by adding nitric, perchloric and hydrofluoric acids and evaporating to dense white fumes (123). These

techniques resulted in > 90% dissolution of the fume samples. Samples for total chromium analysis were also prepared by the alternative method of  $\text{KHSO}_4$  fusion followed by dissolution of the product in 3M sulphuric acid (124). All solutions (standards and unknowns) for the AAS analyses were made in 0.1M hydrochloric acid. AA measurements were made on an Instrumentation Laboratory Model 551 Instrument using flame atomisation with automatic background correction in the double beam mode. The air-acetylene flame was used for all elements except aluminium, calcium and chromium, for which nitrous oxide-acetylene was used. Standard measuring conditions (wavelength, hollow cathode lamp setting, slit width, etc.) were used (80). The wavelength corresponding to the highest sensitivity was chosen. Appropriate ionisation suppressants and releasing agents were added to both standards and unknowns for the analysis of sodium, magnesium, aluminium, potassium and calcium (122).

(ii) Cr(VI): Samples for total Cr(VI) determinations (0.1g; in duplicate) were prepared by extracting the fumes with sodium carbonate/sodium hydroxide (NIOSH solution) at  $\sim 90^\circ\text{C}$  and  $\text{pH} = 12.5$  (125). A diluted NIOSH solution (124) was used for the AAS analysis. Total Cr(VI) was also determined by colorimetry (85) using sym-diphenylcarbazide (Hitachi Model 101 spectrophotometer; 1cm cuvettes;  $\lambda = 546\text{nm}$ ). Because large concentrations of iron (III) interfere with the determination (125, 126), it was removed by extraction with 8-hydroxyquinoline at pH 4.

(iii) Ion-selective electrode (ISE): For total fluoride analyses, duplicate 0.1g samples of fume from electrodes E01, E04, E05 and E11 were dissolved in 6M hydrochloric acid and those from E12 by digestion in nitric/hydrochloric acid. An Orion Model 901 Ionanalyser and a Model 94-09 fluoride-selective electrode were used. Standards were prepared containing the same concentrations of aluminium and iron (III) as the unknowns. All fluoride concentrations were measured at pH  $\approx$  6 using the trishydroxymethylaminomethane method (127).

#### Water-soluble fume

Fume samples (in duplicate) were dissolved by stirring in water at 60°C for two hours (0.1g fume; 100mL water). For calcium determinations, 0.1g of the fume sample was dissolved in 1L water. Solubility determinations were made by recovering the insoluble portion of the fume by filtration through a 0.45  $\mu$ m nylon membrane filter, drying in a desiccator and weighing to constant weight.

Water-soluble fractions were analysed for:

- (i) metals by AAS as for fume;
- (ii) Cr(VI) using sym-diphenylcarbazide (colorimetry), and by AAS;
- (iii) fluoride using an ion-selective electrode as for fume; and
- (iv) chloride and fluoride by suppressor column ion-chromatography (Korth and Ellis (128) - 3.0 mM  $\text{Na}_2\text{CO}_3$  + 2.4 mM  $\text{NaHCO}_3$  eluent; peak height measurements).

A least-squares linear regression program (Apple II; Pascal) was used to determine the correlation between water-soluble chromium (VI) / total chromium in the fume and Na + K in the flux. All five types of electrodes were considered.

### 7.3 RESULTS

Spectrographic analysis of the mild steel base metal (workpiece) gave:

Fe - 98.02%; Mn - 1.46%; Si - 0.22%; C - 0.10%; Al - 0.05%; V - 0.05%; Cr - 0.02%; P - 0.02%; Nb - 0.02%; Ni - 0.015%; Cu - 0.01%; S - 0.005%; Mo - 0.003% and Sn - 0.002%. The major non-metallic constituents of the flux in the different electrodes were: E01 and E04 -  $\text{CaCO}_3$ ,  $\text{CaF}_2$ , silicates,  $\text{TiO}_2$ ; E05 -  $\text{CaCO}_3$ ,  $\text{CaF}_2$ ,  $\text{K}_2\text{SiO}_3$ ,  $\text{TiO}_2$ ; E11 -  $\text{CaCO}_3$ ,  $\text{CaF}_2$ , silicates,  $\text{TiO}_2$ , cellulose; and E12 -  $\text{CaCO}_3$ ,  $\text{CaF}_2$ , silica, silicates and cellulose. The crystalline compounds identified in the fume from the different electrodes were: E01 and E04 -  $\text{Fe}_3\text{O}_4$ ,  $\text{K}_2\text{CrO}_4$ ,  $\text{CaF}_2$ , NaF; E05 -  $\text{Fe}_3\text{O}_4$ ,  $\text{K}_2\text{CrO}_4$ ,  $\text{CaF}_2$ ; E11 -  $(\text{Fe}, \text{Mn})_3\text{O}_4$ ; and E12 -  $\text{Fe}_3\text{O}_4$ ,  $\text{CaF}_2$ .

The following d-spacing values (Å) were measured from the x-ray diffractograms which could be matched with known compounds in the JCPDS (Joint Committee on Powder Diffraction Standards) card system:

2.53, 2.97, 1.48 ( $\text{Fe}_3\text{O}_4$ ); 3.08, 2.99, 2.96 ( $\text{K}_2\text{CrO}_4$ ); 1.93, 3.15, 1.65

( $\text{CaF}_2$ ); and 2.32, 1.65, 2.68 ( $\text{NaF}$ ). Fume from electrode E11

(high-manganese hardfacing) gave XRD peaks at  $d$  (Å) = 2.56, 3.01, 1.52,

which we ascribed to a  $\text{Fe}_3\text{O}_4$  -  $\text{Mn}_3\text{O}_4$  solid solution (129). The

solubilities of the fumes in water (w/w) were found to be: E01 - 22.5%;

E04 - 28.0%; E05 - 37.5%; E11 - 3.0%; and E12 - 26.3%.

All the analytical data relating to the five types of electrodes are presented in Tables 7.1 - 7.5. Duplicate chemical analyses varied by an average of 2% (maximum of 10%). For total chromium, samples prepared by  $\text{KHSO}_4$  fusion gave similar results to those prepared by acid-digestion.

Table 7.6 shows the concentrations of chromium (III), water-insoluble chromium (VI) and water-soluble chromium (VI) in the fumes from the five types of electrodes. The concentrations of chromium in the weld deposit and in the flux, and of sodium and potassium in the flux, are also included in the table for comparison.

## 7.4 DISCUSSION

The crystalline compounds detected in the welding fumes by x-ray powder diffraction are similar to those identified in other studies (74, 130, 131). The results show magnetite ( $\text{Fe}_3\text{O}_4$ ) and calcium fluoride ( $\text{CaF}_2$ ) to be prominent in the crystal phases of four of the five fumes tested. No transition-metal fluorides were detected in any of the fumes.

**Table 7.1 Analytical data for electrode EO1**  
(medium-chromium hardfacing).

Element	Abundance (%w/w)			
	Weld deposit	Flux	Fume	Water-soluble fume
C	0.4 <sup>a</sup>	5.7 <sup>b</sup>	N.D.	•
F	•	8.4 <sup>c</sup>	8.9 <sup>c</sup> , 7.6 <sup>d</sup>	3.2 <sup>d</sup> , 2.8 <sup>e</sup>
Na	•	0.7 <sup>c</sup>	2.4 <sup>c</sup> , 2.8 <sup>f</sup>	1.2 <sup>f</sup>
Mg	•	0.5 <sup>c</sup>	0.4 <sup>c</sup> , 0.3 <sup>f</sup>	0.2 <sup>f</sup>
Al	•	0.6 <sup>c</sup>	0.4 <sup>c</sup> , 0.4 <sup>f</sup>	0.03 <sup>f</sup>
Si	•	5.3 <sup>c</sup>	2.5 <sup>c</sup>	•
P	•	0.03 <sup>c</sup>	0.03 <sup>c</sup>	•
S	•	0.04 <sup>c</sup>	0.08 <sup>c</sup>	•
Cl	•	0.2 <sup>c</sup>	0.4 <sup>c</sup>	0.4 <sup>e</sup>
K	•	1.5 <sup>c</sup>	7.8 <sup>c</sup> , 8.6 <sup>f</sup>	6.8 <sup>f</sup>
Ca	•	18.7 <sup>c</sup>	9.4 <sup>c</sup> , 9.9 <sup>f</sup>	1.5 <sup>f</sup>
Ti	•	1.9 <sup>c</sup>	0.2 <sup>c</sup>	•
V	0.5 <sup>a</sup>	n.d. <sup>c</sup>	n.d. <sup>c</sup>	•
Cr	7.0 <sup>a</sup>	15.9 <sup>c</sup>	2.5 <sup>c</sup> , 2.6 <sup>f</sup>	•
Cr(VI)	•	•	1.7 <sup>f</sup> , 1.9 <sup>g</sup>	1.5 <sup>f</sup> , 1.5 <sup>g</sup>
Mn	0.3 <sup>a</sup>	2.8 <sup>c</sup>	4.6 <sup>c</sup> , 3.6 <sup>f</sup>	0.003 <sup>f</sup>
Fe	91.3 <sup>h</sup>	8.8 <sup>c</sup>	32.1 <sup>c</sup> , 32.3 <sup>f</sup>	0.05 <sup>f</sup>
Ni	•	0.1 <sup>c</sup>	0.04 <sup>c</sup> , 0.03 <sup>f</sup>	n.d. <sup>f</sup>
Cu	•	N.D.	0.03 <sup>c</sup> , 0.03 <sup>f</sup>	n.d. <sup>f</sup>
Zn	•	< 0.01 <sup>c</sup>	0.04 <sup>c</sup>	N.D.
Zr	•	< 0.1 <sup>c</sup>	< 0.1 <sup>c</sup>	•
Mo	0.5 <sup>a</sup>	0.6 <sup>c</sup>	0.1 <sup>c</sup>	•
Total	100.0	71.8	71.8	14.7

Cont'd.....

Table 7.1 (continued)

- a Data provided by the manufacturer.
- b by combustion.
- c by x-ray fluorescence.
- d by ion-selective electrode.
- e by ion-chromatography.
- f by atomic absorption spectrophotometry.
- g by sym-diphenylcarbazide colorimetric method.
- h by difference.
- = category not applicable.
- N.D. = not determined.
- n.d. = not detected.

Table 7.2 Analytical data for electrode E04 (HSLA steel).

Element	Abundance (%w/w)			
	Weld deposit	Flux	Fume	Water-soluble fume
C	0.07 <sup>a</sup>	2.7 <sup>b</sup>	N.D.	•
F	•	8.1 <sup>c</sup>	14.4 <sup>c</sup> , 13.1 <sup>d</sup>	8.5 <sup>d</sup> , 9.9 <sup>e</sup>
Na	•	0.4 <sup>c</sup>	2.8 <sup>c</sup> , 3.5 <sup>f</sup>	1.5 <sup>f</sup>
Mg	•	0.2 <sup>c</sup>	0.1 <sup>c</sup> , 0.1 <sup>f</sup>	0.06 <sup>f</sup>
Al	•	0.5 <sup>c</sup>	0.5 <sup>c</sup> , 0.6 <sup>f</sup>	0.04 <sup>f</sup>
Si	0.04 <sup>a</sup>	4.7 <sup>c</sup>	2.8 <sup>c</sup>	•
P	•	0.01 <sup>c</sup>	0.02 <sup>c</sup>	•
S	•	0.03 <sup>c</sup>	0.1 <sup>c</sup>	•
Cl	•	0.1 <sup>c</sup>	0.2 <sup>c</sup>	0.2 <sup>e</sup>
K	•	1.2 <sup>c</sup>	13.7 <sup>c</sup> , 13.7 <sup>f</sup>	12.3 <sup>f</sup>
Ca	•	15.0 <sup>c</sup>	7.3 <sup>c</sup> , 9.1 <sup>f</sup>	1.2 <sup>f</sup>
Ti	•	2.5 <sup>c</sup>	0.4 <sup>c</sup>	•
Cr	•	0.07 <sup>c</sup>	0.03 <sup>c</sup> , 0.03 <sup>f</sup>	•
Cr(VI)	•	•	0.03 <sup>f</sup> , 0.03 <sup>g</sup>	0.02 <sup>f</sup> , 0.02 <sup>g</sup>
Mn	1.0 <sup>a</sup>	2.6 <sup>c</sup>	5.0 <sup>c</sup> , 4.4 <sup>f</sup>	0.006 <sup>f</sup>
Fe	97.0 <sup>h</sup>	29.7 <sup>c</sup>	19.8 <sup>c</sup> , 17.8 <sup>f</sup>	0.07 <sup>f</sup>
Ni	1.6 <sup>a</sup>	2.8 <sup>c</sup>	0.2 <sup>c</sup> , 0.1 <sup>f</sup>	n.d. <sup>f</sup>
Cu	•	N.D.	0.03 <sup>c</sup> , 0.06 <sup>f</sup>	n.d. <sup>f</sup>
Zn	•	< 0.01 <sup>c</sup>	0.03 <sup>c</sup>	N.D.
Zr	•	< 0.1 <sup>c</sup>	< 0.1 <sup>c</sup>	•
Mo	0.3 <sup>a</sup>	0.6 <sup>c</sup>	0.1 <sup>c</sup>	•
Total	100.0	71.2	66.9	24.6

a-h, •, N.D., n.d., See footnotes to Table 7.1.

Table 7.3 Analytical data for electrode E05 (HSLA steel).

Element	Abundance (%w/w)			
	Weld deposit	Flux	Fume	Water-soluble fume
C	0.045 <sup>a</sup>	3.1 <sup>b</sup>	N.D.	•
F	•	8.0 <sup>c</sup>	18.7 <sup>c</sup> , 18.5 <sup>d</sup>	8.2 <sup>d</sup> , 10.8 <sup>e</sup>
Na	•	0.4 <sup>c</sup>	1.9 <sup>c</sup> , 2.4 <sup>f</sup>	0.5 <sup>f</sup>
Mg	•	0.1 <sup>c</sup>	0.1 <sup>c</sup> , 0.1 <sup>f</sup>	0.06 <sup>f</sup>
Al	•	1.9 <sup>c</sup>	2.2 <sup>c</sup> , 2.1 <sup>f</sup>	0.05 <sup>f</sup>
Si	0.38 <sup>a</sup>	8.2 <sup>c</sup>	4.5 <sup>c</sup>	•
P	0.022 <sup>a</sup>	0.03 <sup>c</sup>	0.03 <sup>c</sup>	•
S	0.019 <sup>a</sup>	0.06 <sup>c</sup>	0.08 <sup>c</sup>	•
Cl	•	n.d. <sup>c</sup>	0.1 <sup>c</sup>	0.1 <sup>e</sup>
K	•	2.4 <sup>c</sup>	16.3 <sup>c</sup> , 17.3 <sup>f</sup>	15.1 <sup>f</sup>
Ca	•	19.1 <sup>c</sup>	9.5 <sup>c</sup> , 12.5 <sup>f</sup>	2.1 <sup>f</sup>
Ti	•	5.2 <sup>c</sup>	0.9 <sup>c</sup>	•
Cr	2.12 <sup>a</sup>	4.2 <sup>c</sup>	0.5 <sup>c</sup> , 0.7 <sup>f</sup>	•
Cr(VI)	•	•	0.6 <sup>f</sup> , 0.7 <sup>g</sup>	0.7 <sup>f</sup> , 0.6 <sup>g</sup>
Mn	0.72 <sup>a</sup>	2.2 <sup>c</sup>	3.9 <sup>c</sup> , 3.6 <sup>f</sup>	0.006 <sup>f</sup>
Fe	95.74 <sup>h</sup>	11.6 <sup>c</sup>	11.6 <sup>c</sup> , 11.5 <sup>f</sup>	0.04 <sup>f</sup>
Ni	•	0.02 <sup>c</sup>	0.02 <sup>c</sup> , 0.01 <sup>f</sup>	n.d. <sup>f</sup>
Cu	•	N.D.	0.03 <sup>c</sup> , 0.04 <sup>f</sup>	n.d. <sup>f</sup>
Zn	•	< 0.01 <sup>c</sup>	0.05 <sup>c</sup>	N.D.
Zr	•	< 0.1 <sup>c</sup>	< 0.1 <sup>c</sup>	•
Mo	0.95 <sup>a</sup>	1.9 <sup>c</sup>	0.1 <sup>c</sup>	•
Total	100.0	68.4	72.5	28.1

a - h, •, N.D., n.d., See footnotes to Table 7.1.

Table 7.4 Analytical data for electrode E11 (high-manganese hardfacing).

Element	Abundance (%w/w)			
	Weld deposit	Flux	Fume	Water-soluble fume
C	0.65 <sup>a</sup>	3.7 <sup>b</sup>	N.D.	•
F	•	0.2 <sup>c</sup>	1.5 <sup>c</sup> , 2.2 <sup>d</sup>	1.5 <sup>d</sup> , 0.8 <sup>e</sup>
Na	•	1.0 <sup>c</sup>	4.1 <sup>c</sup> , 3.5 <sup>f</sup>	0.9 <sup>f</sup>
Mg	•	1.5 <sup>c</sup>	0.4 <sup>c</sup> , 0.2 <sup>f</sup>	0.1 <sup>f</sup>
Al	•	0.05 <sup>c</sup>	0.1 <sup>c</sup> , 0.1 <sup>f</sup>	n.d. <sup>f</sup>
Si	0.14 <sup>a</sup>	3.0 <sup>c</sup>	1.1 <sup>c</sup>	•
P	≤ 0.05 <sup>a</sup>	0.03 <sup>c</sup>	0.03 <sup>c</sup>	•
S	0.01 <sup>a</sup>	0.08 <sup>c</sup>	0.08 <sup>c</sup>	•
Cl	•	n.d. <sup>c</sup>	0.1 <sup>c</sup>	0.1 <sup>e</sup>
K	•	0.08 <sup>c</sup>	0.3 <sup>c</sup> , 0.1 <sup>f</sup>	0.1 <sup>f</sup>
Ca	•	3.1 <sup>c</sup>	0.4 <sup>c</sup> , 0.5 <sup>f</sup>	0.15 <sup>f</sup>
Ti	•	5.7 <sup>c</sup>	0.4 <sup>c</sup>	•
Cr	•	0.2 <sup>c</sup>	0.05 <sup>c</sup> , 0.05 <sup>f</sup>	•
Cr(VI)	•	•	0.03 <sup>f</sup> , 0.03 <sup>g</sup>	0.03 <sup>f</sup> , 0.02 <sup>g</sup>
Mn	14.5 <sup>a</sup>	36.3 <sup>c</sup>	26.1 <sup>c</sup> , 31.0 <sup>f</sup>	0.05 <sup>f</sup>
Fe	80.75 <sup>h</sup>	7.2 <sup>c</sup>	28.1 <sup>c</sup> , 27.3 <sup>f</sup>	0.09 <sup>f</sup>
Ni	3.2 <sup>a</sup>	8.2 <sup>c</sup>	1.4 <sup>c</sup> , 2.0 <sup>f</sup>	n.d. <sup>f</sup>
Cu	•	N.D.	0.03 <sup>c</sup> , 0.07 <sup>f</sup>	n.d. <sup>f</sup>
Zn	•	< 0.01 <sup>c</sup>	0.02 <sup>c</sup>	N.D.
Zr	•	< 0.1 <sup>c</sup>	< 0.1 <sup>c</sup>	•
Mo	0.75 <sup>a</sup>	2.3 <sup>c</sup>	0.4 <sup>c</sup>	•
Total	100.0	72.6	67.0	2.7

a-h, •, N.D., n.d., See footnotes to Table 7.1.

Table 7.5 Analytical data for electrode E12 (high-chromium hardfacing).

Element	Abundance (%w/w)			
	Weld deposit	Flux	Fume	Water-soluble fume
C	4.5 <sup>a</sup>	17.1 <sup>b</sup>	N.D.	•
F	•	14.7 <sup>c</sup>	6.8 <sup>c</sup> , 5.2 <sup>d</sup>	2.7 <sup>d</sup> , 1.9 <sup>e</sup>
Na	•	< 0.01 <sup>c</sup>	1.9 <sup>c</sup> , 1.4 <sup>f</sup>	0.4 <sup>f</sup>
Mg	•	0.3 <sup>c</sup>	0.6 <sup>c</sup> , 0.3 <sup>f</sup>	0.2 <sup>f</sup>
Al	•	0.2 <sup>c</sup>	4.7 <sup>c</sup> , 4.1 <sup>f</sup>	0.01 <sup>f</sup>
Si	•	12.2 <sup>c</sup>	13.3 <sup>c</sup>	•
P	•	0.02 <sup>c</sup>	0.01 <sup>c</sup>	•
S	•	0.01 <sup>c</sup>	0.07 <sup>c</sup>	•
Cl	•	0.2 <sup>c</sup>	3.6 <sup>c</sup>	4.5 <sup>e</sup>
K	•	0.02 <sup>c</sup>	1.9 <sup>c</sup> , 2.4 <sup>f</sup>	2.2 <sup>f</sup>
Ca	•	19.5 <sup>c</sup>	14.5 <sup>c</sup> , 16.0 <sup>f</sup>	3.9 <sup>f</sup>
Ti	•	0.02 <sup>c</sup>	0.03 <sup>c</sup>	•
Cr	32.5 <sup>a</sup>	0.1 <sup>c</sup>	4.7 <sup>c</sup> , 5.5 <sup>f</sup>	•
Cr(VI)	•	•	1.7 <sup>f</sup> , 1.2 <sup>g</sup>	0.4 <sup>f</sup> , 0.5 <sup>g</sup>
Mn	3.3 <sup>a</sup>	0.3 <sup>c</sup>	6.5 <sup>c</sup> , 6.5 <sup>f</sup>	0.02 <sup>f</sup>
Fe	59.7 <sup>h</sup>	1.0 <sup>c</sup>	11.1 <sup>c</sup> , 13.2 <sup>f</sup>	0.03 <sup>f</sup>
Ni	•	0.1 <sup>c</sup>	0.04 <sup>c</sup> , 0.03 <sup>f</sup>	n.d. <sup>f</sup>
Cu	•	N.D.	0.03 <sup>c</sup> , 0.05 <sup>f</sup>	n.d. <sup>f</sup>
Zn	•	< 0.01 <sup>c</sup>	0.05 <sup>c</sup>	N.D.
Zr	•	< 0.1 <sup>c</sup>	< 0.1 <sup>c</sup>	•
Mo	•	< 0.01 <sup>c</sup>	< 0.01 <sup>c</sup>	•
Total	100.0	65.8	70.9	14.0

<sup>a-h</sup>, •, N.D., n.d., See footnotes to Table 7.1.

Table 7.6 Comparison of chromium (III) and chromium (VI)  
concentrations in the welding fume with chromium and  
alkali-metal concentrations in the flux and weld deposit.

Source	Species	% element (w/w)				
		E01*	E04	E05*	E11	E12*
Fume	total Cr	2.6	0.03	0.7	0.05	5.1
	Cr(III)	0.8	0.0	0.0	0.02	3.6
	wis <sup>a</sup> Cr(VI)	0.3	0.01	0.0	0.0	1.0
	ws <sup>b</sup> Cr(VI)	1.5	0.02	0.7	0.03	0.5
Weld deposit	Cr	7.0 <sup>c</sup>	≈0 <sup>d</sup>	2.12 <sup>c</sup>	≈0 <sup>d</sup>	32.5
Flux	Cr	15.9	0.07	4.2	0.2	0.1
	Na	0.7	0.4	0.4	1.0	< 0.01
	K	1.5	1.2	2.4	0.08	0.02

<sup>a</sup> wis = water-insoluble.

<sup>b</sup> ws = water-soluble.

<sup>c</sup> Mainly from flux, i.e., no Cr in the electrode core metal.

<sup>d</sup> Not determined by manufacturer, implying negligible concentration.

\* Fume E05 (HSLA steel electrode) is similar to fume from E316L-16 rutile-coated stainless steel electrodes (Chapter 4), i.e., all the chromium is water-soluble Cr(VI); fumes E01 and E12 (hardfacing electrodes) contain water-insoluble Cr(VI), and Cr(III), in addition to water-soluble Cr(VI).

Crystalline silica ( $\text{SiO}_2$ ) and/or metal silicates were also not observed in the x-ray diffractograms of any of the fumes, implying that silicon was present as amorphous silica or silicates. Although crystalline silica could potentially act as a tumour enhancing agent due to chronic irritative and tissue wounding effects, there is no evidence relating to any biological activity of amorphous silica (3). The presence of crystalline potassium chromate ( $\text{K}_2\text{CrO}_4$ ) in fume from electrode E04 (soluble Cr(VI) - 0.02%) and its absence in fume from electrode E12 (soluble Cr(VI) - 0.5%; K - 2%) is somewhat puzzling. It is possible that only amorphous Cr(VI) compounds were formed in the fume from electrode E12, which may be due to the unfavourable rates of evaporation and condensation for nucleation and crystalline formation (129).

The AAS and XRF techniques together provide analytical data for all elements except oxygen. Where elements were determined by both methods, the agreement was excellent (Tables 7.1 - 7.5). Volatilisation losses during fusion at  $1050^\circ\text{C}$  with  $\text{Li}_2\text{B}_4\text{O}_7$  /  $\text{LiBO}_2$  probably contribute to some of the lower Na, K and Ca concentrations measured by XRF. Ion-chromatography and ion-selective electrode methods for measuring water-soluble fluorides varied on an average by  $\pm 10\%$  (maximum variation  $\pm 30\%$ ). Ion-chromatography (132) has not been used before in welding fume analysis and is probably the more accurate technique. Ionic interferences with ion-selective electrodes are common

(127, 133) and may not have been completely eliminated by our matrix matching methods.

Mass balances (up to 85-95% of total) may be obtained for the flux, fume and water-soluble fume by including the mass of oxygen which would be associated with elements such as Si ( $\text{SiO}_2$ ,  $\text{SiO}_3^{2-}$ ),

Ti ( $\text{TiO}_2$ ,  $\text{TiO}_3^{2-}$ ), Cr ( $\text{Cr}_2\text{O}_3$ ,  $\text{CrO}_4^{2-}$ ), Al ( $\text{Al}_2\text{O}_3$ ,  $\text{Al}_2\text{O}_4^{2-}$ ),

Mn ( $\text{MnO}$ ,  $\text{MnO}_2$ ,  $\text{Mn}_2\text{O}_3$ ,  $\text{Mn}_3\text{O}_4$ ,  $\text{MnO}_4^{2-}$ ) and Fe ( $\text{Fe}_2\text{O}_3$ ,  $\text{Fe}_3\text{O}_4$ ,  $\text{FeO}_4^{2-}$ )

(74). The anions  $\text{OH}^-$ ,  $\text{CO}_3^{2-}$  and  $\text{SiO}_3^{2-}$  were not determined in the water-soluble fume fractions.

The enrichment of fume in flux elements (expressed as the ratio of their concentrations in fume and flux) generally follows the order:

$\text{K} > \text{Na} > \text{F} > \text{Si} > \text{Ca} > \text{Ti}$ . This is related to the volatility of the associated compounds and to the prevailing chemical-thermodynamics. The enormous enrichment of fume in Na, K and Cl for electrode E12 may be due to the formation of highly volatile compounds such as NaCl, NaF, KCl and KF.

Iron is the most abundant element in the fumes. Stokinger (134) has reviewed the literature on iron oxides and concluded that they are essentially non-carcinogenic and biologically inert. The relatively low iron content (11.5%) of the fume from electrode E05 (Table 7.3), correlates with the low fume generation rate (FGR) of the electrode. Similarly, the high iron content (28%) of the fume from electrode E11 (Table 7.4), correlates with the high FGR of the electrode. Both results may be

explained by considering the differences in electrode flux composition, and the volatilities of the flux constituents; for example, the low iron content of fume from electrode E05 may be due to the low volatility of iron oxides compared to that of fluorides (8% w/w F in flux and 18.5% w/w F in fume), at the relatively low arc temperatures associated with low FGRs.

The fluorine compounds present in welding fumes have been found to be physiologically active (135, 136). Basic electrodes (99) give rise to mainly NaF, KF and  $\text{CaF}_2$  in the fume (137) [all the electrodes used in the present study are basic electrodes, except E11 (high-manganese hardfacing), which is a neutral electrode (99)]. The transition-metal fluoro-complexes found in the water-soluble fume fractions from basic electrodes may lower the biological activity of fluoride (135). Our results show that the actual amount of fluoride formed in the fume is the same for the four types of basic electrodes, i.e., 2.2 - 2.4 g/kg electrode melted (See Chapter 5 for FGR data). This means that there is an inverse relationship between fluoride concentration and FGR. The result is not unexpected and may be explained by comparing the volatilities of NaF, KF and  $\text{CaF}_2$  (94) with those of other fume components: only the fluorides are highly volatile at the low arc temperatures concomitant with low FGRs. There is no significant correlation between the percentage of fluoride in the fume and the percentages of fluoride, sodium, potassium or calcium in the flux (Tables 7.1 - 7.5). It appears therefore that fluoride formation in

the fume does not result from specific high temperature reactions but mainly from the volatilisation/condensation process which occurs at a constant rate. The differences in concentrations of NaF, KF and  $\text{CaF}_2$  in the flux from the different electrodes are probably manifested in the slag compositions and/or in the concentrations of chromates, silicates, etc., in the fumes.

The chromium speciation results (Table 7.6) deserve special attention. Chromium (III) compounds are biologically inert (29) and  $\text{Cr}_2\text{O}_3$  has in fact been used in nutritional medicine (138). Chromium (VI) compounds can penetrate cell membranes more easily and oxidise biological material, thereby adversely affecting cellular function and causing toxic effects (29). The carcinogenic activities of chromium (VI) compounds are related to their solubilities in body fluids (3, 139). Relatively insoluble Cr(VI) compounds (e.g.,  $\text{CaCrO}_4$ ,  $\text{ZnCrO}_4$ ,  $\text{PbCrO}_4$ ) have been clearly shown to be carcinogenic in laboratory animals (3). However, the carcinogenicity of highly soluble Cr(VI) compounds (e.g.,  $\text{Na}_2\text{CrO}_4$ ,  $\text{K}_2\text{CrO}_4$ ,  $\text{CrO}_3$ ) is not yet well established (3). Our results indicate that Cr(III), water-insoluble Cr(VI) and water-soluble Cr(VI) in the fume originate both from the electrode core and flux. Chromium in the core metal forms mainly Cr(III) compounds (e.g.,  $\text{Cr}_2\text{O}_3$ ,  $\text{FeCr}_2\text{O}_4$ ) (67). The most important finding from the results in Table 7.6 is that there is a high

correlation ( $r = 0.92$ ) between water-soluble Cr(VI) / total Cr in the fume and the Na + K in the flux. Kimura et al. (130) tested several types of flux-coated electrodes and have reported a similar finding with each type of electrode when varying amounts of Na and K silicates were added to the flux. Although the electrodes used in our study are of five different types, it seems that the sodium and potassium compounds in the flux have reactivities similar to each other. Reduction of the Na + K content of electrode fluxes may be a useful means of reducing the proportion of Cr(VI) in welding fumes (130).

## 7.5 SUMMARY AND CONCLUSIONS

There is an inverse relationship between the fluoride concentrations in the fumes and the FGRs. The water-soluble chromium (VI) / total chromium in the fume is highly correlated with the percentage of Na + K in the flux ( $r = 0.92$ ).  $\text{Fe}_3\text{O}_4$ ,  $\text{K}_2\text{CrO}_4$ ,  $\text{CaF}_2$  and NaF were the only crystalline compounds detected in the fumes by qualitative x-ray diffraction. Mass balances (> 90% of total) were obtained for the flux, fume and water-soluble fume fractions. Excellent agreement was found between x-ray fluorescence and atomic absorption methods. The results from the various quantitative analyses were reproducible to within  $\pm 5\%$ .

The results obtained in the current investigation (especially Cr(VI)) may be used to calculate ventilation requirements in welding

workshop environments by applying the relevant threshold limit value (TLV) indices (2, 79) and the fume generation rate (FGR) data given in Chapter 5. The present results relate to fumes produced and collected under controlled conditions at the recommended optimum welding current and voltage. It should be recognised that fume composition may vary with arc voltage (55) and to a lesser extent with AC and DC welding (79).

The data presented in this chapter may provide guidance to industrial hygienists and occupational health physicians in appraising specific situations related to fume exposure, fume toxicity and health status of welders. These data make up the first rigorous chemical analysis of flux, fume and water-soluble fume, using both major and supplementary methods. Attention has been paid to the fact that nearly all methods of chromium analyses are subject to uncertainties, due to volatilisation losses, and oxidation-reduction reactions (67, 68, 124).

## CHAPTER 8

### MUTAGENICITY OF METAL IONS IN BACTERIA

## 8.1 INTRODUCTION

Organic chemical carcinogens, with the exception of hormone analogs, organohalides and known tumour promoters, have been shown to be readily detected as mutagens in bacterial test systems, particularly the Salmonella/mammalian microsome assay (35, 140, 141). However, the Salmonella assay has as yet shown little promise in detecting inorganic compounds, even of those known to be carcinogenic in laboratory animals or humans (36, 142, 143).

The difficulties encountered in assays of metals have been described by Rossman (142). In particular, metal ions such as  $\text{Ni}^{2+}$ ,  $\text{Co}^{2+}$ ,  $\text{Cd}^{2+}$ ,  $\text{Zn}^{2+}$ ,  $\text{Mg}^{2+}$  and  $\text{Mn}^{2+}$  may be precipitated as their insoluble phosphates by orthophosphate ions ( $\text{PO}_4^{3-}$ ) in the normal bacteriological culture medium and may not be detected as mutagens for this reason. Not surprisingly, chromate ( $\text{CrO}_4^{2-}$ ), the only metal ion consistently mutagenic in microbial assays, is anionic and therefore not precipitated by orthophosphate ions. For the detection of mutagenicity, it is important to maintain metal ions in solution in a labile form, preferably as biological complexes, and accessible to the target cells.

A modified culture medium, for both the Salmonella assay and for fluctuation tests with Salmonella and E. coli, utilising trimetaphosphate ions ( $\text{P}_3\text{O}_9^{3-}$ ) as the sole phosphorus source in place of orthophosphate, is described in this chapter. The trimetaphosphate complexes of all the

metal ions tested are soluble in the modified test media. The results obtained using modified and standard media are compared.

【The Ames test (42) involves the treatment of *Salmonellae* bacteria on Petri plates with the substance in question, and enumeration of mutant colonies which develop either spontaneously (background) or are induced by the action of a mutagenic substance. Strains of *Salmonellae* used in this test are selected for their sensitivity to various types of damage to their genetic material, deoxyribosenucleic acid (DNA). These strains of *Salmonellae* are more permeable to chemicals, and have increased tendencies to spontaneously mutate. All of the Ames tester organisms are auxotrophic mutants, that is, require histidine (an essential amino acid) to grow. Under the influence of mutagenic substances these undergo back-mutations into prototrophs, which no longer require histidine. Culture on a selective medium, lacking histidine, allows detection of back-mutants (revertants).

The fluctuation test, as used here, also detects reversion of auxotrophs. The test is applied to

screening chemicals that are toxic, or that have weak or undetectable activity when tested by the usual Ames plate-incorporation assay (36, 44). The test involves treating auxotrophs with the chemical, diluting the treated cells to low concentration, and then distributing in 100 tubes containing medium with limiting amounts of required nutrients. After incubation for 3-4 days the number of tubes with fully grown cell populations is counted. One reason very weak mutagens can be detected by this procedure may be that spontaneous and mutagen-induced mutation rates are determined from populations of cells equal in number (36).

The addition of an exogenous metabolic system (36) was not considered important in the testing of metal salts. Furthermore, chromium (VI) may be deactivated to chromium (III) in such systems (36). ]

## 8.2 MATERIALS AND METHODS

### Chemicals

Inorganic compounds used in this study are listed by name, source (M. & B. = May and Baker; B.D.H. = British Drug Houses), purity (%), chemical

formula and Chemical Abstracts Service (CAS) Registry Number as follows:

Ammonium molybdate, Ajax, Univar (81%),  $(\text{NH}_4)_6\text{Mo}_7\text{O}_{24} \cdot 6\text{H}_2\text{O}$ ,

[11098 - 84 - 3];

Ammonium metavanadate, M. & B. (99%),  $\text{NH}_4\text{VO}_3$ ,

[11115 - 67 - 6];

Beryllium nitrate, B.D.H., L.R.,  $\text{Be}(\text{NO}_3)_2$ ,

[13597 - 99 - 4];

Beryllium sulphate, B.D.H., L.R. (98%),  $\text{BeSO}_4 \cdot 4\text{H}_2\text{O}$ ,

[13510 - 48 - 0];

Cadmium chloride, M. & B. (98%),  $\text{CdCl}_2 \cdot 2.5\text{H}_2\text{O}$ ,

[7790 - 78 - 5];

Cadmium nitrate, B.D.H., L.R.,  $\text{Cd}(\text{NO}_3)_2 \cdot 4\text{H}_2\text{O}$ ,

[10022 - 68 - 1];

Chromium sulphate, B.D.H., A.R.,  $\text{Cr}_2(\text{SO}_4)_3 \cdot 8\text{H}_2\text{O}$ ,

[13520 - 66 - 6];

Cobalt chloride, B.D.H., A.R. (97.5%),  $\text{CoCl}_2 \cdot 6\text{H}_2\text{O}$ ,

[13815 - 10 - 6];

Copper (II) chloride, M. & B. (98%),  $\text{CuCl}_2 \cdot 2\text{H}_2\text{O}$ ,

[10125 - 13 - 0];

Lead nitrate, Ajax, Univar (99%),  $\text{Pb}(\text{NO}_3)_2$ ,

[10099 - 74 - 8];

Manganese chloride, B.D.H., A.R. (99.8%),  $\text{MnCl}_2 \cdot 4\text{H}_2\text{O}$ ,

[13446 - 34 - 9];

Mercury (II) chloride, B.D.H., A.R.,  $\text{HgCl}_2$ ,

[7487 - 94 - 7];

Nickel chloride, M. & B.,  $\text{NiCl}_2 \cdot 6\text{H}_2\text{O}$ ,

[7791 - 20 - 0];

Nickel sulphate, Ajax, Univar,  $\text{NiSO}_4 \cdot 6\text{H}_2\text{O}$ ,

[10101 - 97 - 0];

Osmium chloride, Aldrich,  $\text{OsCl}_3$ ,

[13444 - 93 - 4];

Potassium antimonate, B.D.H., A.R. (94%),  $\text{KSb}(\text{OH})_6$ ,

[12208 - 13 - 8];

Potassium chromate, M. & B. (99%),  $\text{K}_2\text{CrO}_4$ ,

[11073 - 34 - 0];

Potassium permanganate, Ajax, Univar (99.5%),  $\text{KMnO}_4$ ,

[7722 - 64 - 7];

Disodium hydrogen arsenate, Ajax, Univar (98.5%),  $\text{Na}_2\text{HAsO}_4 \cdot 7\text{H}_2\text{O}$ ,

[10048 - 95 - 0];

Sodium fluoride, Merck, A.R. (99%), NaF,

[7681 - 49 - 4];

Sodium metaarsenite, Sigma, NaAsO<sub>2</sub>,

[7784 - 46 - 5];

Sodium metabismuthate, B.D.H., A.R., NaBiO<sub>3</sub>,

[12232 - 99 - 4];

Sodium selenate, Sigma, Na<sub>2</sub>SeO<sub>4</sub>,

[13410 - 01 - 0];

Sodium selenite, B.D.H., L.R. (99%), Na<sub>2</sub>SeO<sub>3</sub>,

[10102 - 18 - 8].

Purities, where given, are the minimum assay for those samples (Univar reagents comply with specifications of the Committee on Analytical Reagents of the American Chemical Society; A.R. reagents comply with Analar Standards for Laboratory Chemicals; L.R. reagents are high purity raw materials). Chromium sulphate and cadmium nitrate supplied by B.D.H. were both recrystallised twice, using triple-distilled water. Early mutagenicity assays were conducted with beryllium nitrate, but this was later replaced by beryllium sulphate because of concern about the questionable purity of the former. Nickel sulphate was included in the study as well as nickel chloride, because of the unknown purity of the latter.

Stock solutions of chemicals were prepared at 0.1 or 0.01M concentrations in double glass-distilled water, sterilised by membrane filtration and held in sealed glass bottles at room temperature. Aliquots of these stock solutions were used for mutagenicity assays at nontoxic concentrations, determined by preliminary toxicity assays with *Salmonella* TA100, separately conducted for plate-incorporation and fluctuation assays. At the time of assay, serial half-log dilutions of each test chemical were prepared in distilled water.

### Bacterial strains

*Salmonella* strains TA98, TA100, TA1535, TA1537 and TA1538 were obtained from Professor B.N. Ames and all procedures followed published methods (42). The *E. coli* strain (DG1153) employed only in fluctuation tests was obtained from Dr D.G. MacPhee (La Trobe University). This strain requires tryptophan, is sensitive to uv light (*uvrA*) and is resistant to ampicillin (due to the presence of the R plasmid, pKm 101).

### Plate-incorporation assay

For the normal or "standard" assay, plastic Petri plates (100 x 15 mm style, Medical Plastics) were filled with 25 mL of autoclave-sterilised minimal glucose agar medium, consisting of 1.5% Difco-Bacto agar in Vogel-Bonner Medium E ( $\text{MgSO}_4 \cdot 7\text{H}_2\text{O}$ , 0.2 g/L;  $\text{K}_2\text{HPO}_4$ , 10 g/L;  $\text{NaNH}_4\text{HPO}_4$ , 3.5 g/L; citric acid monohydrate, 2 g/L) with 2% D-glucose. Various modifications of this medium were developed

for use in metal mutagenicity assays. However, the modified media chosen for comparison with the standard procedure were based on the Vogel-Bonner medium, with orthophosphate ions replaced by trimetaphosphate ions. A similar buffering capacity to that of the normal medium was provided, as well as equivalent ionic strength. This modified medium contained  $\text{MgSO}_4 \cdot 7\text{H}_2\text{O}$ , 0.2 g/L; KCl, 8.5 g/L; NaCl, 1.0 g/L;  $\text{NH}_4\text{Cl}$ , 1.0 g/L;  $\text{Na}_3\text{P}_3\text{O}_9$ , 1.0 g/L; tris (hydroxymethyl) aminomethane, 9 g/L; citric acid monohydrate, 2 g/L; and D-glucose 20 g/L. The pH of this medium was adjusted to either 7.2 or 7.8 before pouring into plates. All plates were stored at 4°C and warmed to room temperature before use.

Top agar, consisting of 6 g/L Difco-Bacto agar and 5 g/L NaCl was prepared by adding 100 mL/L of a sterile stock solution containing 0.01 g L-histidine and 0.012 g biotin, and was dispensed in 2 mL amounts into sterile plastic tubes at 45°C immediately prior to each assay.

Into each 2 mL of top agar was added 100  $\mu\text{L}$  of the appropriate *Salmonella* strain from an overnight broth culture, followed by 100  $\mu\text{L}$  of test chemical, prepared in serial half-log working dilutions. The top agar was mixed and poured over the surface of a minimal agar plate. After the agar had set, plates were inverted and incubated at 37°C for 3-5 days. Unless stated otherwise, assay results are those from plates incubated for 3 days. Colony numbers were determined manually and plates were examined microscopically for evidence of lawn toxicity and for colony

appearance. Each assay was repeated at least once. Criteria of positive plate assays are those given elsewhere (42, 144) and include a reproducible, dose-related increase in revertant colonies, with at least a doubling of colony numbers on test plates compared with background control values.

### Fluctuation assay

The microtitre fluctuation test was performed according to the method of Gatehouse (145). In the normal or "standard" assay, Davis-Mingioli Medium (DMM) containing  $K_2HPO_4$ , 3.5 g/L;  $KH_2PO_4$ , 1.0 g/L;  $(NH_4)_2SO_4$ , 1.0 g/L; trisodium citrate dihydrate, 0.2 g/L;  $MgSO_4 \cdot 7H_2O$ , 0.1 g/L; and D-glucose, 8 g/L was supplemented with 0.3  $\mu$ g/mL biotin and 0.2  $\mu$ g/mL L-histidine for assays with *Salmonella typhimurium*, and with 0.125  $\mu$ g/mL L-tryptophan for *E. coli* assays. A modified medium was also developed for use in fluctuation assays and contained  $(NH_4)_2SO_4$ , 1.0 g/L; trisodium citrate dihydrate, 0.2 g/L;  $MgSO_4 \cdot 7H_2O$ , 0.1 g/L;  $Na_3P_3O_9$ , 1.0 g/L; tris (hydroxymethyl) aminomethane, 9 g/L; and D-glucose, 8 g/L with pH adjusted to 7.2 before use.

Test chemical dilutions were added to 20 mL amounts of complete DMM or modified medium, to give the required final dilution. Then 1 mL of a 1/10 dilution of 3- to 4- h broth cultures of bacteria was added in each 20 mL test or control bottle, which was mixed and dispensed in 0.2 mL amounts into the 96 wells of Linbro/Titertek trays (Flow Laboratories).

Trays with lids were tightly wrapped in plastic to minimise evaporation and incubated at 37°C for 3 days. To determine bacterial growth, 20 µL of bromothymol blue (600 µg/mL) was added to each well: negative wells appeared blue-green and positive wells appeared yellow. Where metals affected the colour of the indicator dye, wells were assessed for turbidity, based on absorbance measurements in a MicroELISA Auto Reader (Dynatech Model MR580) at 630 nm. The significance of fluctuation test results was determined using the  $\chi^2$  test (146).

### 8.3 RESULTS

#### Plate-incorporation assays

Only two ions, chromate and selenate were found to be mutagenic in Salmonella assays using standard media. Both were also detected using modified media (Fig. 8.1). Selenate ions were mutagenic to strain TA1535 (Fig. 8.1a) and appeared to be equally active in the modified medium at either pH 7.2 or pH 7.8, although the highest test concentration in modified media was toxic. Toxicity was not observed using standard assay techniques and, consequently, higher revertant colony numbers were found under standard conditions at higher selenate concentrations. Selenate ions were not mutagenic to strain TA100 in any assay. Chromate ions, on the other hand, were mutagenic to strains TA1537, TA98, and TA100 and the standard medium was the most sensitive for detecting their mutagenicity. Results obtained with TA100 are shown in Fig. 8.1b, with the modified

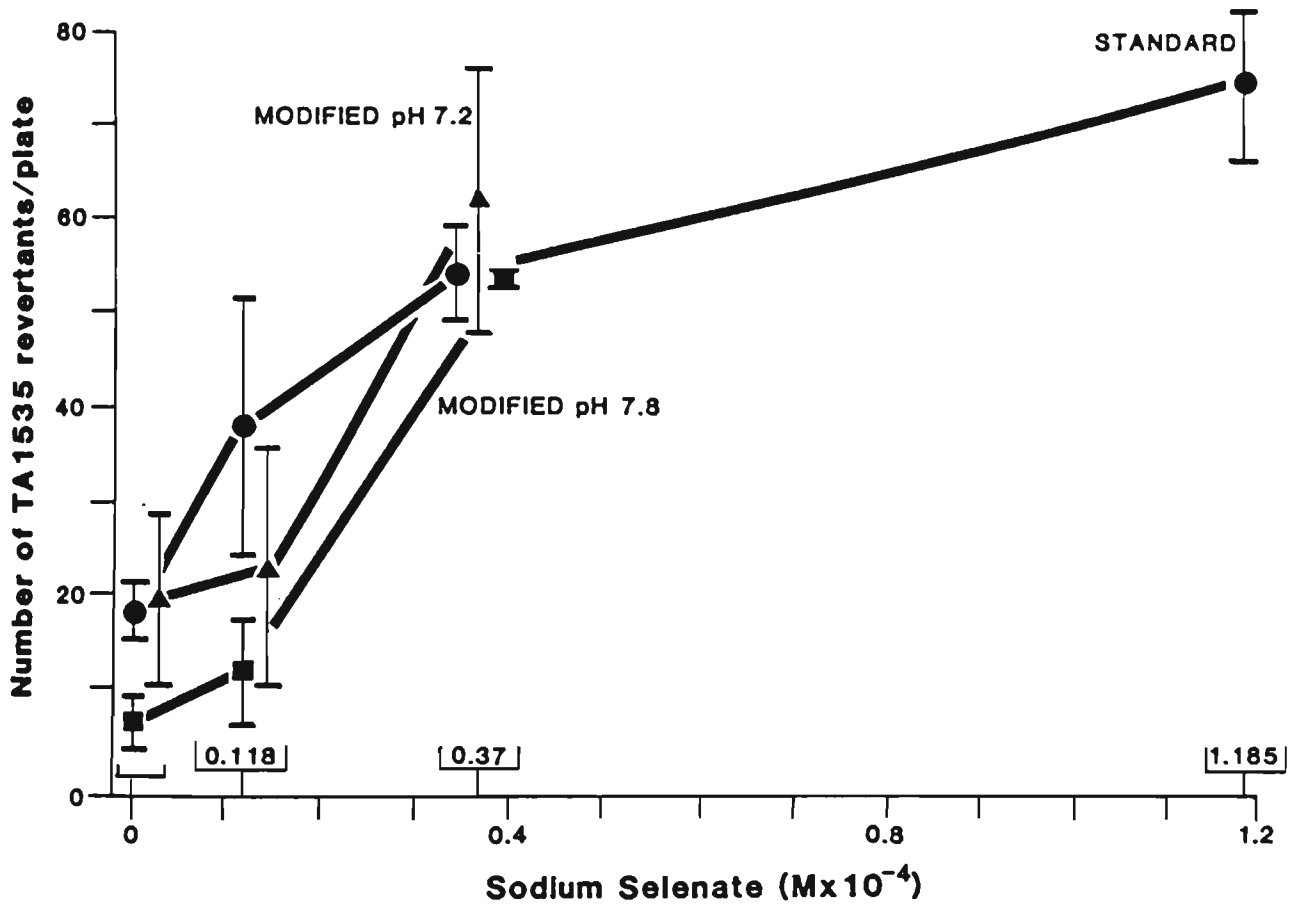


**Fig. 8.1a** Dose-response curve for plate-incorporation assays of sodium selenate with Salmonella TA1535. Points represent means of results from two experiments. Bars indicate standard error for an average of 4 plates per dose point.

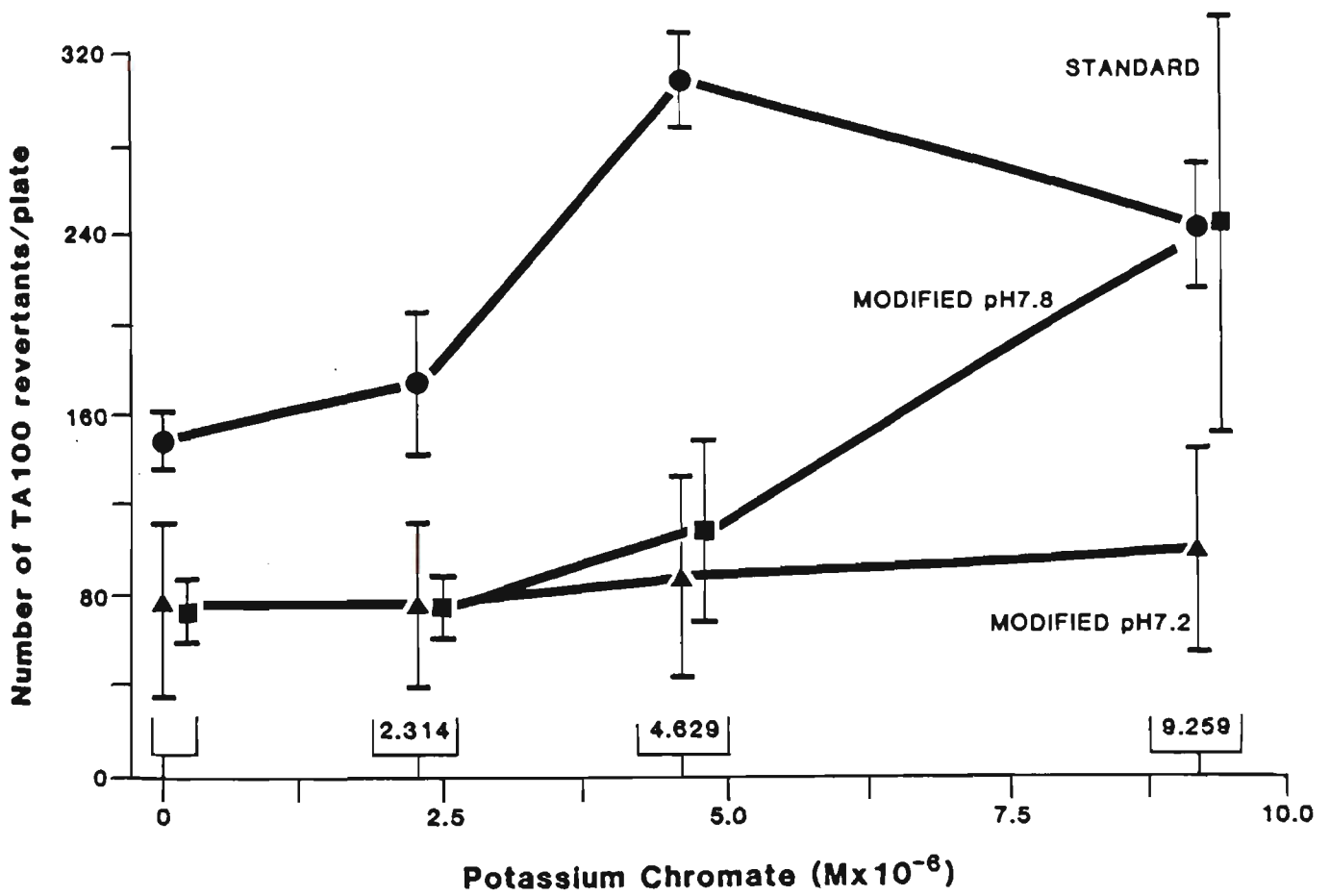


**Fig. 8.1b** Plate-incorporation assays of potassium chromate with *Salmonella* TA100. Other details as given in Fig. 8.1a.

pH 7.8 medium providing marginally higher revertant colony counts than pH 7.2 medium.

Of the remaining 22 metal salts tested, only ammonium metavanadate was found to be mutagenic in a plate-incorporation assay. Metavanadate ions were mutagenic only with strain TA1535 in modified medium at pH 7.8 when an approximate doubling of revertant colonies was observed at the highest subtoxic dose tested (Table 8.1). Although this result was reproducible, a clear dose-response was not demonstrated in all experiments.

Table 8.1 Mutagenicity of vanadate with Salmonella TA1535 in modified plate-incorporation assays at pH 7.8.

Ammonium vanadate concentration (Mx10 <sup>-7</sup> )	Revertant colonies per plate			
	Expt. 1	$\bar{x}_1$	Expt. 2	$\bar{x}_2$
3.7	47,90,120	85.6	83,88,114,118	100.8
1.17	41,57,68	55.3	50,52,61,68	57.8
0.37	56,57,59	57.3	40,43,46,53	45.5
0.12	32,50,68	50.0	42,43,43,45	43.2
0	39,45,47	43.7	39,44,46,46	43.8

Some compounds gave conflicting results in repeat assays, and were therefore not assessable in the present study. They included (i) potassium permanganate in modified pH 7.8 medium with TA1535; (ii) sodium metabismuthate in both standard and modified pH 7.2 media with TA1535; (iii) sodium metaarsenite in modified pH 7.8 medium with TA1535; and (iv) beryllium nitrate in modified pH 7.2 medium with TA98.

### Fluctuation assays

Four ions were found to be mutagenic in the fluctuation assays: chromate, metavanadate, beryllium (II) and cadmium (II). Only chromate ions were found to be mutagenic using both modified and standard media in the fluctuation assay (Table 8.2); the fluctuation and plate-incorporation assays had similar sensitivities for this mutagen.

Metavanadate ions were positive in two standard fluctuation assays with TA100 (Table 8.3) at concentrations far in excess of those able to be used in plate-incorporation assays for reasons of toxicity. These results support our positive findings for metavanadate in plate-incorporation assays using TA1535. Both TA100 and TA1535 contain the same point mutation (his G46) and are consequently both able to detect substances causing reverse mutations by base-pair substitution. Metavanadate ions were not mutagenic to any *Salmonella* strains other than TA100 in the fluctuation test (including TA1535), nor to any of the strains using modified media.

Table 8.2 Comparison of standard and modified (pH 7.2) fluctuation assays for detecting chromate mutagenicity.

Potassium chromate concentration (Mx10 <sup>-5</sup> )	standard <sup>(a)</sup> fluc. test		modified <sup>(a)</sup> fluc. test	
	TA100 <sup>(b)</sup>	E.C. <sup>(b)</sup>	TA100	E.C.
2.5	36 <sup>(c)</sup>	42 <sup>(c)</sup>	17 <sup>(c)</sup>	78 <sup>(c)</sup>
1.25	26	33 <sup>(c)</sup>	9	34 <sup>(c)</sup>
0.625	23	28	14	17
0	18	19	6	15

- (a) Number of wells positive, out of 96.
- (b) TA100 = Salmonella TA100.  
E.C. = Escherichia coli WP2.
- (c)  $\chi^2 > 3.84$ ;  $p < 0.05$ .

Selenate ions were negative in all fluctuation assays. Cadmium and beryllium ions were mutagenic in standard media with E. coli and Salmonella TA100 respectively, but negative to other Salmonella strains and negative with all fluctuation assays using modified media. The difference in sensitivity between the fluctuation and plate-incorporation techniques did not appear to be due to the toxicity of the species being tested. For instance, cadmium ions appeared to be equally toxic using both techniques and beryllium ions were conspicuously nontoxic up to the highest doses used in either technique. It should be noted that cadmium ions were positive in fluctuation assays with E. coli, but negative in a

separate plate-incorporation assay using E. coli.

Table 8.3 Standard fluctuation assays of vanadate, cadmium and beryllium salts.

Salt	Concentration (M)	Standard fluctuation test <sup>(a)</sup>	
		Expt. 1	Expt. 2
Ammonium metavanadate <sup>(b)</sup>	$1.6 \times 10^{-5}$	28	54 <sup>(d)</sup>
	$5.0 \times 10^{-6}$	53	54 <sup>(d)</sup>
	$1.6 \times 10^{-6}$	58 <sup>(d)</sup>	58 <sup>(d)</sup>
	0	44	35
Cadmium nitrate <sup>(c)</sup>	$1.6 \times 10^{-5}$	31	47
	$5.0 \times 10^{-6}$	33	53 <sup>(d)</sup>
	$1.6 \times 10^{-6}$	34 <sup>(d)</sup>	53 <sup>(d)</sup>
	0	21	37
Beryllium sulphate <sup>(b)</sup>	$5.0 \times 10^{-2}$	36 <sup>(d)</sup>	11
	$1.6 \times 10^{-3}$	32 <sup>(d)</sup>	21
	$5.0 \times 10^{-4}$	30 <sup>(d)</sup>	26 <sup>(d)</sup>
	0	15	18

(a) Number of wells positive, out of 96.

(b) With Salmonella TA100.

(c) With E. coli WP2.

(d)  $\chi^2 > 3.84$ ;  $p < 0.05$ .

Some compounds gave conflicting results in repeat fluctuation assays, and were therefore not assessable in the present study. They were: (i) potassium permanganate in modified fluctuation assay with TA100 and *E. coli*; (ii) cadmium chloride in modified fluctuation assays with *E. coli*; and (iii) potassium antimonate in standard fluctuation assays with TA100.

#### 8.4 DISCUSSION

The mutagenicity of hexavalent chromium and lack of mutagenicity of trivalent chromium in microbial assays has been well established in the literature. Various chromate salts have been shown to be active in *Salmonella* (147-151) or *E. coli* (147, 152) plate-incorporation assays, whereas trivalent chromium salts are negative (150-152). Our results further confirm the mutagenicity of chromate in bacterial systems.

Selenate ions have been shown to be mutagenic in other *Salmonella* plate-incorporation assays (149, 153). The report that selenite is weakly mutagenic in TA100 (153) is neither in agreement with other published results (149) nor with the present study.

This study provides reproducible evidence for bacterial mutagenicity of cadmium (II), beryllium (II), and metavanadate (V) ions. Cadmium ions were consistently positive in an *E. coli* fluctuation assay, despite having been found negative by previous workers using *Salmonella* (150) and *E. coli* (152) plate-incorporation assays. Few other microbial

studies and no plate-incorporation assays have been reported for beryllium (II) or vanadium (V) salts. Nor is there any information concerning osmium, bismuth or copper salts which we found nonmutagenic. As in the present study, assays of manganese (150), mercury (152), fluoride (154, 155), and nickel (146, 156) salts have all proven negative. Mutagenicity of lead chromate has been attributed to its chromate content (148). Arsenite and arsenate salts were found negative here as in previous *Salmonella* plate-incorporation assays (149) though arsenite has been reported to be both negative (157) and positive (158) in *E. coli* WP2 mutagenicity assays. Molybdate ions, which we found negative, have also given conflicting results in *E. coli* WP2 and WP2 *uvrA* plate-incorporation tests (152, 158).

Mutagenicity of certain compounds, including chromate, has been claimed to be enhanced by the *uvrA* deficiency in *E. coli* (158), though conflicting evidence has also been published (152). If true, it might have been expected that *E. coli uvrA* pKm 101 would readily respond to arsenite and molybdate ions in the present study. Although this was not so, the *E. coli* strain proved useful in detecting the mutagenicity of cadmium ions and in providing additional evidence of chromate mutagenicity.

The fact that modified culture media did not significantly improve detection of a range of mutagenic metals demonstrates that solubility problems in media containing high concentrations of orthophosphate are not a major factor in preventing detection of metal mutagens in

plate-incorporation assays. It was significant that the fluctuation assay proved valuable for detecting two metal ions, viz., cadmium and beryllium, which were not detected in any plate-incorporation assays. In particular, the demonstration that beryllium is only mutagenic with *Salmonella* TA100 in the fluctuation assay shows that plate-incorporation is inadequate in some other unidentified way, at least for detection of this element.

The mutagenicity of vanadate ions showed a complex dependence on bacterial strain, medium (standard vs modified), and/or assay type (plate-incorporation vs fluctuation assay). In the plate-incorporation assay, vanadate was mutagenic to TA1535 only using the modified medium; there was no effect with the standard medium. In the fluctuation assay, vanadate was mutagenic to TA100 (but not TA1535) with the standard medium only. The main difference between the two assays is the presence of agar in the plate-incorporation assay. However, the absence of a clear dose-response relationship in some positive tests on this system precludes any firm conclusions concerning possible interaction between vanadate and agar or vanadate and the phosphate species present in the respective media.

There are a number of compounds, known to be active in microbial DNA repair assays, which were not detected here. They include salts of cobalt (159), manganese (153, 160), antimony (159, 160), arsenic (158-161), mercury (159-161), molybdenum (158, 159), and osmium (159).

This suggests that some forms of DNA damage either do not play a significant role in the induction of point mutations or are not detected using current microbial gene mutation techniques (142).

## 8.5 SUMMARY AND CONCLUSIONS

The mutagenicity of 24 metal salts was investigated in plate-incorporation and fluctuation assays with *Salmonella* TA strains or *E. coli* WP2 *uvrA* pKm 101. Chromate (VI) and selenate (VI) ions were found to be mutagenic in plate-incorporation assays employing conventional media. On the other hand, cadmium (II), beryllium (II), chromate (VI), and metavanadate (V) ions were detected in conventional fluctuation assays, indicating the importance of this technique in detection of metal mutagens.

Modified culture media, with trimetaphosphate ions in place of orthophosphate as the sole phosphate source for bacterial growth, were also used in this study. The media modifications prevented precipitation of metals such as nickel and cadmium as their insoluble phosphates, and allowed detection of the mutagenicity of metavanadate ions in plate-incorporation assays. However, the fluctuation technique using standard media was shown to detect a wider range of mutagenic metal ions than tests with modified media.

It is notable that metaarsenite (III), arsenate (V), and nickel (II) ions, were found not to be mutagenic in any of the assays although they are

known to be carcinogenic and are mutagenic in other test systems. The lack of mutagenicity of nickel (II) in the modified media indicates that precipitation of this ion as orthophosphate is not the reason for its lack of activity in standard bacterial assays. It is possible that bacterial systems such as the Ames and fluctuation test systems are not sensitive to lipid peroxidation and oxidative damage to DNA (162) and that nickel (II) may exert a mutagenic action by this means.

## CHAPTER 9

CHROMIUM (VI) AND APPARENT PHENOTYPIC

REVERSION IN SALMONELLA TA100

## 9.1 INTRODUCTION

Occasional reports suggest that some apparently mutagenic chemicals fail to induce true reverse mutations in microbial assays, even though macroscopic colony numbers may be increased on test plates.

Examples of treatments which result in such 'false' or phenotypic reversion include:

- (i) accidental addition of an essential nutrient to test plates containing nutritional mutants (e.g., histidine added to *Salmonella* TA strain cultures in assays of inadequately prepared urine concentrates (163));
- (ii) treatment with test compounds which may act as analogues of essential nutrients (e.g., amitrole, which occasionally gives spurious results in *Salmonella* assays, possibly due to its ability to interfere in histidine metabolism and to compete with histidine for incorporation into protein (164, 165));
- (iii) treatment with cytotoxic chemicals or distilled water (e.g., in microbial assays where suppression of lawn colony growth may increase the availability of a limiting nutrient, allowing subsequent growth of auxotrophic colonies to sizes similar to those of prototrophs (166)).

The occurrence of 'false' revertant colonies in *Salmonella* assays of chromium (VI) has been reported by Pedersen et al. (167). Pedersen et al. in their study tested a number of welding fumes and concluded that

Cr(VI) Ames assay results are valid only at low Cr(VI) doses. The present investigation was undertaken to determine whether 'false' reversion adversely affects quantitative estimates of chromium (VI) mutagenesis in *Salmonella*, as has been suggested.

## 9.2 MATERIALS AND METHODS

### Test chemical

Chromate (VI) ions were added as potassium chromate (May and Baker) determined to be 99% pure.

### Plating method

The plate-incorporation assay with *Salmonella* TA100 follows the method of Maron and Ames (168). Briefly, the technique used in this investigation employed basal agar medium containing Vogel-Bonner medium E supplemented with 2% D-glucose. Top agar (6 g/L Difco-Bacto agar and 5 g/L NaCl) to which traces of histidine and biotin were added (10 mg L-histidine and 12 mg biotin/L final concentration) was inoculated with 100 µL of an overnight broth culture and 100 µL of test chemical prepared in serial half-log working dilutions. Plates were routinely incubated at 37°C for 3 days, though additional incubation periods from 4-8 days were necessary to allow for late development of colonies.

### Characterisation of revertant colony genotype

Colonies developing on both control and test plates were stab-inoculated onto sterile minimum agar plates containing excess

biotin, but lacking histidine. A fine platinum wire needle was used to manually transfer colonies to biotin plates which were then incubated for 1-2 days. (The biotin was necessary because the mutation that has deleted the bio gene in TA100 cannot be reverted (168)).

More detailed studies were also carried out on colonies identified by their inability to replicate directly on biotin plates. After 24 hours incubation on nutrient agar, these colonies were retested on biotin plates.

#### Determination of chromium (VI)

The standard spectrophotometric method using s-diphenylcarbazide was employed to determine chromium (VI) concentrations in aqueous solutions (169). Here 40 mg of s-diphenylcarbazide in 100 mL of a solution of 95% ethanol (20 mL) and 10% sulphuric acid (80 mL) was freshly prepared and 1 mL of this solution was added to 4 mL test solutions in plastic cuvettes. Absorbances were measured at 546 nm using a Pye-Unicam SP6-550 UV-visible spectrophotometer.

#### Electron microscopy

Transmission electron microscopy was undertaken with glutaraldehyde-fixed *Salmonella* TA100, either untreated or after overnight incubation in a broth culture containing various concentrations of chromium (VI).

### 9.3 RESULTS

#### Appearance of colonies and bacterial cells exposed to chromium

At toxic concentrations of chromate ( $< 3.7 \times 10^{-5}\text{M}$ ), well-formed colonies did not appear until 5-7 days of incubation. Beforehand, colonies exhibited various unusual features. Some satellite colony development was seen at this and at lower concentrations ( $1.85 \times 10^{-5}\text{M}$ ). These comprised small peripheral colonies within a zone of 2-3 mm around central larger colonies. Other colonies occurred in the form of small discrete clusters, which were also observed in a culture of wild-type ( $\text{his}^+$ ) organisms grown in the presence of  $3.7 \times 10^{-5}\text{M}$  chromate, suggesting that these probably originated by fragmentation of larger colonies. At chromium concentrations above  $1.85 \times 10^{-5}\text{M}$ , large numbers of minute colonies (0.1 mm) were observed by low-power microscopy, presumably resulting from growth inhibition of  $\text{his}^+$  revertants by chromate. Normal background lawn growth was evident under these conditions.

Chromate appeared to exert an effect not unlike that of penicillin, when bacterial cells were observed under the light microscope. Pleiomorphic shapes and distortions of cell walls were common. To determine whether this effect of chromium was occurring at the level of the cell wall, chromate-treated cells were observed under the electron microscope (Fig. 9.1). Although unusual cytoplasmic inclusions were seen at  $1.85 \times 10^{-5}\text{M}$  chromate, there were no obvious alterations in the cell wall structure.

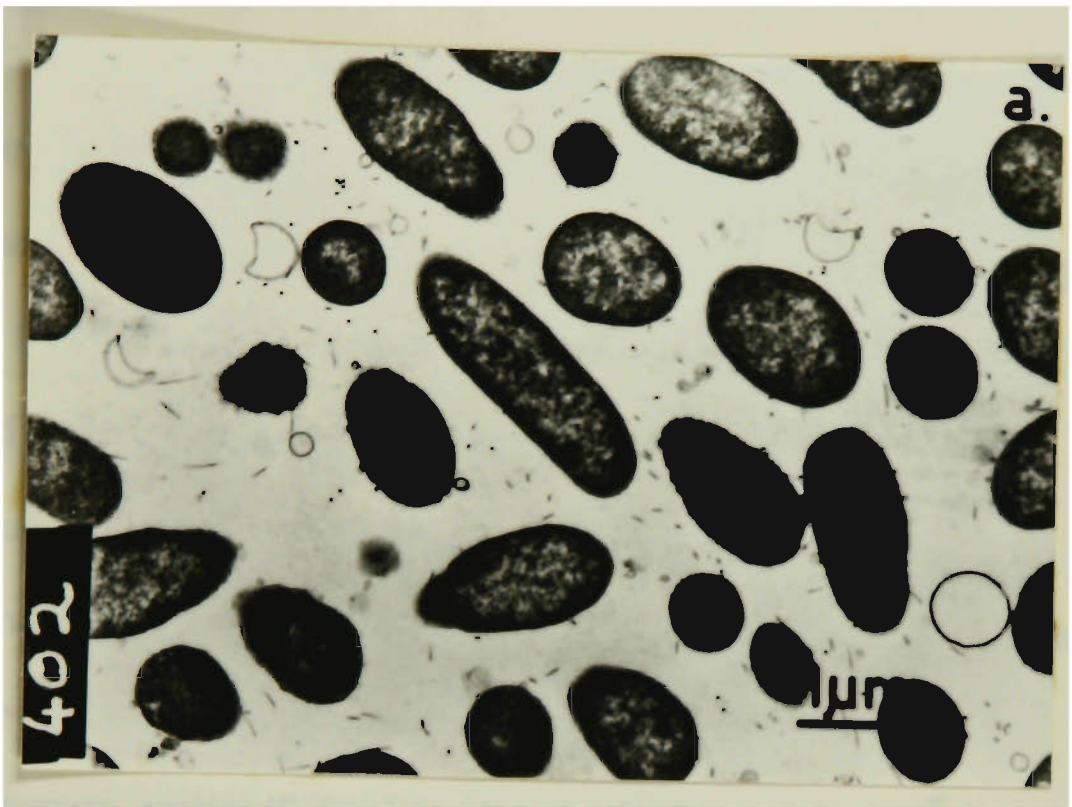


**Fig. 9.1a** Electron micrograph showing *Salmonella* TA100 cells after incubation in an overnight broth culture.

**Fig. 9.1b** TA100 cells after incubation overnight in broth containing  $1.85 \times 10^{-5} \text{ M}$  chromate. Vacuolar inclusions are prominent, together with occasional disrupted cells. At higher magnification, cells containing arrays of electron-dense fibrillar inclusions were also observed.

### Evaluation of non-replicating revertant colonies

Using the stab-inoculation method, almost all colonies on control plates were shown to be capable of growth on fresh plates containing biotin (Tables 9.1, 9.2). However, some colonies on test plates containing chromate failed to subculture, and the proportion of TA100 colonies confirmed as *his*<sup>+</sup> by subculturing varied with the time of incubation of test plates (Table 9.1). At the highest concentration of chromate, well-formed revertant colonies were not observed until 7 days incubation. Most were identified as *his*<sup>+</sup> by their replication on biotin-containing plates. However, earlier (5 days) scoring of colonies on  $3.7 \times 10^{-5}\text{M}$  chromate plates showed a significant proportion of non-replicating colonies. Very few could be detected between 3-5 days because of poor bacterial growth. At  $1.85 \times 10^{-5}\text{M}$  chromate, the occurrence of non-replicating colonies was also confirmed, though they were now equivalent to only 24% of the colony population.

There was a possibility that chromium (VI) might suppress growth of bacterial cells due to toxicity, and that this might be exacerbated under conditions of nutrient deprivation i.e., on minimal agar plates. Thus, colonies initially failing to replicate on biotin plates could do so after a longer incubation period. Biotin plates were therefore examined at both 1 and 2 days of incubation. There was little difference in results (not shown) on either day.

Table 9.1 Effect of chromate (VI) concentration and incubation time on proportion of TA100 colonies scored as his<sup>+</sup>.

Potassium chromate concentration <sup>(a)</sup> (M x 10 <sup>-5</sup> )	<u>Number of replicating revertant colonies (%)</u> Total number of colonies investigated		
	<u>Incubation time</u>		
	3 days	5 days	7 days
3.7	n.d. <sup>(b)</sup>	3/ 12 (25%)	198/200 (99%)
1.85	123/161 (76%)	350/353 (99%)	-
0.92	207/251 (82%)	244/246 (99%)	-
0.37	173/194 (89%)	-	-
Control	99/102 (97%)		

- (a) Concentration initially added to plates.
- (b) Could not be determined due to poor growth on test plate.

Alternatively, colonies might be more satisfactorily identified after an intervening culture period on nutrient agar. Table 9.2 shows that 28% of colonies from plates containing 3.7 x 10<sup>-5</sup>M chromate failed to replicate directly on biotin plates. However, after 24 hours intervening culture on nutrient agar, the majority of these colonies were scored as his<sup>+</sup> when retested on biotin plates. Under the same conditions his<sup>-</sup> colonies picked from a nutrient agar culture of Salmonella TA100 remained incapable of growth on biotin plates.

Table 9.2 Proportion of  $his^-$  colonies identified as  $his^+$  after culture on nutrient agar.

Potassium chromate concentration <sup>(a)</sup> (M x 10 <sup>-5</sup> )	Incubation time (days)	Colonies investigated	Non-replicating colonies ( $his^-$ ?)	Colonies identified as $his^+$ on retest <sup>(b)</sup>
3.7	6	142	40	29
1.85	4	354	10	8
0.92	3	248	0	-
Control	3	255	6	6

(a) As for Table 9.1.

(b) After 24 hours' growth on nutrient agar, retested on biotin plates.

Other replica plating methods were also attempted, including the velvet template technique. These did not provide the accuracy obtained with the stab-inoculation method, and incorporate the risk of transferring significant traces of histidine to the replica plate. In addition, minute colonies were not satisfactorily carried over using the velvet template.

#### Effect of incubation time on colony development

Because of observations that well-formed revertant colonies appeared later on plates incorporating higher chromium concentrations, the effect of incubation time on colony numbers/plate was investigated (Fig. 9.2). Clearly maximum colony numbers did not develop at

$1.85 \times 10^{-5}\text{M}$  chromate until 6-7 days, whereas at  $0.92 \times 10^{-5}\text{M}$  plateau colony development was reached by 4-5 days and at  $0.37 \times 10^{-5}\text{M}$  by 3-4 days. The significant colony-growth-retarding effect of  $1.85 \times 10^{-5}\text{M}$  chromate seen at 3-4 days was reversed with prolonged incubation. The results show that colony numbers on all test plates increased during the 8-day incubation period until reaching plateau levels proportional to the initial chromate concentration.

#### Effect of time on the bioavailability of chromium in agar plates

The reversibility of colony growth inhibition by chromate suggested that chromium (VI) bioavailability in agar plates decreased with time of incubation. To test this possibility, a first overlay, containing  $0.92 \times 10^{-5}\text{M}$  chromate only was poured onto test plates. A second overlay containing bacteria and trace quantities of histidine and biotin was then added, on the same day as the first overlay or 1-4 days thereafter (Fig. 9.3).

Chromium (VI) mutagenicity, as a measure of chromium (VI) bioavailability, decreased with time between addition of chromate and addition of target organisms. Allowing for the lag in colony development seen at this dose level (i.e., allowing for growth of most revertant colonies) the mutagenic action of chromate was completely lost by day 3, where colony numbers are similar to those on control plates ( $93 \pm 16$ ;  $n = 10$ ). The cytostatic effect of chromium (VI) was monitored in this experiment by prolonged incubation of plates following addition of

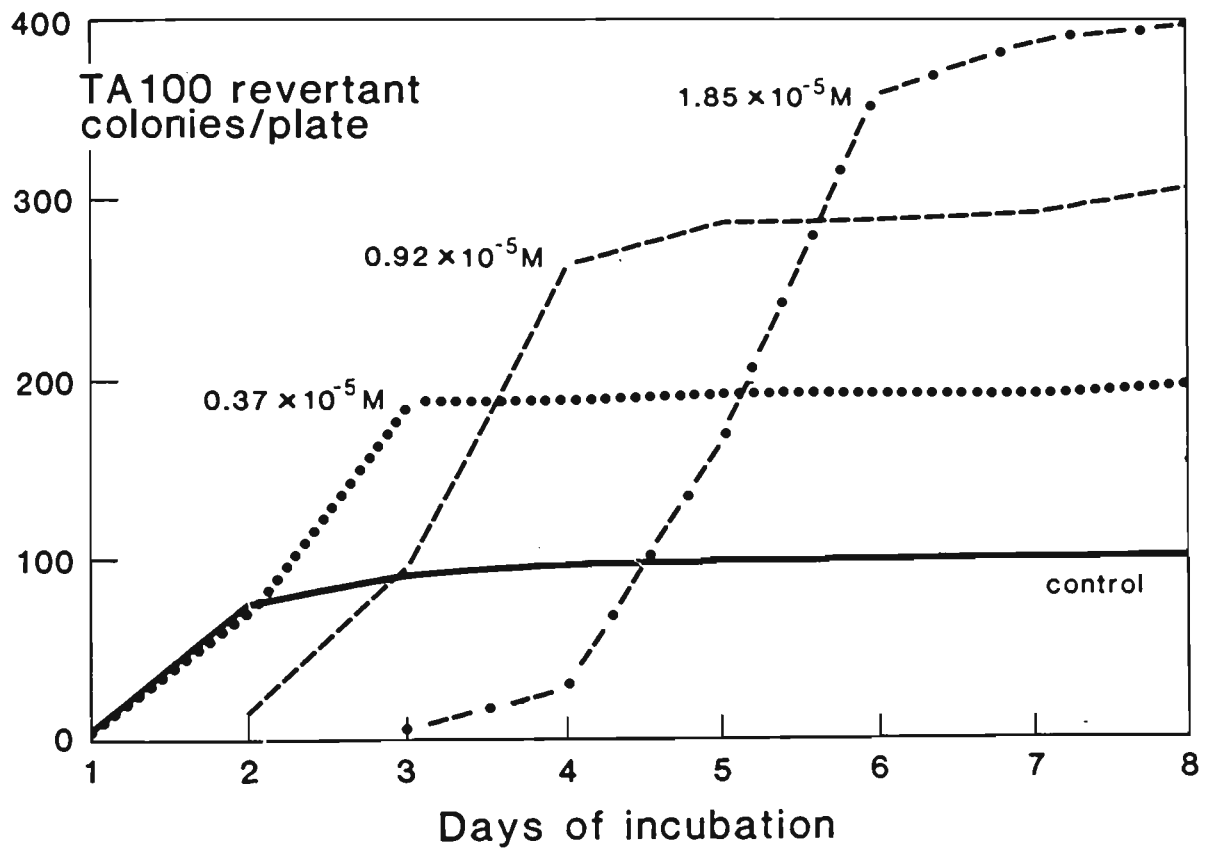


**Fig. 9.2** Delayed TA100 colony development due to chromate (VI). Duplicate dishes were counted and then reincubated each day. Data include both replicating and non-replicating colonies.

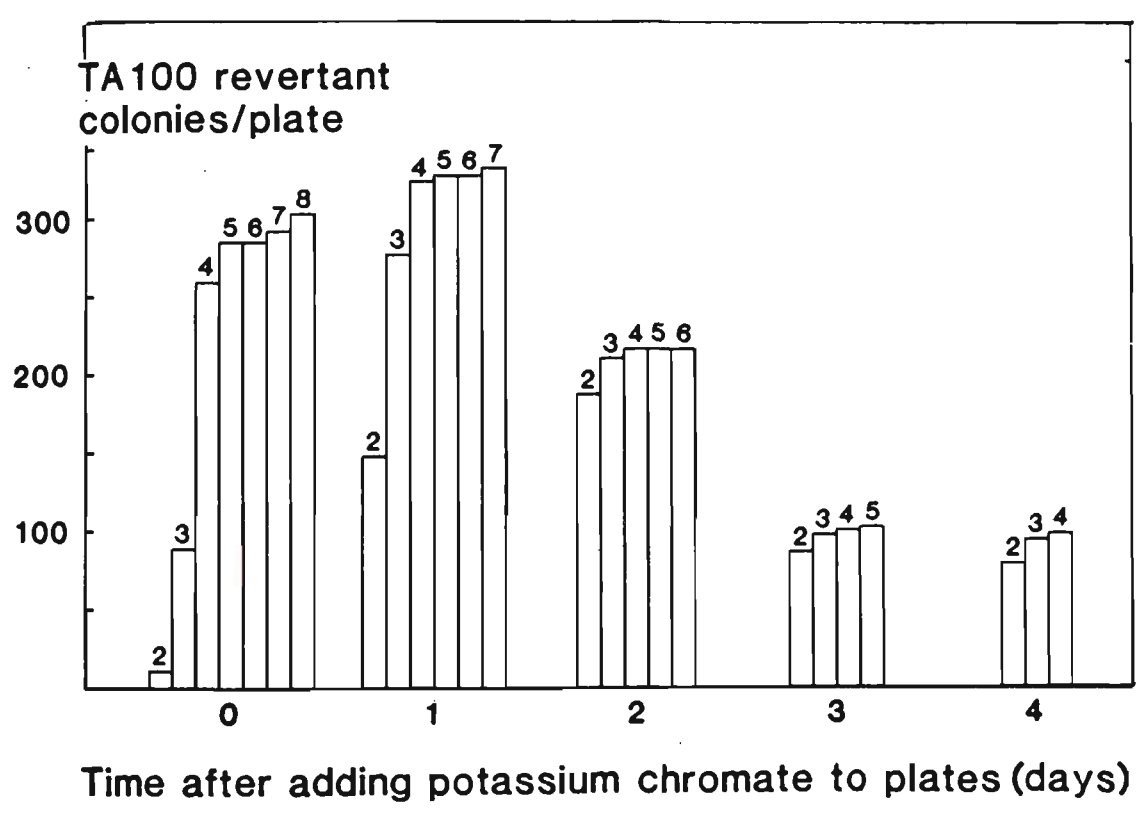


**Fig. 9.3** Loss of mutagenic potency and of cytostatic effect following preincubation of chromate ( $0.92 \times 10^{-5}M$ ) on agar plates. Graphed data represent total colony counts over successive days of incubation after adding second (bacterial) overlay. The latter incubation time is indicated by numbers above each bar on the histogram.

the second (bacterial) overlay (Fig. 9.3). The retarding effect of chromium (VI) on colony development also diminished with preincubation of chromate on agar plates.

When chemical analyses were made of the chromate remaining in media at different times, it was found that spectrophotometrically detectable chromium (VI) decreased steadily with time (Fig. 9.4). In the present case, measurements of chromium (VI) were made in the absence of agar because of problems in spectrophotometric measurements with agar media. However, all other constituents were as in the solid media. Separate estimates of chromate (VI) in media containing salts, glucose, citric acid or combinations thereof (data not shown) indicated that citric acid and glucose together accounted for most of the chromium (VI) reduction detected in liquid media. These components are almost certainly responsible for the reduction in mutagenic and cytostatic effects of chromate incorporated in test plates.

#### 9.4 DISCUSSION

*Salmonella* TA100, cultured for periods of 3-5 days in the presence of high concentrations of potassium chromate, gave rise to substantial numbers of colonies which could not be transferred to biotin-containing replica plates. Pedersen et al. (167) have attributed these non-replicating colonies to 'false' revertants, which it was reported, account for 50-80% of all colonies at  $0.37 \times 10^{-5} \text{M}$  dichromate. In our

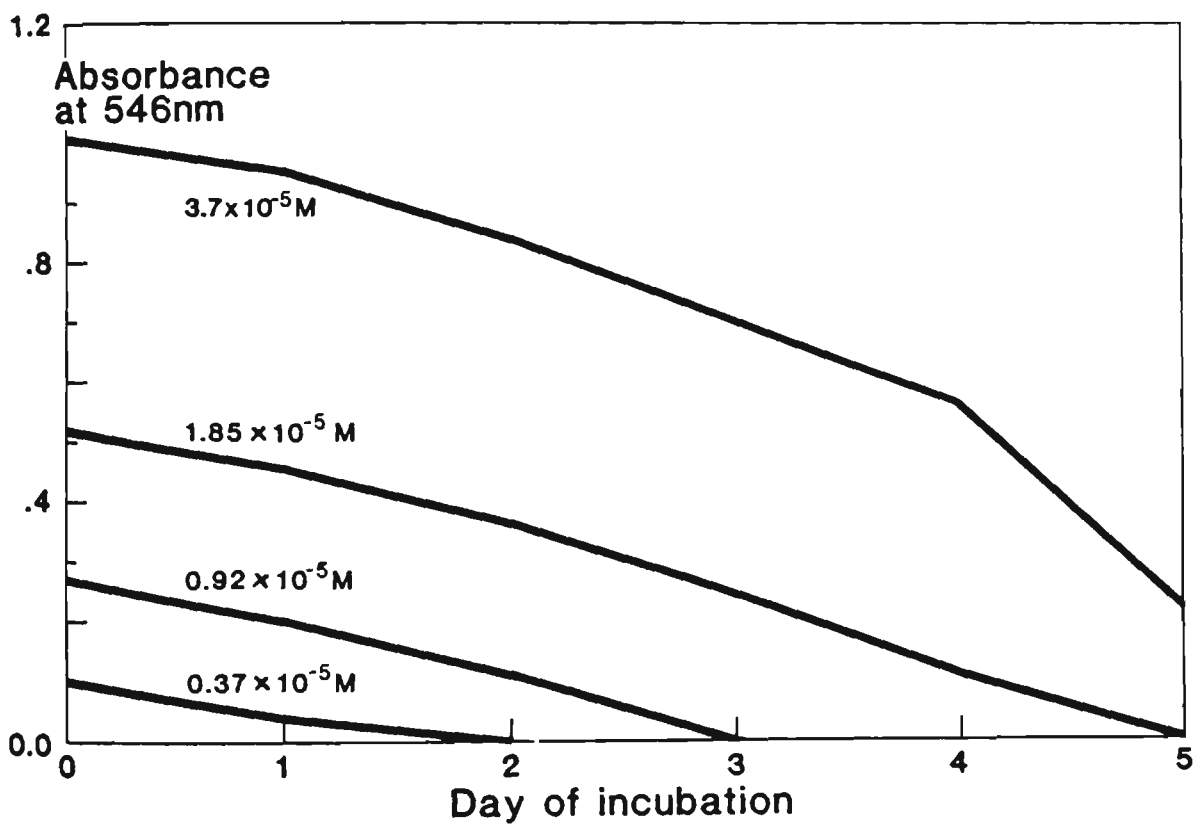


**Fig. 9.4** Spectrophotometric measurement of chromium (VI) in a liquid medium consisting of Vogel-Bonner medium E with 2% added D-glucose, incubated at 37°C for up to 5 days.

study 11-18% of colonies were non-replicating at concentrations of  $0.37 - 0.93 \times 10^{-5} \text{M}$  chromate. These differences may be due to the use of a different replica plating technique in the former study, and to the apparent use of minimal agar replica plates without biotin.

In the present case, the occurrence of non-replicating colonies was closely related to retardation of colony development due to chromate. Both effects were reversible with prolonged incubation, almost certainly as a result of the gradual chemical reduction of chromium (VI) by normal components of bacteriological culture media. Reduction of hexavalent chromium to its trivalent form has been previously demonstrated to occur in the presence of the S9 fraction from rat liver (170) and with reducing agents added to Salmonella test plates (169).

These findings demonstrate that difficulties in establishing the his<sup>+</sup> character of some colonies from chromate-containing plates is probably due to temporary growth inhibition by chromium (VI), which could in turn be a result of accumulated cellular damage (ultramicroscopic lesions were evident at relevant concentrations of chromate). The fact that low numbers of slow growing his<sup>+</sup> cells were present in inocula from chromate plates was illustrated by the use of an intervening nutrient agar subculture procedure. This allowed positive identification as his<sup>+</sup> of a majority of non-replicating colonies from chromate plates, while similarly treated his<sup>-</sup> colonies remained true to type. 'False' or phenotypic reversion therefore plays an insignificant role in chromium

(VI) mutagenesis. On the other hand, the cytostatic action of chromium (VI) does adversely affect the dose-response relationship.

## 9.5 SUMMARY AND CONCLUSIONS

After treatment with potassium chromate at concentrations causing ultramicroscopic cellular lesions, a significant proportion (up to 75%) of *Salmonella* TA100 colonies fail to replicate on fresh minimal plates containing biotin. This suggests that chromium(VI) may not always induce his<sup>-</sup> reversion to his<sup>+</sup> in *Salmonella* TA100. The terms 'false' or phenotypic reversion have been used to distinguish such instances from 'true' or genotypic reversion, where progeny his<sup>+</sup> cells readily grow on biotin replica plates.

Results of the present study indicate that the majority of chromate-exposed colonies, initially scored as his<sup>-</sup>, are identifiable as his<sup>+</sup> after 24 hours culture on nutrient agar. Moreover, chromate exerts a cytostatic effect on TA100 since early colony development is suppressed at high chromate concentrations. A gradual chemical reduction of chromium (VI) ions by normal media compounds is probably responsible for the re-emergence of colony growth during prolonged incubation of test plates.

Thus, temporary growth inhibition at high chromate concentration appears to be responsible for most of the non-replicating colonies detected in mutagenicity assays of chromium (VI). The observations made

and the conclusions reached in this study are of importance in the Ames testing of stainless steel and other chromium-containing welding fumes.

## CHAPTER 10

ACTION OF WELDING FUMES FROM HARDFACING AND  
HSLA STEEL ELECTRODES ON CULTURED MAMMALIAN CELLS

## 10.1 INTRODUCTION

The inadequacy of bacterial test systems for hazard evaluation of inorganic compounds, inert particles and fibres has been alluded to in the literature (171). Lack of agreement between prokaryotic (e.g., Ames test) and eukaryotic (e.g., SCE test) assays has been a major barrier for proper evaluation of the genetic toxicity of nickel, cadmium and arsenic compounds (44) and also of welding fume which contains these putative carcinogens.

The present study utilises three types of hardfacing and two types of HSLA steel flux-coated welding rods which yield fumes of different composition, in order to further explore the role of fume in sister chromatid exchange (SCE) induction, and mitotic inhibition in mammalian cells. The chief advantage of the SCE assay employed here is its sensitivity to inorganic compounds of beryllium, nickel, arsenic and chromium, including relatively insoluble compounds such as chromium (III) oxide (172).

[The sister chromatid exchange test has been referred to in Sections 2.3 and 2.5. The test is discussed in detail in Refs 45, 46. The labelling protocol is described in the next section. The SCE test was chosen because it is objective, easy to score (no overall change in chromosome morphology), more sensitive than the micronucleus test (a test related

to chromosomal breakage), and amenable to dose-response studies (38, 45, 46). Because SCEs occur with higher frequency than chromosome aberrations, fewer cells are needed in the SCE test to determine whether a compound has a significant effect; often, very large increases in SCE are observed at concentrations of chemicals that induce few if any chromosome aberrations (45, 46).

Sister chromatid exchanges were first described by Taylor (46) who found that if chromosomes were allowed to replicate once in the presence of tritiated thymidine and then again in its absence, autoradiographs showed that only one chromatid of each chromosome was labelled (i.e., carried radioactive DNA) as a semi-conservative replication of DNA. Occasional symmetrical switches in this label between sister chromatids were observed, and Taylor called these, 'sister chromatid exchanges'. The method did not find favour as a routine screen for SCE inducing agents because the resolution was poor and the procedure was time consuming. However, a more powerful technique was made possible by the observation that incorporation of the chemical

5-bromodeoxyuridine (BUdR) in place of thymidine quenches the reaction of chromosomes with the dye Hoechst 33258 (BUdR is a thymidine analogue). This can be seen as a decrease in fluorescence (dim vs intense) or a decrease in staining with Giemsa's solution (light vs dark).

The principle of the sister chromatid differential staining method used in the present work is described below. After one round of replication in BUdR, the thymidine in one strand of each DNA duplex is replaced, i.e., each sister chromatid (of a pair) has one labelled and one unlabelled strand. This unifilar substitution results in a uniform reduction in the staining or fluorescence of the chromosomes. Following segregation of the chromatids (of a pair) at mitosis, a second round of replication in BUdR generates a sister chromatid pair, consisting of one chromatid whose DNA is unifilarly substituted (one strand labelled and the other strand unlabelled), and the other chromatid in which both strands of the DNA duplex are labelled, i.e., possess BUdR in place of thymidine (bifilarly substituted). When treated with the dye Hoechst 33258 and stained with Giemsa, the

unifilar chromatid is much darker than the bifilar chromatid: bifilar substitution results in a much greater decrease in staining or fluorescence than unifilar substitution. A sister chromatid exchange is seen as an exchange of label between the two chromatids.]

## 10.2 EXPERIMENTAL

### Welding fume production

Fume was generated using an automatic arc welding apparatus (see Chapter 3) under precise and reproducible conditions of voltage and current, and collected on glass-fibre media. The fume particles were brushed from the glass-fibre substrates and dried at 100°C prior to storage in sealed glass vials in a dessicator at 4°C. Chemical analyses were completed within 2-4 weeks following fume collection. Cell culture experiments were carried out over a total period of 4-20 weeks, initial experiments on all fumes being completed within the first few weeks of fume storage.

The electrodes employed in this study and their operating conditions are described in Tables 5.1 and 5.2.

### Chemical and biological analyses

Composition of the welding fumes and water-soluble fume fractions as determined by x-ray fluorescence, x-ray diffraction, atomic

absorption spectrophotometry, ion-selective electrode and ion-chromatography, etc., are described in Chapter 7. The results for the water-insoluble fraction are given in Table 10.1 and were obtained by difference.

For SCE and mitotic inhibition assays, the welding fumes were tested either as insoluble particles (i.e., washed fume, following removal of soluble components by stirring in water at 60°C for 2 h and filtering through a 0.45 µm nylon membrane) or as a water extract of total fume (whole fume mixed with high purity deionised water for 10 min at 45°C and filtered through a 0.45 µm nylon membrane). Half-log dilutions of insoluble particles or freshly prepared soluble extract were made with complete culture medium immediately before each assay.

#### Sister chromatid exchange (SCE) assays

Chinese hamster lung (Don) cells (American Type Culture Collection CCL16) and SCE assay techniques have been described by Baker et al. (173). In this study, Don cells cultured in Ham's F-12 medium (Flow) supplemented with 10% heat-inactivated foetal bovine serum (Flow), were inoculated at  $8 \times 10^4$ /mL in 4 mL of culture medium into 25 cm<sup>2</sup> culture flasks (Lux) and incubated at 37°C in an atmosphere containing 5% CO<sub>2</sub> in air and at 95% relative humidity. After 6 h incubation cell attachment was complete and the growth medium was changed.

After overnight incubation, the medium was again replaced with

fresh medium or medium containing insoluble particles, soluble fume components or the positive control compound, mitomycin-C (MMC). After a further 4 h incubation, 5-bromodeoxyuridine was added to 10  $\mu$ M concentration and all flasks were incubated in the dark for a further 20 h. Fresh medium containing colcemid (1  $\mu$ M) was added for a further 3 h before harvesting metaphase cells. Fluorescence plus Giemsa (FPG) -stained spreads (174) on glass microscope slides were coded for analysis of 30 metaphases at each experimental point. Individual data points represent mean SCE/metaphase spread from single flasks. Generally, each water-soluble extract was tested three times at a range of doses. Each insoluble fume was tested once. For comparison,  $K_2CrO_4$  was assayed in six experiments and results of  $K_2CrO_4$  assays are expressed as means  $\pm$  standard deviations.

### Assays of mitotic inhibition

Sister chromatid differential staining is an extremely sensitive indicator of mitotic inhibition, because of the requirement for two complete cell cycles of incorporation of 5-bromodeoxyuridine to achieve differential chromatid staining. This feature of the SCE technique was used to determine the lowest concentration of insoluble or soluble fume preparations able to block differential staining, but without causing overt cytotoxicity or loss of cell viability. Under these conditions, failure of differential staining can occur due to a slowing, but not necessarily a complete cessation, of cell division.

## Statistical analyses

Curve-fitting, estimation of slopes and probability values were determined using a microcomputer program (175). A p-value  $< 0.05$  for linearity indicates that the line does not adequately describe this data. Significance of SCE results was determined using a 2-tail Student t-test.

## 10.3 RESULTS

### Mitotic inhibition and fume chemistry

The concentrations of Cr, Ni and F in the five fume preparations are given in Table 10.1. All of the water-soluble chromium is chromium (VI), though not all chromium (VI) is water-soluble e.g.,  $\text{CaCrO}_4$  is much less soluble than  $\text{K}_2\text{CrO}_4$ , particularly in the complex fume matrix. Chromium (III) in these fumes is water-insoluble. There is also very little water-soluble nickel, since nickel is present in the fumes only in the form of insoluble oxides. Of the fluorides detected here, NaF and KF are water-soluble, whereas  $\text{CaF}_2$  is insoluble. A detailed analysis of the fume and water-soluble fume fractions is given in Tables 7.1-7.6 (pp. 91-97).

Each of the five fumes has a distinctive chemical composition which may be useful for comparative investigations of their biological activities. For example, fume E01 has the highest concentration of water-soluble hexavalent chromium and the highest iron content (32%) amongst the five fumes. Fume<sup>E</sup>04 has the lowest concentration of

Table 10.1 Chemical composition and mitotic-inhibitory activity of welding fume preparations.

Fraction	Composition <sup>(a)</sup> mitotic inhibition	Fume				
		E01	E04	E05	E11	E12
Water-soluble	Cr(VI)	1.5	0.02	0.7	0.03	0.5
	F	3.0	9.4	9.5	1.2	2.3
	Inhibitory level <sup>(b)</sup>	10	25	10	1000	10
Water-Insoluble	Cr(VI)	0.3	0.01	0.0	0.0	1.0
	Cr(III)	0.8	0.0	0.0	0.02	3.6
	Ni	0.04	0.2	0.02	1.7	0.04
	F	5.3	4.3	9.1	0.7	3.7
	Inhibitory level <sup>(b)</sup>	> 500	500	100	> 500	100

- (a) % w/w with respect to total fume.
- (b) Lowest test concentration (µg total fume or washed fume/mL) at which significant mitotic inhibition was evident. The inhibition level for K<sub>2</sub>CrO<sub>4</sub> corresponds to 0.61 µg/mL K<sub>2</sub>CrO<sub>4</sub> or 0.162 µg/mL Cr(VI).

water-soluble chromium (VI). Fume E05 has the highest content of both water-soluble and insoluble fluorides. There is very little water-soluble material in fume E11 which contains considerably more nickel than the other fumes and 28% iron, all of which is water-insoluble. Moreover, fume E11 contains 25-30% manganese, approximately 100% of which is present as insoluble manganese oxides. Finally, fume E12 possesses the highest concentration of insoluble chromium (VI) and also of insoluble chromium(III).

Mitotic inhibition (Table 10.1) is a very sensitive indicator of biological activity of welding fume since it occurs at subtoxic concentrations. Most of the soluble metal salts tested cause mitotic inhibition in Don cells at doses below cytotoxic levels (172). Exceptions are NaF and  $\text{MnCl}_2$ . Thus, investigations of mitotic inhibitory activity in soluble fume indicates that  $\text{E01} = \text{E05} = \text{E12} > \text{E04} > \text{E11}$ , which did not and would not be expected to parallel their fluoride or manganese content. However, the two soluble fractions with lowest mitotic inhibitory activity were from fumes with lowest water-soluble chromium (VI) content.

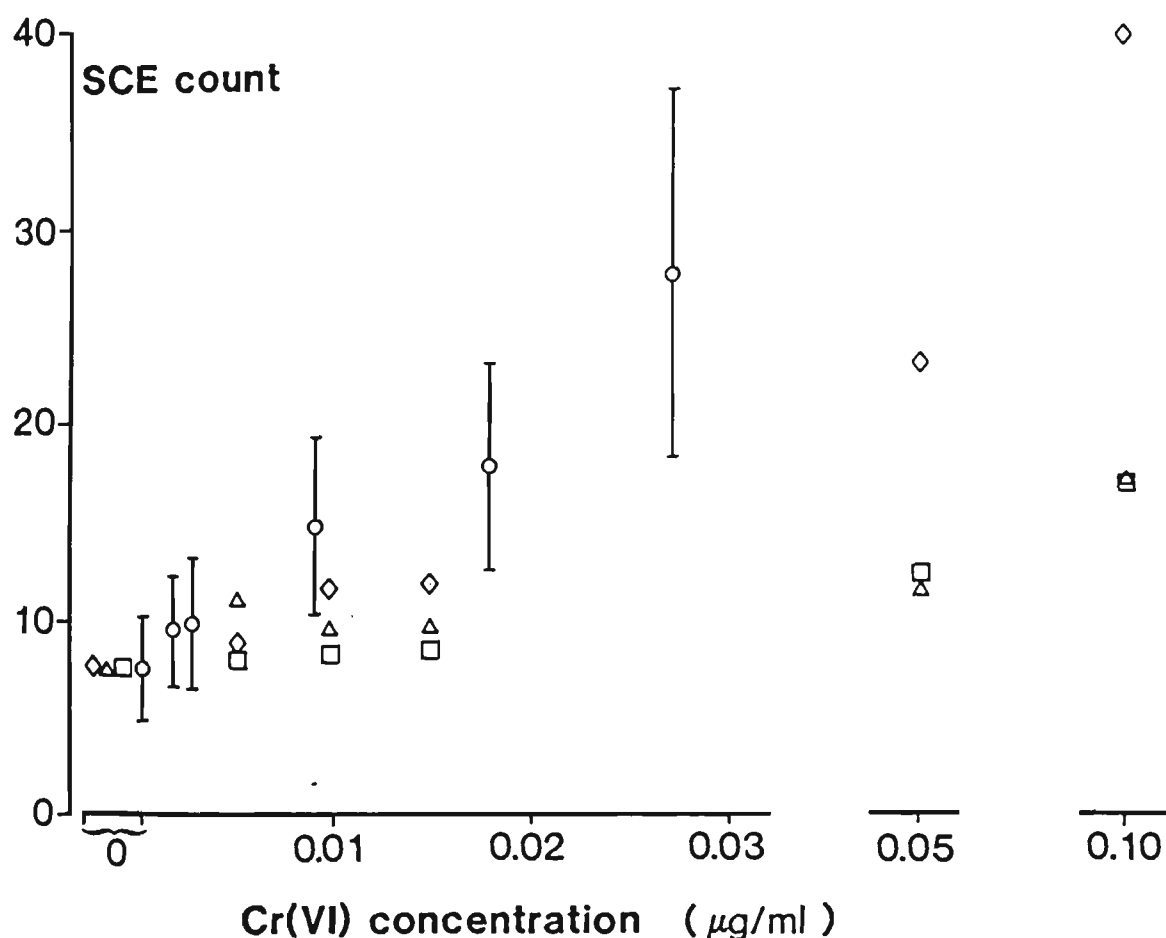
Water-insoluble fume particles were much less active than the water extracts of the respective fumes. The results correlate partially, though not completely, with insoluble chromium (VI) content (fume E05 being an exception). Amongst the five fumes, the insoluble particles of E05 and E12 were the more active in mitotic inhibition. It is possible that insoluble silicates, which were highest in these two fumes (4.5% Si in E05 and 13.3% Si in E12) might contribute to this.

### SCE Induction

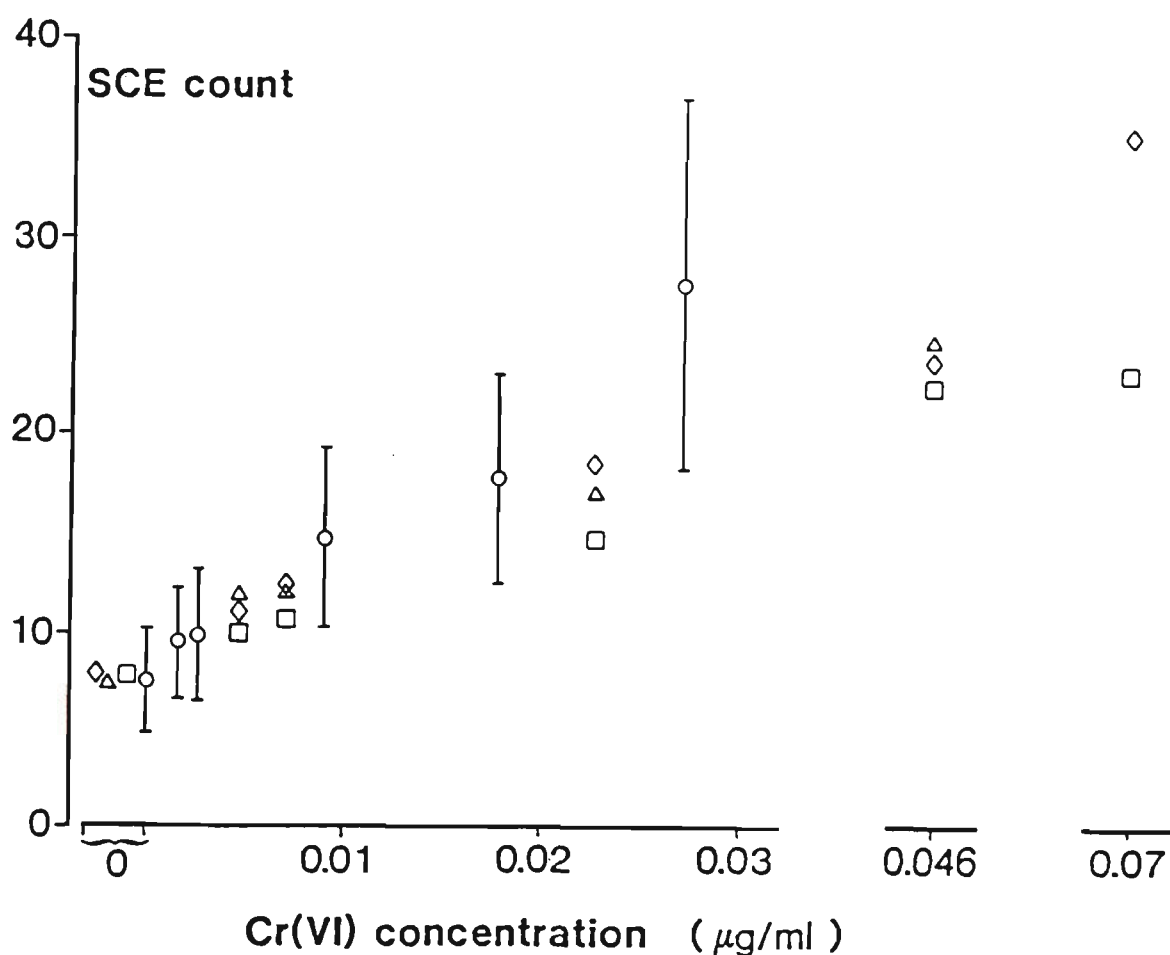
Water extracts of the five welding fume preparations all induced SCE in Don cells (Fig. 10.1 a-d). Fume SCE values were significantly higher ( $p < 0.01$ ) than control values from cell cultures without fume. In order to compare SCE induction with chromium (VI) content of the soluble extracts,

the activity of  $K_2CrO_4$  was determined and has been superimposed on the fume data. In each case, SCE induction by the water-soluble fraction can be accounted for solely by its chromium (VI) content. However, only the soluble components of E04 (Fig. 10.1 d), E05 (Fig. 10.1 b) and E12 (Fig. 10.1 c) have activity coincident with that of  $K_2CrO_4$ . Soluble fractions of fumes E11 and E01 (Figs 10.1 d and 10.1 a) are marginally less active than  $K_2CrO_4$ , and in the case of E01, SCE induction may have decreased with time of storage of fume, perhaps due to reduction of chromium (VI) by iron (II), in the presence of moisture in the fume matrix (50).

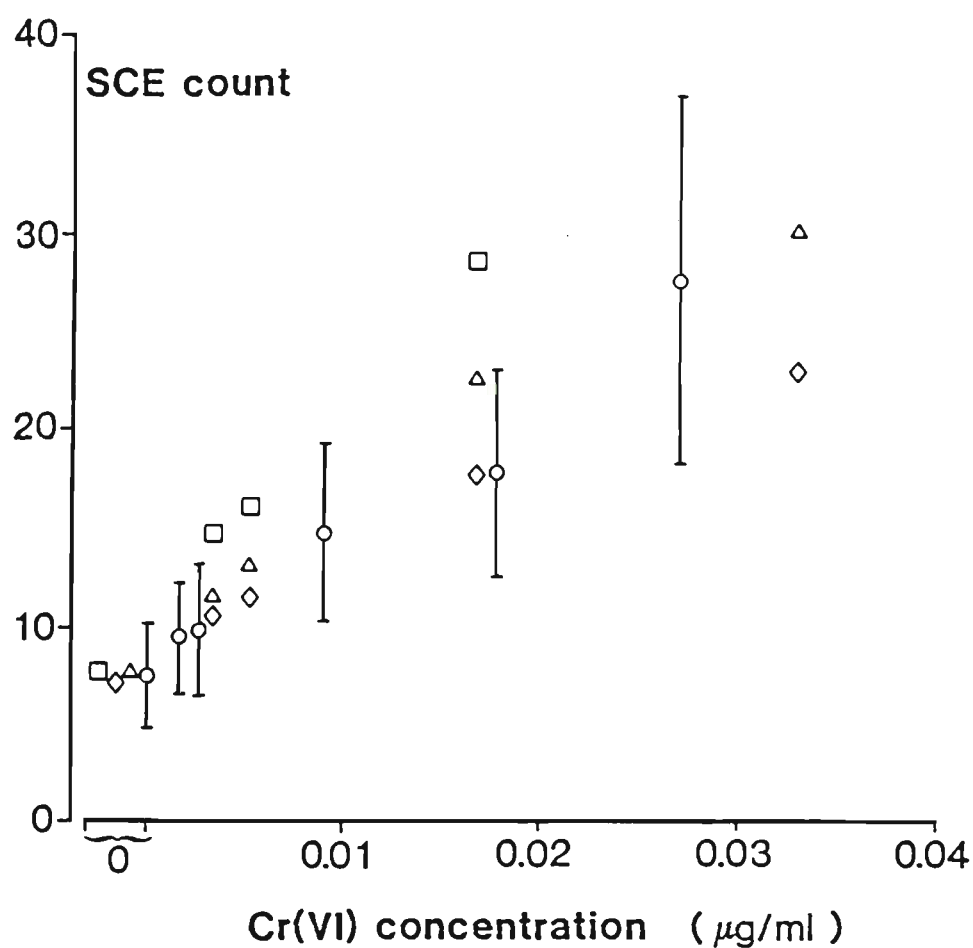
Overall SCE activity of soluble fractions and insoluble fume particles is depicted in Fig. 10.2. This data has been expressed as SCE/ $\mu$ g total or washed fume/mL for purposes of direct comparison. In every case the slopes of SCE induction curves for the soluble extracts are greater than those of the insoluble material. Comparison of the water extracts shows  $E12 > E01 > E05 > E04 > E11$ . On the other hand, activities of the insoluble fume particles indicate a different order from those of the soluble extracts, with  $E12 > E05 > E01 > E11 > E04$ . Thus, SCE inducing activity shows a high correlation with mitotic inhibition by the various fume preparations, except in the case of the insoluble particulates of fumes E01 and E11 which yielded somewhat less mitotic inhibition than E04 (Table 10.1).



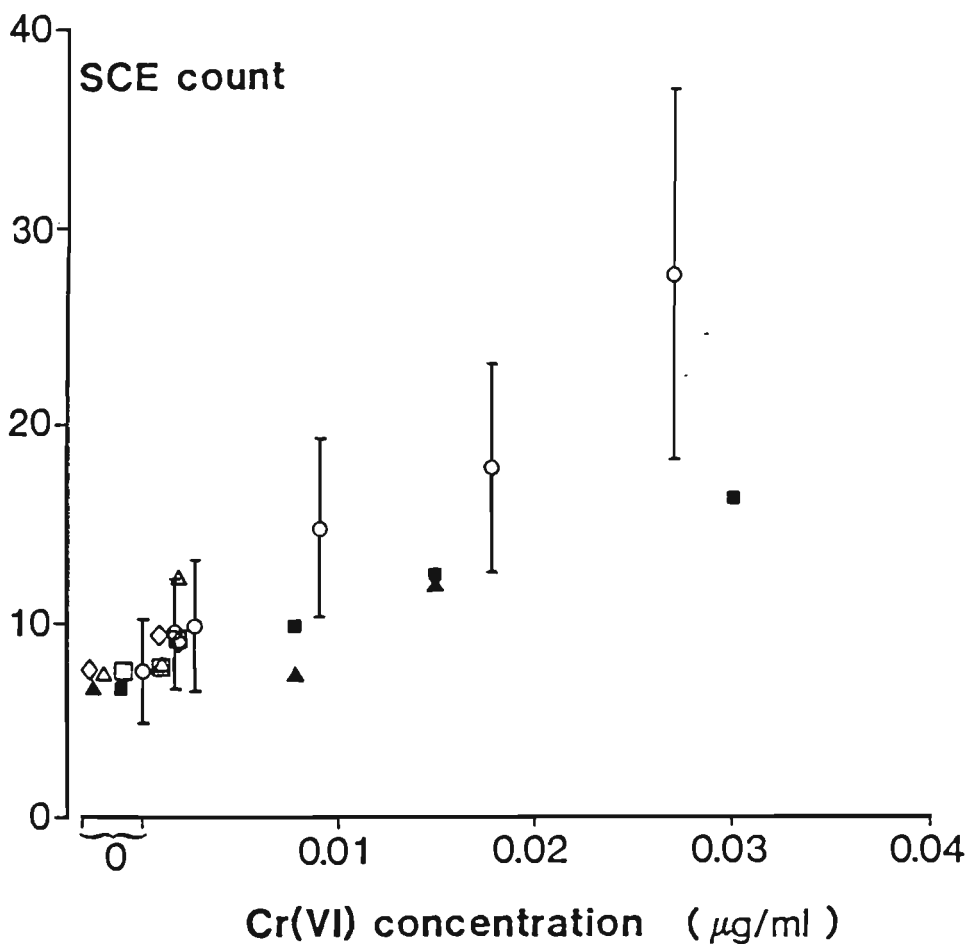
**Fig. 10.1a** Sister chromatid exchanges in Don cells treated with fume extract E01 (three experiments (◇, △, □)), and treated with K<sub>2</sub>CrO<sub>4</sub> (○), as a function of water-soluble chromium (VI) concentration. Results of six experiments with K<sub>2</sub>CrO<sub>4</sub> (○) have been pooled and are superimposed on the graph, each point representing the mean and standard deviation SCE value from 180 metaphase spreads. The average relative standard deviation in the fume data points is 20%.



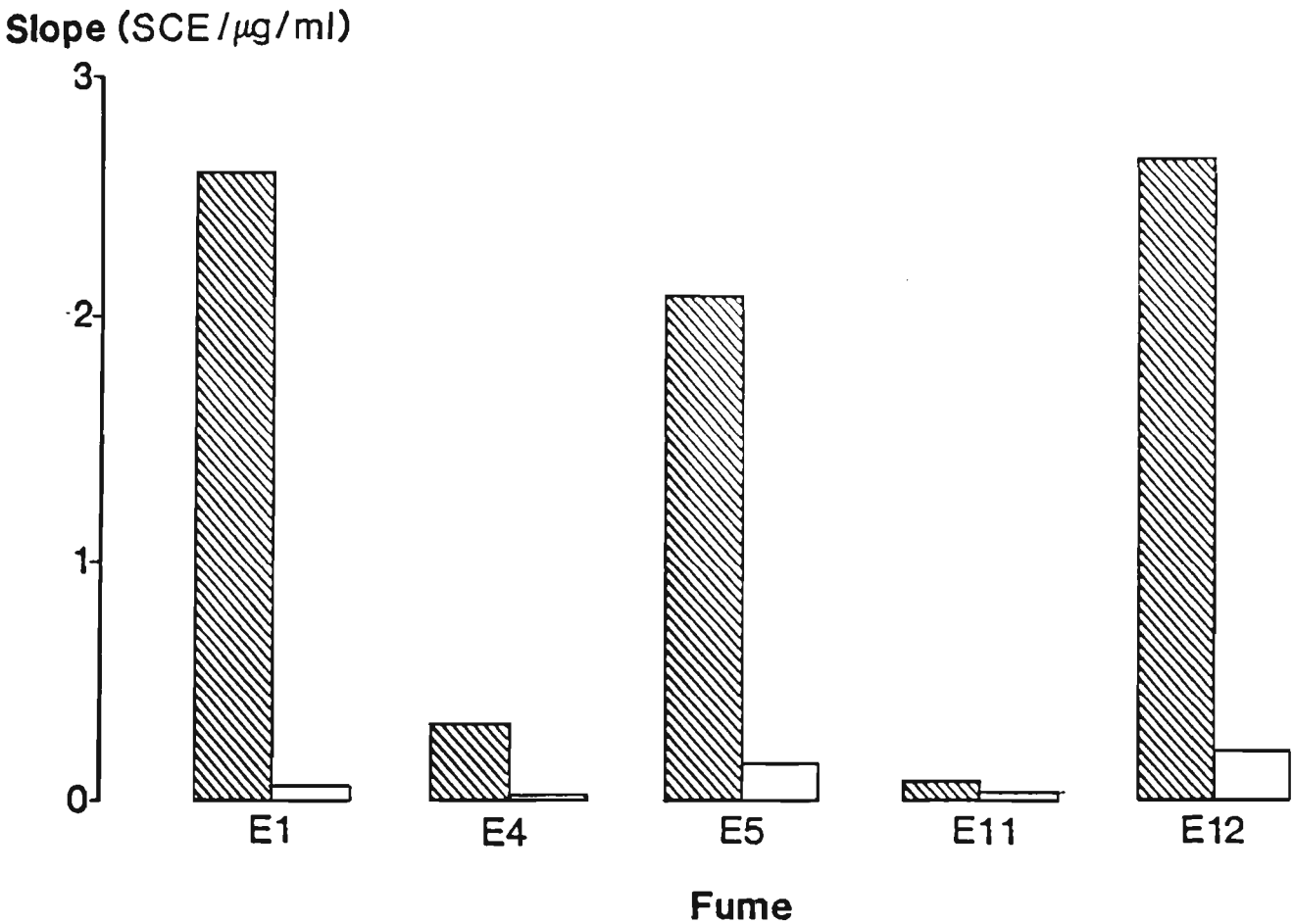
**Fig. 10.1b** Sister chromatid exchanges in Don cells treated with fume extract E05 (three experiments (  $\diamond$  ,  $\triangle$  ,  $\square$  )), and treated with  $K_2CrO_4$  (  $\circ$  ), as a function of water-soluble chromium (VI) concentration.  $K_2CrO_4$  (  $\circ$  ) results as described in Fig. 10.1a. The average relative standard deviation in the fume data points is 25%.





**Fig. 10.1c** Sister chromatid exchanges in Don cells treated with fume extract E12 (three experiments (  $\diamond$  ,  $\triangle$  ,  $\square$  )), and treated with  $\text{K}_2\text{CrO}_4$  (  $\circ$  ), as a function of water-soluble chromium (VI) concentration.  $\text{K}_2\text{CrO}_4$  (  $\circ$  ) results as described in Fig. 10.1a. The average relative standard deviation in the fume data points is 25%.



**Fig. 10.1d** Sister chromatid exchanges in Don cells treated with fume extract E04 (three experiments (  $\diamond$  ,  $\triangle$  ,  $\square$  )), treated with fume extract E11 (two experiments (  $\blacktriangle$  ,  $\blacksquare$  )), and treated with  $\text{K}_2\text{CrO}_4$  (  $\circ$  ), as a function of water-soluble chromium (VI) concentration.  $\text{K}_2\text{CrO}_4$  (  $\circ$  ) results as described in Fig. 10.1a. The average relative standard deviation in the fume data points is 30%.



**Fig. 10.2** SCE-inducing activity of soluble (  ) and insoluble (  ) fume preparations, represented as the slope of the dose-response curves for the soluble extracts from total fume, or for washed fume (i.e., insoluble particles). Slope for each water extract is here expressed as a function of the mass of total fume used in its preparation. P-values for the slopes of soluble fumes E01 to E12 are 1.0, 0.8966, 0.9568, 0.6762 and 0.228, respectively. P-values for slopes of insoluble fumes E01 to E12 are 0.9889, 0.058, 0.996, 0.089 and 0.6121, respectively.

#### 10.4 DISCUSSION

Because of the sensitivity of microbial assays to chromium (VI), inevitably much of the mutagenicity of welding fume was initially attributed to this metal ion (47, 50). Since then, other comparative studies of cytogenetic effects in mammalian cells (53) and of recessive spots in mice (51) have indicated their correlation with soluble chromium (VI) present in fume. Moreover, the cytotoxicity of fume in an established human cell line, in bovine alveolar macrophages (176-178) and in rat lung (179, 180) also appears to be related to its soluble chromium (VI) content.

The present study demonstrates that mitotic inhibition and SCE-induction both correlate well with chromium (VI) in water extracts of fume. From other studies (172), there is evidence that fluoride, nickel and manganese could also contribute to SCE induction by welding fume. However, the concentration of fluoride is too low in the soluble extracts to be sufficient to account for their activity. Furthermore, the fume with highest nickel and manganese concentrations (albeit not water-soluble) was also the least active in both SCE induction and in mitotic inhibition, indicating only a slight contribution, if any, by these metals.

Activity of the insoluble fume particles may be explained in terms of the release of metal ions by slow (< 24 h) leaching from particles phagocytosed by the Chinese hamster lung cells. Nevertheless it is unlikely that the growth inhibitory and genotoxic effects of particles can

be accounted for solely by their chromium (VI) content. Chromium (III) in the form of insoluble  $\text{Cr}_2\text{O}_3$  also induces SCE in Chinese hamster lung cells (172), but the SCE-inducing activity of the fume particles is far greater than that due to chromium (III) alone. Indeed the biological action of E05 particles cannot be explained in terms of known activity of any individual metals, being either due to synergism or to some as yet unidentified component.

The present findings concur with other mammalian cell studies indicating the role of fume-derived soluble chromium (VI) in SCE-induction (53) and in inhibition of cell division (176), but they also indicate the need for care in evaluating the action of water-insoluble fume particulates, particularly since these insoluble components may, due to their persistence, contribute more to chronic lung disease.

## 10.5 SUMMARY AND CONCLUSIONS

Welding fumes from three types of hardfacing and two types of HSLA steel electrodes were water-extracted and both soluble and insoluble fractions were subsequently investigated for mitotic inhibition and sister chromatid exchange (SCE) induction in cultured Chinese hamster lung (Don) cells. In general, activity of the water-soluble extracts of fumes in Don cells paralleled their chromium (VI) content, although a contribution of chromium (III), fluorides, nickel, manganese and other

fume constituents cannot be excluded. In the case of the insoluble fume particles, growth inhibition and genotoxic action cannot be due to chromium (VI) alone.

## APPENDIX 1

### EFFECT OF pH ON CHROMIUM (VI) SPECIES IN SOLUTION

## INTRODUCTION

The analytical chemistry of aqueous chromium (VI) has been described extensively in the literature (181-183) but no tabulation of the abundance of chromium (VI) species at different pH values and metal concentrations has been published apart from a brief account of the  $\text{HCrO}_4^-/\text{CrO}_4^{2-}$  equilibrium. Such data are essential for studies of environmental chromium speciation. Chromium (VI) may be present in aqueous solution as chromate ( $\text{CrO}_4^{2-}$ ), dichromate ( $\text{Cr}_2\text{O}_7^{2-}$ ), hydrogen chromate ( $\text{HCrO}_4^-$ ), dihydrogen chromate (chromic acid,  $\text{H}_2\text{CrO}_4$ ), hydrogen dichromate ( $\text{HCr}_2\text{O}_7^-$ ), trichromate ( $\text{Cr}_3\text{O}_{10}^{2-}$ ) and tetrachromate ( $\text{Cr}_4\text{O}_{13}^{2-}$ ). The last three ions have been detected only in solutions of  $\text{pH} < 0$  or at chromium (VI) concentrations greater than 1M (182-184). Polyanions containing  $> 4$  chromium atoms are not known, and probably do not exist, on account of chromium-oxygen multiple bonding (184). Three pH regions may be distinguished for chromium (VI) species: (i)  $\text{pH} \leq 0$ , where  $\text{H}_2\text{CrO}_4$  is a significant species, (ii)  $\text{pH} = 2-6$ , where  $\text{HCrO}_4^-$  and  $\text{Cr}_2\text{O}_7^{2-}$  occur together, and (iii)  $\text{pH} > 6$ , where  $\text{CrO}_4^{2-}$  predominates.

## EXPERIMENTAL

The published values of the chromium (VI) equilibrium constants used in the calculations in this study are given in Table 1. Contributions

from  $\text{HCr}_2\text{O}_7^-$ ,  $\text{Cr}_3\text{O}_{10}^{2-}$  and  $\text{Cr}_4\text{O}_{13}^{2-}$  are negligible at  $\text{pH} > 1$  and at chromium (VI) concentrations  $\leq 10^{-2}\text{M}$ . The concentration of  $\text{H}_2\text{CrO}_4$  (x) in a solution of hydrogen ion concentration (p) and total chromium (VI) concentration C was obtained by solving the quadratic equation

$$x + \frac{k_1 x}{p} + \frac{k_1 k_2 x}{p^2} + \frac{k_3 k_1^2 x^2}{p^2} - C = 0$$

Table 1. Published values of equilibrium constants<sup>(a)</sup>.

Equilibrium	Ionic Strength (M)	Equilibrium constant (at 25°C)	Reference
$\text{H}_2\text{CrO}_4 \rightleftharpoons \text{H}^+ + \text{HCrO}_4^-$	$\approx 0.16$	$k_1 = 0.18$	(184-186)
$\text{HCrO}_4^- \rightleftharpoons \text{H}^+ + \text{CrO}_4^{2-}$	0.33-0.63	$k_2 = 3.2 \times 10^{-7}$	(186)
$2\text{HCrO}_4^- \rightleftharpoons \text{Cr}_2\text{O}_7^{2-} + \text{H}_2\text{O}$	$< 0.022$	$k_3 = 33.3$	(188)
	1	$k_3 = 98$	(187)
	0	$k_3 = 35.5$	(187)

(a) K-values ( $k_1$ ,  $k_2$  and  $k_3$ ) at the same ionic strength (e.g., at  $\mu = 1$ ) are not available in the literature.

The concentrations of the other chromium (VI) species were obtained from:

$$[\text{HCrO}_4^-] = \frac{k_1 x}{p}$$

$$[\text{CrO}_4^{2-}] = \frac{k_1 k_2 x}{p^2}$$

$$[\text{Cr}_2\text{O}_7^{2-}] = \frac{k_3 k_1^2 x^2}{p^2}$$

The equations were solved on a Univac 1100 computer using a Fortran program (see Table 2 for program).

## RESULTS AND DISCUSSION

Results obtained by using  $k_3 = 98$  are given in Table 3. This value of  $k_3$  was determined at an ionic strength ( $\mu$ ) of unity (187). If a value of  $k_3 = 35.5$  ( $\mu = 0$ ) is used, the dichromate concentrations are approximately half those given in Table 3 and the concentrations of the other species are correspondingly greater. The results in Table 3 are consistent with qualitative and quantitative descriptions of the chromium (VI) system by other authors (181-184, 189) and indicate that at neutral pH the principal species in solution are  $\text{CrO}_4^{2-}$  ( $\approx 80\%$ ) and  $\text{HCrO}_4^-$  ( $\approx 20\%$ ).

Table 2. Fortran program used<sup>(a), (b)</sup>


---

```

1      IMPLICIT REAL*8(A-H,O-Z)
2      REAL*8 K1,K2,KD
3      DIMENSION PH(8),C1(5),KD(2)
4      DATA PH/1.0D-1,1.0D-2,1.0D-3,1.0D-4,1.0D-5,1.0D-6
          1D-7,1D-8/
5      DATA K1/0.18D+0/,K2/3.2D-7/
6      DATA KD/98D+0,35.5D+0/
7      DATA C1/1.0D-2,1.0D-3,1.0D-4,1.0D-5,1.0D-6/
8      DO 10 I=1,2
9      DO 20 J=1,5
10     C= -C1(J)
11     WRITE(6,50) KD(I),C1(J)
12     50  FORMAT(/,1X,' THE KD VALUE IS ',F12.8,2X,' THE C VALUE
          IS ',F12.9)
13     DO 30 K=1,8
14     A=(KD(I)*K1**2)/(PH(K)**2)
15     B=(K1/PH(K))+(K1*K2/PH(K)**2)+1.0D+0
16     X=(-B+DSQRT(B**2-4.0D+0*A*C))/(2.0D+0*A)
17     IF(X.GT.0.0D+0)GO TO 40
18     X=(-B-DSQRT(B**2-4.0D+0*A*C))/(2.0D+0*A)
19     40  X1=(K1/PH(K))*X
20     X2=(K1*K2/PH(K)**2)*X
21     X3=((KD(I)*K1**2)/(PH(K)**2))
22     X3=X3*X**2
23     WRITE(6,60) PH(K),X,X1,X2,X3
24     60  FORMAT(/,1X,' THE PH IS ',F15.9,' THE (H2CR04) IS ',F15.9,
25     $/,1X,' THE (HCR04-) IS ',F15.9,' THE (CR04=) IS ',F15.9,
26     $/,1X,' THE (CR207=) IS ',F15.9)
27     30  CONTINUE
28     20  CONTINUE
29     10  CONTINUE
30     STOP
31     END

```

---

(a) The variable, PH, contains the value of the hydrogen ion concentration.

(b) Both values of  $K_3$  (i.e., 98 and 35.5) are included in the program.

Table 3. Calculated abundances of chromium (VI) species in aqueous solution at pH 1-8 and total chromium (VI) concentrations (C) in the range  $10^{-2}$ - $10^{-6}$  M.

pH	C(M)	abundance (%)			
		$\text{CrO}_4^{2-}$	$\text{Cr}_2\text{O}_7^{2-}$	$\text{HCrO}_4^-$	$\text{H}_2\text{CrO}_4$
1	$10^{-2}$	0.0	23.6	49.1	27.3
	$10^{-3}$	0.0	3.7	61.9	34.4
	$10^{-4}$	0.0	0.4	64.0	35.6
	$10^{-5}$	0.0	0.0	64.3	35.7
	$10^{-6}$	0.0	0.0	64.3	35.7
2	$10^{-2}$	0.0	36.0	60.6	3.4
	$10^{-3}$	0.0	7.5	87.6	4.8
	$10^{-4}$	0.0	1.0	94.0	5.0
	$10^{-5}$	0.0	0.0	95.0	5.0
	$10^{-6}$	0.0	0.0	95.0	5.0
3	$10^{-2}$	0.0	37.7	62.0	0.3
	$10^{-3}$	0.0	8.2	91.3	0.5
	$10^{-4}$	0.0	1.0	98.5	0.5
	$10^{-5}$	0.0	0.1	99.3	0.6
	$10^{-6}$	0.0	0.0	99.4	0.6
4	$10^{-2}$	0.2	37.7	62.1	0.0
	$10^{-3}$	0.3	8.2	91.5	0.0
	$10^{-4}$	0.3	1.0	98.7	0.0
	$10^{-5}$	0.3	0.1	99.5	0.1
	$10^{-6}$	0.3	0.1	99.6	0.0
5	$10^{-2}$	2.0	36.7	61.3	0.0
	$10^{-3}$	2.9	7.8	89.3	0.0
	$10^{-4}$	3.0	1.0	96.0	0.0
	$10^{-5}$	3.1	0.1	96.8	0.0
	$10^{-6}$	3.1	0.0	96.9	0.0

Cont'd.....

Table 3. Continued

pH	C(M)	abundance (%)			
		$\text{CrO}_4^{2-}$	$\text{Cr}_2\text{O}_7^{2-}$	$\text{HCrO}_4^-$	$\text{H}_2\text{CrO}_4$
6	$10^{-2}$	17.3	28.6	54.1	0.0
	$10^{-3}$	23.0	5.0	72.0	0.0
	$10^{-4}$	24.0	0.7	75.3	0.0
	$10^{-5}$	24.2	0.1	75.7	0.0
	$10^{-6}$	24.2	0.0	75.8	0.0
7	$10^{-2}$	72.4	5.0	22.6	0.0
	$10^{-3}$	75.8	0.6	23.6	0.0
	$10^{-4}$	76.2	0.0	23.8	0.0
	$10^{-5}$	76.2	0.0	23.8	0.0
	$10^{-6}$	76.2	0.0	23.8	0.0
8	$10^{-2}$	96.9	0.1	3.0	0.0
	$10^{-3}$	97.0	0.0	3.0	0.0
	$10^{-4}$	97.0	0.0	3.0	0.0
	$10^{-5}$	97.0	0.0	3.0	0.0
	$10^{-6}$	97.0	0.0	3.0	0.0

### SUMMARY AND CONCLUSIONS

In this study, published values of equilibrium constants were used to calculate the percentage of each chromium (VI) species ( $\text{CrO}_4^{2-}$ ,  $\text{Cr}_2\text{O}_7^{2-}$ ,  $\text{HCrO}_4^-$  and  $\text{H}_2\text{CrO}_4$ ) present in aqueous solution at total chromium (VI) concentrations of  $10^{-2}$  -  $10^{-6}\text{M}$ , in the pH range 1-8. This is the first compilation of such data.

The results show that at the Ames test pH ( $\approx 7.4$ ), only  $\text{CrO}_4^{2-}$

( $\approx 80-90\%$ ) and  $\text{HCrO}_4^-$  ( $\approx 10-20\%$ ) are present. The thermochemical radii of the isoelectronic  $\text{CrO}_4^{2-}$ ,  $\text{SO}_4^{2-}$ , and  $\text{PO}_4^{3-}$  ions (tetrahedral) are 2.40 Å, 2.30 Å and 2.38 Å, respectively (190): the size, shape and anionic nature of the  $\text{CrO}_4^{2-}$  ion facilitate its diffusion through biological membranes via the sulphate or phosphate transport systems (191). The analytical data compiled are also applicable to soil, marine and other aquatic environments.

## REFERENCES

1. Stern, R.M., Environ. Health Perspect., 41 (1981) 235.
2. Gray, C.N., Hewitt, P.J. and Dare, P.R.M., Welding and Metal Fabrication, 50 (1982) 318.
3. Baker, R.S., Aust. Weld. J., 27 (1982) 53.
4. Stern, R.M., Arch. Environ. Health, 38 (1983) 148.
5. Akseleson, K.R., Desaeleer, G.G., Johansson, T.B. and Winchester, J.W., Ann. Occup. Hyg., 19 (1976) 225.
6. Jarnuszkiewicz, I., Knapik, A. and Kwiatkowski, B., Bull. Inst. Mar. Med. Gdansk, 17 (1976) 73.
7. Clapp, D.E. and Owen, R.J., Weld. J., 56 (1977) 380-s.
8. Ulfvarson, U., Scand. J. Work Environ. Health, 7 Suppl. 2 (1981) 1.
9. Beck Hansen, E., Danish Welding Institute Report SF77.01.
10. Welding Fume. Sources. Characteristics. Control. Vols 1 and 2. Welding Institute, Abington, U.K. (1981).
11. Fumes and Gases in the Welding Environment. American Welding Society, Miami, Florida (1979).
12. Lunau, F.W., Ann. Occup. Hyg., 10 (1967) 174.
13. Morley, R. and Silk, S.J., Ann. Occup. Hyg., 13 (1970) 101.
14. Doig, A.T. and McLaughlin, A.I.G., Lancet, 1 (1936) 771.
15. Parkes, W.R., Occupational Lung Diseases, Butterworths, London, 1974.

16. Stern, R.M., Extended bibliography pertinent to studies of toxic substances to which welders are exposed and the resulting health effects. The Danish Welding Institute, Copenhagen (1981).
17. Stern, R.M., Danish Welding Institute Report No. 81.31.
18. Newhouse, M.L. and Murray, R., Welding Institute Report Publication, Abington, U.K. (1981).
19. Lob, M., Soudure, Z (1979) 178.
20. Oxhoj, H., Bake, B., Wedel, H. and Wilhemsen, L., Arch. Environ. Health, 34 (1979) 211.
21. Franchini, I., Mutti, A., Cavatorta, A., Corradi, A., Cosi, A., Olivetti, G. and Borghetti, A., Contr. Nephrol., 10 (1978) 98.
22. Jindrichova, J., Z. Gesamte Hyg., 24 (1978) 86.
23. Kalliomaki, P.-L., Kalliomaki, K., Kelha, V., Sortti, V. and Korhonen, O., Welding in the World, 18 (1980) 67.
24. Keskinen, H., Kalliomaki, P.-L. and Alanko, K., Clin. Allergy, 10 (1980) 151.
25. Mutti, A., Cavatorta, A., Pedroni, C., Borghi, A., Giaroli, C. and Franchini, I., Int. Arch. Occup. Environ. Health, 43 (1979) 123.
26. Stettler, L.E., Groth, D.H. and Mackay, G.R., Am. Ind. Hyg. Assoc. J., 38 (1977) 76.
27. Tola, S., Kilpio, J., Virtamo, M. and Haapa, K., Scand. J. Work Environ. Health, 3 (1977) 192.

28. Hewitt, P.J. and Gray, C.N., Am. Ind. Hyg. Assoc. J., 44 (1983) 727.
29. Langard, S., in Biological and Environmental Aspects of Chromium, Ed. Langard, S., Elsevier Biomedical Press, Amsterdam, 1982, pp. 149-169.
30. Gottlieb, M.S., J. Occup. Med., 22 (1980) 384.
31. Putoni, R., Vercelli, M., Merlo, F., Valerio, F. and Santi, L., Ann. N.Y. Acad. Sci., 330 (1979) 353.
32. Grice, H.C., The Testing of Chemicals for Carcinogenicity, Mutagenicity and Teratogenicity. Department of Health and Welfare, Ottawa (1973).
33. Stolz, D.R., Tox. Appl. Pharmacol., 29 (1974) 157.
34. Bridges, B.A., Nature (Lond), 261 (1976) 195.
35. Purchase, I.F.H., Longstaff, E., Ashby, J., Styles, J.A., Andersen, D., Lefevre, P.A. and Westwood, F.R., Br. J. Cancer, 37 (1978) 873.
36. Hollstein, M., McCann, J., Angelosanto, F.A. and Nichols, W.W., Mutation Res., 65 (1979) 133.
37. Macphee, D.G., in Cancer, Causes and Control, Ed. Metcalf, D., Australian Academy of Science Symposium, Canberra, May 1980, pp. 37-55.
38. Rohrborn, G., Arch. Toxicol., Suppl. 4 (1980) 3.
39. Rees, K.R., J. Royal Soc. Med., 73 (1980) 261.
40. Andersen, D. and Longstaff, E., Analyst, 106 (1981) 1.
41. Hoffmann, G.R., Environ. Sci. Technol., 16 (1982) 560A.

42. Ames, B.N., McCann, J. and Yamasaki, E., *Mutation Res.*, 31 (1975) 347.
43. Jacobs, M., *J. Environ. Pathol. Toxicol.*, 2 (1979) 1205.
44. Baker, R.S.U., *Toxicol. Environ. Chem.*, 2 (1984) 191.
45. Perry, P.E., in *Chemical Mutagens, Principles and Methods for Their Detection*, Vol. 6, Ed. de Serres, F.J. and Hollaender, A., Plenum Press, New York, 1980, pp. 1-39.
46. Perry, P.E. and Thomson, E.J., in *Handbook of Mutagenicity Test Procedures*, Ed. Kilbey, B.J., Legator, M., Nichols, W. and Ramel, C., Elsevier Science Publishers, Amsterdam, 1984, pp. 495-529.
47. Hedenstedt, A., Jensson, D., Lidsten, B.-M., Ramel, C. and Stern, R.M., *Scand. J. Work Environ. Health*, 3 (1977) 203.
48. Maxild, J., Andersen, M., Kiel, P. and Stern, R.M., *Mutation Res.* 57 (1978) 235.
49. Stern, R.M., in *The In Vitro Effects of Mineral Dusts*, Ed. Brown, R.C., Chamberlain, M., Davies, R. and Gormley, I.P., Academic Press, London, pp. 203-209.
50. Stern, R.M., Thomsen, E., Andersen, M., Kiel, P. and Larsen, H., *J. Appl. Toxicol.*, 2 (1982) 122.
51. Knudsen, I., *Acta Pharmacol. Toxicol.*, 47 (1980) 66.
52. Knudsen, I. and Stern, R.M., *Danish Welding Institute Report No.* 80.28.
53. Koshi, K., *Ind. Health*, 17 (1979) 39.

54. Dare, P.R.M. and Hewitt, P.J., Welding and Metal Fabrication, 52 (1984) 56.
55. Gray, C.N., Hewitt, P.J. and Dare, P.R.M., Welding and Metal Fabrication, 51 (1983) 52.
56. Kobayashi, M., Maki, S. and Ohe, I., IIW Doc. VIII-670-76.
57. Dare, P.R.M., Ph.D. thesis, University of Bradford, 1983.
58. Swedish National Standard, "Classification of MMA welding electrodes into fume classes", Utgiven 1975 AC, Svetkommisioner Ingenjorvetenskapadienen.
59. Welding Fume. Sources. Characteristics. Control. Vol. 1. Welding Institute, Abingdon, U.K. (1981).
60. Japan Welding Engineering Society, IIW Doc. VIII-1007-82.
61. Gray, C.N., Hewitt, P.J. and Dare, P.R.M., IIW Doc. VIII-1018-82.
62. Evans, M.J., Ingle, J., Molyneaux, M.K., Sharp, G.T.H. and Swain, J., Ann. Occup. Hyg., 22 (1979) 1.
63. Carlson, T.A., Photoelectron and Auger Spectroscopy, Plenum Press, New York, 1975.
64. Bauer, H.H., Christian G.D. and O'Reilly, J.E., Chapter 15 in Instrumental Analysis, Allyn and Bacon, Inc., Massachusetts, 1978.
65. Lautner, G.M., Carver, J.C. and Konzen, R.B., Am. Ind. Hyg. Assoc. J., 39 (1978) 651.
66. Bohgard, M., Jangida, B.L. and Akseleson, K.R., Ann. Occup. Hyg., 22 (1979) 241.

67. Thomsen, E. and Stern, R.M., Danish Welding Institute Report No. 81.09.
68. Ferguson, W.S., Am. Ind. Hyg. Assoc. J., 44 (1983) B-16.
69. Voítkevich, V.G., Avt. Svarka, 3 (1982) 51.
70. Stern, R.M., IIW Doc. VIII-779-78.
71. Stern, R.M., IIW Doc. VIII-861-80.
72. Morita, N. and Tanigabi, T., IIW Doc. VIII-727-77.
73. Dahberg, G.A., IIW Doc. VIII-475-72.
74. Characterization of Arc Welding Fume. American Welding Society, Miami, Florida (1983).
75. Pedersen, P., Thomsen, E. and Stern, R.M., Danish Welding Institute Report No. 82.16.
76. Kimura, Y., Ichahara, I. and Kobayashi, M., IIW Doc.VIII-574-74.
77. Technical Committee Welding Filler Metal Division, The Japan Welding Engineering Society, IIW Doc.II-956-81.
78. Kimura, S., Kobayashi, M. and Maki, S., IIW Doc.VIII-687-76.
79. Miller, T.M. and Jones, R.C., Aust. Weld. Res., 6 (1979) 1.
80. Instrumentation Laboratory atomic absorption methods manual, Massachusetts, U.S.A., 1979.
81. Handbook of Chemistry and Physics, 55th edition, Chemical Rubber Co., Cleveland, Ohio, 1974-75.
82. Leonard, A. and Lauwerys, R.R., Mutation Res., 76 (1980) 227.

83. Gray, C.N., Hewitt, P.J. and Hicks, R., Weld Pool Chemistry and Metallurgy International Conference, London, 15-17 April, 1980.
84. Kubaschewski, O. and Evans, E.L., Metallurgical Thermochemistry, Pergamon, London, 1958.
85. Abbell, M.T. and Carlberg, J.R., Am. Ind. Hyg. Assoc. J., 35 (1974) 229.
86. Asami, K., J. Electron Spectrosc., 9 (1976) 469.
87. Wagner, C.D., Riggs, W.M., Davis, L.E., Moulder, J.F. and Muilenberg, G.E., Handbook of x-ray Photoelectron Spectroscopy, Perkin-Elmer Corporation, Minnesota, U.S.A., 1979.
88. Wagner, C.D., Anal. Chem., 44 (1972) 1050.
89. Blazek, A., Thermal Analysis, Van Nostrand Reinhold, London, 1973.
90. Mackenzie, R., Differential Thermal Analysis, Academic Press, London, 1970.
91. Wagner, C.D., Gale, L.H. and Raymond, R.H., Anal. Chem., 51 (1979) 466.
92. Wagner, C.D., Zatko, D.A. and Raymond, R.H., Anal. Chem., 52 (1980) 1445.
93. Gray, C.N., Hewitt, P.J. and Dare, P.R.M., Welding and Metal Fabrication, 50 (1982) 393.
94. Aylward, G.H. and Findlay, T.J.V., Chemical Data Book, John Wiley, New York, 1966.

95. Mercer, P.D. and Payling, R., Nuclear Instruments and Methods, 191 (1981) 283.
96. de Angelis, B.A., J. Electron Spectrosc., 9 (1976) 81.
97. American Welding Society, Welding Handbook, Vol. 1, 7th edition, Miami (1976).
98. Welding Industries of Australia (WIA) Catalogue 2012/20/180.
99. Sandvik, A.B. Sandviken, Sandvik Welding Handbook, Sandvik, Goteborg, Sweden (1977).
100. Laboratory method for measuring fume generation rates and total fume emission of welding and allied processes. American Welding Society, Miami (1979) (IIW Doc. VIII-932-81).
101. AWRA standard laboratory method for measuring fume generation rates and total fume emission from wire welding processes. Australian Welding Research Association, AWRA Panel 9-8-82.
102. General Metal Works Inc. Ohio, Glass-fibre filter specifications.
103. Eichhorn, F., Trosken, F. and Oldenburg, T., Paper presented at the special DVS conference on "Health and Safety during Welding" held in Essen, W. Germany on 16 and 17 February 1982 (Sweissen und Schneiden Translation 2/1982).
104. Houldcroft, P.T., Welding Processes, Cambridge University Press, London, 1967.

105. Glickstein, S.S., in Trends in Welding Research in the United States, Ed. David, S.A., American Society for Metals, Ohio, 1983, pp. 3-51.
106. Brunauer, S., Emmett, P.H. and Teller, E., J. Am. Chem. Soc., 60 (1938) 309.
107. Broekhoff, J.C.P. and Linsen, B.G., in Physical and Chemical aspects of Adsorbents and Catalysts, Ed. Linsen, B.G., Academic Press, New York, 1970, pp. 1-62.
108. Burton, R.M., Howard, J.N., Penley, R.L., Ramsay, P.A. and Clark, T.A., 65th annual meeting of the Air Pollution Control Association, Miami Beach, Florida, 1972.
109. Operating manual for Andersen Samplers, Inc. high volume particle size samplers. October 1, 1979. Andersen Samplers, Inc. Atlanta, Georgia, U.S.A., TR // 76 - 900018.
110. Blezard, R.G., Chem. Ind. (London), 16 (1983) 626.
111. Draft for development - methods for the sampling and analysis of fume from Welding and allied processes. Part I. Particulate matter. IIW Doc. VIII-729-77.
112. Hesketh, H.E., Fine particles in Gaseous Media, Ann Arbor, Michigan, 1977.
113. Ludwig, F.L., Environ. Sci. Technol., 2 (1966) 547.
114. Ranz, W.E. and Wong, J.B., Ind. Eng. Chem. 44 (1952) 1371.

115. Alexander Rihm Jr. P.E., Evaluation of a particle sizing attachment for high-volume samplers. New York Department of Environmental Conservation Report No. BTS-3 (1972).
116. Serita, F., Ind. Health, 21 (1983) 67.
117. Heile, R. and Hill, D., Weld. J., 54 (1975) 201-s.
118. Hewitt, P.J., Ann. Occup. Hyg., 15 (1972) 341.
119. Hewitt, P.J., Hicks, R. and Lam, H.F., Ann. Occup. Hyg., 21 (1978) 159.
120. Luckey, T.D. and Venugopal, B., Metal Toxicity in Mammals, Vol. 1, Plenum Press, New York, 1977.
121. Venugopal, B. and Luckey, T.D., Metal Toxicity in Mammals, Vol. 2, Plenum Press, New York, 1978.
122. Varian Techtron. Analytical methods for flame spectroscopy. Australia 9/72.
123. Japanese Welding Engineering Standard 9003K-1976. Methods for chemical analysis of welding fumes. IIW Doc. VIII-717-77.
124. Working Group F. Interlaboratory calibration of a standardised analytical method of hexavalent and total chromium in welding fumes. IIW Doc. VIII-1036-82.
125. NIOSH Measurements Research Branch. Latest NIOSH method for hexavalent chromium. 319-1-319-7, 1981.
126. Sandell, E.B., Colorimetric Determination of Traces of Metals, 3rd edition, Interscience Publishers, New York, 1959.

127. Orion Research Incorporated. Orion ionanalyzer instruction manual. Form IM 94, 96-09/7721, Massachusetts, 1977.
128. Korth, W. and Ellis, J., *Talanta*, 31 (1984) 467.
129. Kubaschewski, O. and Hopkins, B.E., *Oxidation of Metals and Alloys*, Butterworths, London, 1962.
130. Kimura, S., Kobayashi, M., Godai, T. and Minato, S., *Weld. J.*, 59 (1979) 195-s.
131. Stern, R.M., Danish Welding Institute Report No. 76.00.
132. Pohl, C.A. and Johnson, E.L., *J. Chromatogr. Sci.*, 18 (1980) 442.
133. Willard, H.H., Merritt Jr. L.L., Dean, J.A. and Settle Jr. F.A., *Instrumental Methods of Analysis*, Wadsworth Publishing Company, Belmont, California, 1981.
134. Stokinger, H.E., *Am. Ind. Hyg. Assoc. J.*, 45 (1984) 127.
135. Pantucek, M.B., *Ann. Occup. Hyg.*, 18 (1975) 207.
136. Sjogren, B., *Brit. J. Ind. Med.*, 41 (1984) 192.
137. Pantucek, M., *Am. Ind. Hyg. Assoc. J.*, 32 (1971) 687.
138. Mertz, W., *Nutr. Rev.*, 33 (1975) 129.
139. Koshi, K. and Iwasaki, K., *Ind. Health*, 21 (1983) 57.
140. McCann, J. and Ames, B.N., *Proc. Natl. Acad. Sci. U.S.A.*, 73 (1976) 950.

141. Sugimura, T., Yahagi, T., Nagao, M., Takeuchi, M. and Kawachi, T., in Screening Tests in Chemical Carcinogenesis, Ed. Montesano, R., Bartsch, M. and Tomatis, L., IARC Scientific Publications No. 12, Lyon, 1976, pp. 81-101.
142. Rossman, T.G., Environ. Health Perspect., 40 (1981) 189.
143. McCann, J. and Ames, B.N., in Origins of Human Cancer, Ed. Hiatt, H.R., Watson, J.D. and Winsten, J.A., Cold Spring Harbor Conferences on Cell Proliferation, 4, 1977, pp. 1431-1449.
144. de Serres, F.J. and Shelby, M.D., Mutation Res., 64 (1979) 159.
145. Gatehouse, D., Mutation Res., 53 (1978) 289.
146. Green, M.H.L., Muriel, W.J. and Bridges, B.A., Mutation Res., 38 (1976) 33.
147. Tindall, K.R., Warren, G.R. and Skaar, P.D., Mutation Res., 53 (1978) 90.
148. Nestmann, E.R., Matula, T.I., Douglas, G.R., Bora, K.C. and Kowbel, D.J., Mutation Res., 66 (1979) 357.
149. Lofroth, G. and Ames, B.N., Mutation Res., 53 (1978) 65.
150. de Flora, S., Carcinogenesis, 2 (1981) 283.
151. Petrilli, F.L. and de Flora, S., Appl. Environ. Microbiol., 33 (1977) 805.
152. Venitt, S. and Levy, L.S., Nature, 250 (1974) 493.
153. Noda, M., Takano, T. and Sakurai, H., Mutation Res., 66 (1979) 175.

154. Martin, G.R., Brown, K.S., Matheson, D.W., Lebowits, H., Singer, L. and Ophaug, R., Mutation Res., 66 (1979) 159.
155. Gocke, E., King, M.-T., Eckhardt, K. and Wild, P., Mutation Res., 90 (1981) 91.
156. Buselmaier, W., Rohrborn, G. and Propping, P., Biol. Zentralbl., 91 (1972) 311.
157. Rossman, T.G., Stone, D., Molina, M. and Troll, W., Environ. Mutagen., 2 (1980) 371.
158. Nishioka, H., Mutation Res., 31 (1975) 185.
159. Kanematsu, N., Hara, M. and Kada, T., Mutation Res., 77 (1980) 109.
160. Warren, G., Rogers, S.J. and Abbott, E.H., in Inorganic Chemistry in Biology and Medicine, Ed. Martell, A.E., ACS Symposium Series No. 140, 1980, pp. 227-236.
161. Yagi, T. and Nishioka, H., The Science and Engineering Review of Doshisha University, 18 (1977) 1.
162. Ames, B.N., Hollstein, M.C. and Cathcart, R., in Lipid Peroxide in Biology and Medicine, Ed. Yagi, K., Academic Press, New York, 1981.
163. Yamasaki, E. and Ames, B.N., Proc. Natl. Acad. Sci. U.S.A., 74 (1977) 3555.
164. Rinkus, S.J. and Legator, M.S., in Chemical Mutagens, Ed. de Serres, F.J. and Hollaender, A., Plenum Press, New York, 1980, pp. 365-473.

165. Rosenkranz, H.S., Speck, W.T. and Gutter, B., in *In Vitro Metabolic Activation in Mutagenesis Testing*, Ed. de Serres, F.J., Fouts, J.R., Bend, J.R. and Philpot, R.M., Elsevier/North-Holland, Amsterdam, 1976, pp. 337-363.
166. Green, M.H.L. and Muriel, W.J., in *Handbook of Mutagenicity Test Procedures*, Ed. Kilbey, B.J., Legator, M., Nichols, W. and Ramel, C., Elsevier/North-Holland, Amsterdam, 1977, pp. 65-94.
167. Pedersen, P., Thomsen, E. and Stern, R.M., *Environ. Health Perspect.*, 51 (1983) 227.
168. Maron, D.M. and Ames, B.N., *Mutation Res.*, 113 (1983) 173.
169. Petrilli, F.L. and de Flora, S., *Mutation Res.*, 54 (1978) 139.
170. de Flora, S., *Nature (Lond)*, 271 (1978) 455.
171. Stern, R.M., Possible inadequacy of Ames test systems for metallic aerosols. Publication from the Working Environment Group. The Danish Welding Institute, Copenhagen (1978).
172. Baker, R.S.U., Arlauskas, A., Tandon, R.K., Crisp, P.T. and Ellis, J., unpublished results.
173. Baker, R.S.U., Mitchell, G.A., Meher-Homji, K.M. and Podobna, E., *Mutation Res.*, 118 (1983) 103.
174. Goto, K., Maeda, S., Kano, Y. and Sugiyama, T., *Chromosoma*, 66 (1978) 351.
175. Moore, D. and Felton, J.S., *Mutation Res.*, 119 (1983) 95.

176. White, L.R., Jakobsen, K. and Ostgaard, K., Environ. Res., 20 (1979) 366.
177. White, L.R., Richards, R.J., Jakobsen, K. and Ostgaard, K., in The In Vitro Effects of Mineral Dusts, Ed. Brown, R.C., Chamberlain, M., Davies, R. and Gormley, I.P., Academic Press, New York, 1980, pp. 211-218.
178. White, L.R., Marthinsen, A.B.L., Jakobsen, K. and Eik-Nes, K.B., Environ. Health Perspect., 51 (1983) 211.
179. White, L.R., Hunt, J., Tetley, T.D. and Richards, R.J., Ann. Occup. Hyg., 24 (1981) 93.
180. White, L.R., Hunt, J., Richards, R.J. and Eik-Nes, K.B., Toxicol. Lett., 11 (1982) 159.
181. Cresser, M.S. and Hargitt, R., Talanta, 23 (1976) 153.
182. Lingane, J.J., Analytical Chemistry of Selected Elements, Reinhold, New York, 1966.
183. Beattie, J.K. and Haight Jr. G.P., Prog. Inorg. Chem., 17 (1972) 93.
184. Cotton, F.A. and Wilkinson, G., Advanced Inorganic Chemistry, Wiley, New York, 1972, pp. 841-842.
185. Freiser, H. and Fernando, Q., Ionic Equilibria in Analytical Chemistry, Wiley, New York, 1966, pp. 296-297.
186. Neuss, J. D. and Rieman, W., J. Am. Chem. Soc., 56 (1934) 2238.
187. Tong, J.Y. and King, E.L., *ibid.*, 75 (1953) 6180.
188. Davies, W.G. and Prue, J.E., Trans. Faraday Soc., 51 (1955) 1045.

189. Kolthoff, I.M., Sandell, E.B., Meehan, E.J. and Bruckenstein, S.,  
Quantitative Chemical Analysis, 4th Ed., Macmillan, London, 1969,  
pp. 1053-1054.
190. Ball, M.C. and Norbury, A.H., Physical Data for Inorganic Chemists,  
Longman, London, 1974, pp. 145-146.
191. Jenette, K.W., Environ. Health Perspect., 40 (1981) 233.

LIST OF PUBLICATIONS

1. Variations in the chemical composition and generation rates of fume from stainless steel electrodes under different AC arc welding conditions, Tandon, R.K., Crisp, P.T., Ellis, J. and Baker, R.S., Aust. Weld. J., 28 (1983) 27.
2. Effect of pH on chromium (VI) species in solution, Tandon, R.K., Crisp, P.T., Ellis, J. and Baker, R.S., Talanta, 31 (1984) 227.
3. Fume generation and melting rates of shielded metal arc welding electrodes, Tandon, R.K., Ellis, J., Crisp, P.T. and Baker, R.S., Weld. J., 63 (1984) 263-s.
4. Chromium (VI) and apparent phenotypic reversion in Salmonella TA100, Baker, R.S.U., Bonin, A.M., Arlauskas, A., Tandon, R.K., Crisp, P.T. and Ellis, J., Mutation Res., 138 (1984) 127.
5. Generation rate, particle-size and chemical measurements of fume from some hardfacing and HSLA-steel electrodes, Tandon, R.K., Crisp, P.T., Ellis, J. and Baker, R.S., Welding and Metal Fabrication, 53 (1985) 43.
6. Application of x-ray photoelectron spectroscopy to the analysis of stainless-steel welding aerosols, Tandon, R.K., Payling, R., Chenhall, B.E., Crisp, P.T., Ellis, J. and Baker, R.S., Appl. Surf. Sci., 20 (1985) 527.

7. Mutagenicity of metal ions in bacteria, Arlauskas, A., Baker, R.S.U., Bonin, A.M., Tandon, R.K., Crisp, P.T. and Ellis, J., Environ. Res., 36 (1985) 379.
8. Toxic and genotoxic action of electric-arc welding fumes on cultured mammalian cells, Baker, R.S.U., Arlauskas, A., Tandon, R.K., Crisp, P.T. and Ellis, J., Submitted to J. Appl. Toxicol.
9. Chemical investigation of some electric arc welding fumes and their potential health effects, Tandon, R.K., Crisp, P.T., Ellis, J., Baker, R.S. and Chenhall, B.E., To be submitted to Weld. J.

#### PAPERS PRESENTED AT CONFERENCES

1. An automatic arc welder and fume collector system for the chemical investigation of welding fume and its potential health effects, Tandon, R.K., Crisp, P.T., Ellis, J. and Baker, R.S., Paper presented at the 30th Annual Convention of the Australian Welding Institute, Hobart, 9-15 October, 1982.
2. "False" mutation by chromium (VI): exploding a myth, Arlauskas, A., Bonin, A.M., Baker, R.S.U., Tandon, R.K., Crisp, P.T. and Ellis, J., Paper presented at the 8th Annual Meeting of the Australia New Zealand Environmental Mutagen Society, CSIRO Division of Molecular Biology, North Ryde, 22-25 February, 1984.